TOPOGRAPHY OF THE BASEMENT ROCK

BENEATH THE

NORTHERN GUAM LENS AQUIFER

AND ITS

IMPLICATIONS FOR GROUNDWATER EXPLORATION AND DEVELOPMENT

by
David T. Vann
Vivianna M. Bendixson
Douglas F. Roff
Christine A. Simard
Robert M. Schumann
Nathan C. Habana
John W. Jenson

WERI
WATER AND ENVIRONMENTAL RESEARCH INSTITUTE
OF THE WESTERN PACIFIC
UNIVERSITY OF GUAM

Technical Report No. 142

August 2014

TOPOGRAPHY OF THE BASEMENT ROCK
BENEATH THE
NORTHERN GUAM LENS AQUIFER
AND ITS
IMPLICATIONS FOR GROUNDWATER EXPLORATION AND DEVELOPMENT

by
David T. Vann[1]
Vivianna M. Bendixson[1]
Douglas F. Roff [2]
Christine A. Simard[1]
Robert M. Schumann[3]
Nathan C. Habana[1]
John W. Jenson[1]

[1]Water and Environmental Research Institute of the Western Pacific
University of Guam UOG Station, Mangilao, Guam 96923

[2]AECOM Technical Services
7807 Convoy Court, Suite 200
San Diego, CA 92111

[3]AECOM Technical Services
10461 Old Placerville Road, Suite 170
Sacramento, CA 95827

Technical Report No. 142
August 2014

Acknowledgements: Initial work described herein was funded by the Guam Hydrologic Survey through the University of Guam Water and Environmental Research Institute of the Western Pacific. The most recent work was funded by the Pacific Islands Water Science Center, U.S. Geological Survey, Department of the Interior: "Hydrogeological Database of Northern Guam," grants numbered G10AP0092 and G11AP20225. The authors wish to thank Todd Presley, Travis Hylton, and Kolja Rotzoll for helpful comments and suggestions, and Steve Gingerich for contributions and detailed reviews of both the map and technical report. The final draft benefited from careful proofing by Joe Rouse and Gary Denton.

Updates and Revisions: Subsequent editions of this report and the accompanying map will be issued as the database and understanding of the aquifer improve. Please advise WERI of any errors, discrepancies, or updates via J.W. Jenson (jjenson@uguamlive.uog.edu) or N.C. Habana (nchabana@uguamlive.uog.edu).

Author Contributions

Vann collected, researched, and compiled the voluminous and disparate historical data from which the initial map was built; researched, selected, applied, and described the interpolation methodology; prepared the initial interpolation for the current map in consultation and collaboration with the co-authors; and drafted the core of this technical report as part of the requirements for the Master of Science Degree in Environmental Science at the University of Guam.

Bendixson prepared and finalized the master database, derived from *The Northern Guam Lens Aquifer Database*, which she built as part of the requirements for the Master of Science Degree in Environmental Science at the University of Guam. She worked closely with Vann to scrutinize and evaluate the reliability of the data and select data for construction of the map. She worked with the rest of the co-authors to edit the technical report, and compile the appendices, along with other supporting materials.

Roff and Schuman led the NAVFACPAC exploratory drilling program, and interpreted the results of the drilling, contributing fresh insights into general aquifer hydrogeology as well as into specific hydrogeological conditions at particular locations. They collaborated with the rest of the co-authors in the critical evaluation of the map and the development of the recommendations of this report.

Simard contributed to the critical assessment of the para-basal zone geometry using information derived from her research thesis as part of the requirements for the Master of Science Degree in Environmental Science at the University of Guam.

Habana contributed to the composition and editing of the report and consolidated and compiled the final map. His contributions include critical examination and refinement of the basement interpretations, including integration of surface boundary conditions from other data sources, field-checking and re-interpretation of selected features, development of the design and layout of the map, and descriptions of the associated methodologies and map features.

Jenson served as project/thesis advisor to Vann, Bendixson, and Simard. He collaborated with Roff and Schuman in the interpretations and implications of the hydrogeology, consulted with Habana on the development of the final map, and coordinated the compilation and editing of the technical report among all the co-authors.

ABSTRACT

Subterranean hills and valleys in the non-productive volcanic basement rock underlying the water-bearing limestone bedrock of the Northern Guam Lens Aquifer partition it into six semi-contiguous groundwater basins. Within each basin are three zones, which pose different challenges for developing and managing water production and quality. An accurate and detailed map of basement topography is thus of central importance for successful groundwater exploration, development, and management. The pivotal 1982 *Northern Guam Lens Study* produced the first comprehensive map of basement topography, and has been in use ever since. The purpose of the project reported herein was to produce an up-to-date, state-of-the-art map to support groundwater exploration and development, and aquifer modeling, management, and protection. This revision applies the latest data screening and spatial analysis techniques to evaluate 697 records, from which 148 internal control points (80 from borehole data, 68 from geophysical surveys) were selected and applied along with 24 boundary conditions (2 Light Detection and Ranging raster-points, 17 bathymetric points, 5 specified points) to model basement topography. Elevations across the basement surface were thus estimated from 173 control points that pinned the interpolated surface to 132 positive control points. The interpolated surface was adjusted at 16 negative control points at which the deepest known depths of limestone showed it to be too high. For each control point, the new map displays the *type of data* (boundary condition, borehole, seismic, or Time Domain Electromagnetic), *type of control* (positive or negative), and *precision* (distinct or indistinct). The new map updates and more precisely defines the boundaries of the aquifer's six groundwater basins and provides for more accurate and detailed demarcation within each basin of its *basal zone* (at least 75% of the aquifer, where freshwater is underlain by saltwater), *para-basal zone* (probably less than 5% of the aquifer, where freshwater is underlain by basement rock below sea level), and *supra-basal zone* (about 20% of the aquifer, where conduits and discontinuous patches of freshwater are underlain by basement rock above sea level). The new map also incorporates new insights regarding groundwater occurrence gained from the broad-ranging 2010 Exploratory Drilling Program funded by *Naval Facilities Engineering Command Pacific*. Names from the 1982 map are retained but formal names are also assigned to previously unnamed significant features. New basin boundaries are also proposed. This report describes the elements and methodology used, including definitions of essential terms and concepts; the conceptual model of the basement geology; procedures for assembling the dataset; and the steps in preparing, statistically evaluating, and editing the interpolated basement surface. It also describes the geologic and geographic symbols used. The report concludes with recommendations regarding groundwater exploration, aquifer development, and maintenance and improvement of the basement map.

Keywords: Northern Guam Lens Aquifer, groundwater exploration, groundwater models

This page intentionally left blank.

CONTENTS

LIST OF FIGURES

LIST OF TABLES

MAP

SUPPLEMENTARY MATERIALS

Supplementary materials, including copies or links to the following and other references and appendices cited in this report can be found on the WERI website, under "Basement Map of Northern Guam: Supplementary Materials."

1. CDM, 1982, Final Report, Northern Guam Lens Study, Groundwater Management Program, Aquifer Yield Report, Camp, Dresser and McKee, Inc. in assoc. with Barrett, Harris & Associates *for* Guam Environmental Protection Agency. (Including, Plate 1, orginal basement map.)

2. AECOM Technical Services Inc., 2011, Guam Water Well Testing Study to Support US Marine Corps Relocation to Guam: Naval Facilities Engineering Command, Pacific.

   http://www.guambuildupeis.us/documents/final/volume_9/Vol9_AppK_Additional_Reports_Utilities_PartII.pdf

3. PCR Environmental, Inc., 2012, Spring 2012 Long Term Groundwater Monitoring Report: Main Base and MARBO Annex Operable Units, Andersen Air Force Base, Guam: for Naval Facilities Engineering Command, Marianas.

ABBREVIATIONS AND ACRONYMS

36 CES	36th Civil Engineering Squadron
AAFB	Andersen Air Force Base
amsl	above mean sea level
BBE	Bottom Borehole Elevation
CWMP	Comprehensive Water Monitoring Program
DEM	Digital Elevation Model
DKDLE	Deepest Known Depths of Limestone Elevations
GEPA	Guam Environmental Protection Agency
GHS	Guam Hydrologic Survey
GIS	Geographic Information System
gpm	gallons per minute
GWA	Guam Waterworks Authority
IDW	Inverse Distance Weighting
IRP	Installation Restoration Program
LiDAR	Light Detection and Ranging
MARBO	Marianas-Bonin Island Command
NAVFACPAC	Naval Facilities Engineering Command Pacific
NGLA	Northern Guam Lens Aquifer
NGLS	Northern Guam Lens Study
PUAG	Public Utility Agency of Guam
PWC	Public Works Center
TDEM	Time Domain Electromagnetic
USEPA	US Environmental Protection Agency
USGS	US Geological Survey
WERI	Water & Environmental Research Institute of the Western Pacific

REGARDING UNITS: ENGLISH AND METRIC

The map is published in both English and metric versions, English to support engineering and management applications, and metric to support modeling and other scientific activities. This report therefore cites both unit types together. In general, English units are cited first, with the equivalent quantity in metric units (usually rounded to the nearest whole unit) following in parentheses. The order reflects the fact most of the original data (drilling, construction, and meteorological) are in English units, while modeling and other scientific applications are done in metric units. Where original data are in metric units, however, the metric quantity is cited first.

Regarding depths and intervals of basement topographic contours, it should be noted that English-metric unit pairs cited in the report are not equivalent conversions of one another, but are rather merely the closest analogues of intervals from the different systems. Such pairs are cited with the conjunction “or” rather than with one following the other in parentheses. Thus, for example, a reference in the report to “the 120-ft or 40-m contour” refers to the analogous, but different, depths used on separate versions of the map, rather than implying identical depths (in which, for example, 120 ft would convert to 36.6 rather than 40 m).

EXECUTIVE SUMMARY

TOPOGRAPHY OF THE BASEMENT ROCK
BENEATH THE
NORTHERN GUAM LENS AQUIFER
AND ITS
IMPLICATIONS FOR GROUNDWATER EXPLORATION AND DEVELOPMENT

Subterranean hills and valleys in the non-productive volcanic basement rock that underlies the water-bearing limestone bedrock of the Northern Guam Lens Aquifer (NGLA) partition it into six basins, within each of which are three zones that require unique approaches for exploration and development. An accurate and detailed map of the basement topography is therefore the first prerequisite for successful exploration and development of new wells and for diagnosing and correcting problems in existing ones. In addition to improving the odds for success in exploration, investments in greater accuracy and resolution of the map facilitate more accurate diagnoses and more effective remediation of saltwater intrusion and other forms of contamination. An accurate basement map is also essential for supporting other groundwater research and the development of other tools, including numerical flow and transport models.

I. BACKGROUND

A. Geology & Groundwater Zones in the Northern Guam Lens Aquifer

Basement topography partitions the NGLA into six partially contiguous groundwater basins; within each are three groundwater zones:

1. *Basal zone*: freshwater lens underlain by saltwater, occupies the area between the coast and the flanks of basement rises and ridges that stand above sea level

2. *Para-basal zone*: ribbon-like zone where the headward edge of the freshwater lens laps onto the flank of basement rises and ridges

3. *Supra-basal zone*: patchy zone, contains fractures, cavern systems, and natural impoundments filled with water flowing downward along the basement contact

B. History of Map Development

- 1982: The $1.2M *Northern Guam Lens Study* (NGLS) was the first comprehensive aquifer study, and produced the first detailed basement map from seismic and drilling data.

- 1992: NGLS update incorporated new geophysical data (Time Domain Electromagnetic (TEDM)) in parts of the 1982 map.

- 2000: Borehole data acquired from exploratory drilling in the 1990s were incorporated into an unpublished map by D.T. Vann at the Water & Environmental Research Institute of the Western Pacific (WERI).

- 2010: Renewal of exploration by Naval Facilities Engineering Command Pacific (NAVFACPAC) rekindled interest and support for a state-of-the-art basement map.

II. SCOPE & OBJECTIVES

The purpose of this project was to produce, from historical as well as newly acquired data, an up-to-date, state-of-the-art map of NGLA basement topography to support aquifer research, exploration, development, and management.

III. METHODOLOGY

Six-Step Spatial Analysis Procedure

Step 1: Key elements and conceptual model rigorously defined

Step 2: Data from all sources, historical and current, collected and consolidated

Step 3: Data set assembled (from more than 697 prospective points)

- Four *types* of data
  1. *Boundary conditions* (24 points) from LiDAR-based DEM, bathymetry, etc.
  2. *Borehole* (200 points), historical up through 2010 NAVFACPAC study
  3. *Seismic lines* (45 points) from the original 1982 map
  4. *TDEM* (23 points) from 1992 NGLS update

- Two types of internal *control*
  1. *Positive*: where basement surface is located: 132 points
  2. *Negative*: where basement surface is not: 16 points

- Two levels of data *quality*
  1. *Distinct*: precise control (within a foot or two—most boreholes)
  2. *Indistinct*: approximate control (more than foot or two—all seismic, TDEM)

Step 4: Candidate interpolation methods selected and tested using latest Geographic Information System (GIS) tools

Step 5: Selection of most reliable interpolation from tested candidates

Step 6: Corrections and editing of selected interpolation, and assembly of map

IV. RESULTS: ADDITIONS AND INNOVATIONS TO THE MAP

A. Display of control points. The map displays each of the 172 control points, with map symbols that differentiate among:

- Boundary conditions: 2 LiDAR-derived DEM points, 17 bathymetry depths (2 off of map), 5 specified
- Borehole data, positive control: 65 points (and whether distinct or indistinct)
- Borehole data, negative control: 16 points (active)
- Seismic, positive control: 45 points, from 1982 NGLS map (inherently indistinct)
- TDEM, positive control: 23 points, from 1992 NGLS update (inherently indistinct)

B. Geologic and hydrogeologic features. The map includes GIS enhancements for terrain analysis, and overlays of LiDAR data, satellite imagery, and selected geologic features:

1. Basement topography is depicted with hill-shading and conventional contour lines using standard symbols, including those for closed-contour depressions. In addition:

- *Hill-shade* rendering of the topography
- *Formal names* assigned to basement features:
  - *Rises*: *Mataguac, Pati Point, Santa Rosa, Adacao,* and *Barrigada*
  - *Ridges: Santa Rosa*
  - *Saddles: Santa Rosa-Adacao* and *Adacao-Barrigada*
  - *Valleys: Yigo Valley, YigoTrough*, *Haputo, Tarague,* and *Anao*

2. **Hydrologically significant geologic features added**
   - Ground surface from LiDAR data
   - Mapped faults from previous geologic maps
   - *Hagåtña Argillaceous Member of the Mariana Limestone*

3. **Infrastructure relevant to water resources management**
   - WERI-US Geological Survey (USGS) *Comprehensive Water Monitoring Program* (CWMP) observation wells
   - AECOM exploratory wells
   - Locations of the production wells
   - Major roads and airfields

4. **Bathymetric boundary conditions**. Bathymetric depths from other maps (17 points used, 15 shown) provided approximate depths to fix the initial boundaries.

5. **Manual editing to incorporate independently mapped positive control points**. The interpolated topography was manually refined where mapped outcrops of the basement or other additional data allowed for refinement of the computer-generated basement topography. Adjustments were also made to correct for anomalies in the computer-generated topography. Such refinements and adjustments were made at about a dozen locations.

6. **Manual editing driven by negative control points**. The initial interpolated surface was corrected at five locations based on 16 drilling records.

7. **Water-table contours**. The map also displays *thin blue contour lines* for the water table calculated from the numerical model (Gingerich & Jenson, 2010; Gingerich, 2013).

8. **Groundwater basins and hydrologic boundaries**. Standard term, “groundwater basin” adopted in lieu of previously used term “sub-basin.” Boundaries revised from 1982 map:
   - Basement hydrologic divides: fixed or “hard” boundaries (bold solid blue lines)
   - Presumed groundwater flow-line boundaries (in absence of knowledge of the karst “plumbing”): mobile or “soft” boundaries (bold dashed blue lines)
   - Basin names from the 1982 map retained, with 2 slight modifications:
   - Hagåtña (in lieu of “Agana” to conform to Chamorro-language lexicography)
   - Yigo-Tumon (in lieu of “Yigo” to better reflect geography of this unit)

9. **Saltwater toe and para-basal/basal boundary**. The map displays an estimated saltwater toe location—defined as the 50% seawater isochlor calculated from the numerical model (blue-green band).

10. **Santa Rosa-Adacao Saddle**. A noticeable revision from previous maps is the slight deepening of the saddle based on results from the 2010 drilling program.

11. **Santa Rosa-Adacao-Barrigada Hydrologic Barrier**. Concurrent research (Rotzoll et al., 2013) suggests an effective barrier from Mount Santa Rosa to the Barrigada Rise, regardless of depths of basement saddles.

V. OBSERVATIONS & RECOMMENDATIONS

A. Applications of the Map to Future Exploration and Sustainable Development

NOTE: General prospects for success in exploratory production wells are 1-in-4 to 1-in-3. Productivity of individual well sites varies greatly within all three groundwater zones. Of the 11 wells drilled in the 2010 NAVFACPAC study only four delivered economical quantities of high-quality water—consistent with the professional wisdom of experienced local drillers. With this in mind, recommendations follow for each zone:

1. **Exploration for basal water.** The 2010 NAVFACPAC exploratory drilling program indicated promising prospects for further development of some basal water (particularly in the Agafa Gumas and Andersen basins), but it should be kept in mind that the risk of saltwater contamination is highest in the basal zone, and that basal water quality can be expected to deteriorate as upstream para-basal and/or supra-basal wells are installed. For this and the other two zones, other current research on local groundwater flow and quality should be considered as well before evaluating prospective effects of new wells on nearby current and planned production wells.

    - In general, seek sites as close as possible to the para-basal zone, and where possible, along the axes of basement valleys, with the following qualifications:

        - Finegayan Basin: High permeability and possibility that fresh water converges on regional-scale karst pathways suggest that basal wells here may be especially susceptible to saltwater contamination.

        - Hagåtña Basin: Development should be avoided in the southeastern portion, which has historically contained high-salinity water, and shows strong seasonal variation in water quality.

        - Mangilao Basin: Lacks such zones of possible higher-thickness basal water, except along the southeast flank of the Barrigada Rise.

2. **Exploration for para-basal water.** Given the important advantages of the para-basal zone, continuing investments should be made in more accurately and precisely determining its boundaries and in locating and developing productive well sites within it:

    - The para-basal zone should continue to be the focus of exploration, particularly in the Agafa Gumas and Andersen Basins, where it remains relatively undeveloped.

        - Prospective sites are limited, however, by current and planned land use.

    - The northwest flank of the Mataguac Rise and head of the Yigo Trough contain shallow, extensive para-basal areas that may be relatively more vulnerable than elsewhere to landward migration of saltwater.

        - This prediction is sensitive to the accuracy of the mapped topography in these areas—finer control on actual basement depths is advisable to support development in these areas.

    - Hagåtña Basin: There may be some remaining potential along the flank of the Pago-Adelup Fault at the southwestern end of the basin.

        - Focused study of the basement topography is also advisable here, however, as the current map is poorly constrained in this area.

- It should be noted that increased development of the para-basal zone in general may degrade the quality of water from basal wells downstream.

    - Application of numerical models could help to evaluate these prospects.

3. **Exploration for supra-basal water.** The supra-basal zone was generally regarded as unproductive until the discovery of what was initially called “perched” water in Andersen Air Force Base (AAFB) *Installation Restoration Program* (IRP) wells during the 1990s:

    - These discoveries were followed by the spectacular successes of a few exploratory production wells, notably Y-15, Y-17, and Y-23 (on the Santa Rosa Rise), which remain high-quality large-capacity producers to this day.

    - In summer of 2010, the latest attempt was made to locate supra-basal water.

        - Although success was limited, insights gained from three of the wells drilled on AAFB should improve the odds for future success.

    - There are at least five positive reasons for pursing development of supra-basal water:

        1. Given that the Santa Rosa-Mataguac-Pati Point complex occupies about 20% of the aquifer and nearly half of the Andersen Basin, it may be cost-effective to pursue development here.

        2. It is immune to contamination by saltwater intrusion.

        3. It lies at the headwaters of groundwater basins, upstream of most of the possible sources of surface contamination.

        4. The map shows prospective locations, with conditions that may be similar to those that provide the consistent high-quality water to Y-15.

        5. Supra-basal wells might also be successful along the axes of the basement valleys.

    - Continued improvements in the accuracy and precision of the basement map could be especially fruitful for supporting nearby residents and adjacent military activities.

    - NOTE: The supra-basal zone is not included in the numerical model of the 2013 Guam Groundwater Availability Study.

        - Flow, storage, and aquifer geometry are too complex and poorly known here to incorporate in numerical models.

        - The numerical model does account for recharge assigned to this area, however, and could be applied to help evaluate the effects of supra-basal extraction on the para-basal and basal zones.

    - NOTE: Wells drilled in the supra-basal zone should be extended all the way to the basement contact. (Local regulations, which prohibit drilling more than 40 ft below static water level, should be adjusted accordingly.)

4. **Other applications: aquifer protection, etc.** The map indicates where the aquifer is partitioned and provides a basis for predicting where karst flow paths might form along the bedrock-basement contacts, or along the axes of the basement valleys.

B. Improvements and Updates of the Map

1. **Annual updates and 5-year revisions of the map.** Under Guam Public Law 24-247, drillers must notify WERI prior to drilling and provide copies of down-hole or geophysical data to be archived at WERI in the Guam Hydrologic Survey (GHS) database. These should be used to develop annual updates and 5-year reviews of the basement map.

2. **Comprehensive hydrogeologic map of northern Guam**. Recommend integrating and overlaying other geologic features that are also of crucial importance for understanding of aquifer potential and performance.

3. **Coastal discharge evaluation.** Field studies suggest concentrations of coastal springs correlate with structural features such as faults, which control flow and transport.

4. **Future surveys of basement topography.** Improvements in geophysical technology in the 30 years since 1982 suggest that new surveys could verify or achieve more accurate and precise measurements of basement topography. The current map provides a basis for selecting areas worthy of additional study.

TOPOGRAPHY OF THE BASEMENT ROCK BENEATH THE NORTHERN GUAM LENS AQUIFER AND ITS IMPLICATIONS FOR GROUNDWATER EXPLORATION AND DEVELOPMENT

Vann, D.T., Bendixson, V.M., Roff, D.F., Simard, C.A., Schumann, R.M., Habana, N.C., Jenson, J.W.

Figure 1. Simplified physiographic map of Guam. The Northern Guam Lens Aquifer is the limestone bedrock covering all but one percent of the northern plateau; interior basement outcrops occur at Mount Santa Rosa, Mataguac Hill, and Palii Hill in the northwest portion of the northern Guam plateau, and in minor exposures along the NE coast.

1 BACKGROUND

1.1 Geologic Setting

First mapped in detail by Tracey et al. (1964), Guam is about 30 miles (50 km) long and four to twelve miles (7-20 km) wide, with a surface area of 214 square miles. It is divided almost evenly into two distinct physiographic provinces by a normal fault trending northwest from Pago Bay on the east central coast to Adelup on the west central coast (Figure 1). The lower-standing northern province is a gently tilted and faulted concave karst plateau (Figure 2) formed on an uplifted (200-600 ft; 60-180 m) Miocene-to-Plio-Pleistocene bank-to-lagoon-and-reef limestone sequence (Siegrist and Randall, 1992a; Tracey et al., 1964) (Figure 3), atop an Oligocene volcanic basement (Figure 4). The karst terrain of the north is devoid of rivers and streams except at its southeastern end, where streams and blind valleys have formed on the argillaceous limestone that abuts the southern highlands on the opposite side of the Pago-Adelup Fault (Figure 2). The northern plateau, including the

Figure 2. The Northern Guam Plateau, seen from the northwest coast, looking to the southeast. Dos Amantes Point, stands at about 300 ft (90 m) elevation in the front and center, with Barrigada Hill, which rises to about 600 ft (180 m) elevation, at the horizon in the far upper right. Occupying 102 mi^2 (264 km^2) area, the plateau surface is the uplifted, eroded remnant of an ancient atoll-like reef-lagoon complex. It is now the catchment for the aquifer composed of the Miocene-Pleistocene limestone bedrock sequence beneath it. (Photo: Hydroguam.net)

argillaceous terrain, is internally drained by a complex network of solution features, including closed depressions, large- and small-scale solution channels, caves, and coastal seeps and springs (Schlanger, 1964). The terrain of the southern province is mostly volcanic upland drained by deeply incised stream valleys formed on deeply weathered Eocene-to-Miocene volcanic rocks (Figure 4). These are overlain in the interior and on the spine of the western cuesta by Miocene limestones, and flanked on the province's eastern and northwestern coasts by younger limestones thought to be penecontemporaneous with the northern limestones (Figure 1).

1.2 The Northern Guam Lens Aquifer & the Carbonate Island Karst Model

Figure 3. The Barrigada Limestone. A fresh excavation of the Miocene-Pliocene Barrigada Limestone, the core and dominant unit of the aquifer, at the Department of Public Works Quarry, Dededo. Patches of orange staining at the center and on the right-hand side mark pathways of percolating vadose water.

The aquifer of the northern plateau, designated the Northern Guam Lens Aquifer (NGLA) (U.S. Environmental Protection Agency, 1978), is composed primarily of two limestone units. The core of the aquifer is the Miocene-to-Pliocene Barrigada Limestone, which consists primarily of detrital deep-to-shallowing foraminiferal bank deposits. The Barrigada Limestone is surrounded and mostly overlain by the Plio-to-Pleistocene Mariana Limestone, which consists primarily of reef and lagoonal facies. The basement beneath the limestone bedrock is the Oligocene Alutom Formation (Figure 4), a complex volcanic unit that dominates the surface in the northern half of the southern highland. Because limestone is soluble in freshwater, the water running through the aquifer dissolves an internal drainage network within it and along the contact between it and the underlying insoluble volcanic basement. The characteristic internally drained topography formed on soluble rocks is called *karst*, and the aquifers formed within them are thus *karst aquifers* (Neuendorf et al., 2011).

Figure 4. The Alutom Formation. Outcrop of layered tuffaceous volcanic rock near the summit of Mount Alutom, the type locale of the Oligocene Alutom Formation, which comprises the basement under the limestone bedrock aquifer beneath the northern plateau.

Mylroie and Jenson (2000) developed the Carbonate Island Karst Model (CIKM) to define the unique type of karst that develops on small carbonate islands such as Guam (Mylroie et al., 2001). In contrast to the classic karst terrain that forms on old limestone on continents and islands composed of continental rocks, carbonate island karst forms on small uplifted carbonate islands composed of geologically young limestone that has

never been buried (Vacher and Mylroie, 2002), and which is supported by a basement of insoluble and much (i.e., orders of magnitude) less permeable volcanic rock (Figure 4 and Figure 5). It has long been known that freshwater in island aquifers accumulates in a thin lens-shaped body supported by the underlying higher-density saltwater, and from which water captured in the interior of the island flows to the coast, whence it discharges in seeps and springs (cf., Fetter, 2001). As relative sea level rises and falls, whether from glacio-eustasy or tectonic subsidence and uplift, the lens migrates up and down through the aquifer. Over geologic time, migrating vertical and horizontal flows of groundwater in island karst aquifers redistribute porosity and permeability in both the vadose and phreatic zones (Mylroie and Carew, 1999; Vacher and Mylroie, 2002) resulting in a complex distribution of aquifer properties between the interior and the perimeter, and throughout the vertical section (Ford and Williams, 2007; Rotzoll et al., 2013; Taborosi et al., 2013a).

Within this context, the CIKM posits four ideal carbonate island types: *simple, carbonate-covered, composite, and complex.* Simple carbonate islands (Figure 5A) are those without volcanic or other non-carbonate basement rock above sea level, and which thus contain a classic, unperturbed freshwater lens. Carbonate-cover (Figure 5B) islands are those in which part of the non-carbonate basement core rises above sea level but is not exposed at the surface. On composite islands (Figure 5C), parts of the non-carbonate core are exposed at the surface. Complex islands (Figure 5D) exhibit any or all of the features of the first three types, along with additional complexity wrought by structural modification (e.g., offset of permeable and impermeable units along faults) and more complicated stratigraphy (e.g., inter-layered volcanic and carbonate units, including "dirty" limestones containing syndepositional volcanic ash and volcanic-derived sediments). Northern Guam contains at least each of the first three ideal types: simple, carbonate-covered, and composite (Mylroie et al., 2001). Recent drilling experience (AECOM Technical Services Inc., 2011) suggests, however, that the hydrogeology around Mount Santa Rosa (Figure 1) may be more structurally complex than has heretofore been recognized.

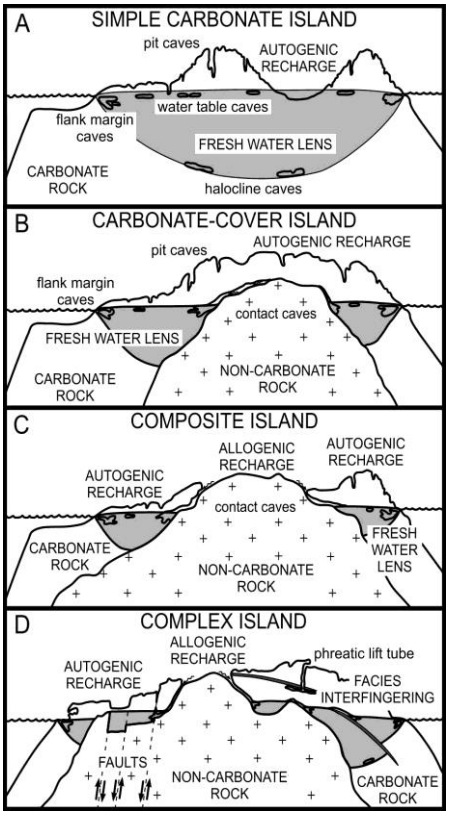

Figure 5. Carbonate Island Karst Model. A) *Simple carbonate islands* contain a classic freshwater lens. Zones of enhanced porosity are thought to form at the top and bottom of the lens during periods of stasis: B) The lens in *carbonate-cover islands* is partitioned where the basement aquiclude stands above sea level; C) On *composite islands* the basement core breaches the surface and weathers to form surface-water catchments that shunt allogenic waters to insurgents formed at the contact with the surrounding limestone terrain; D) Aquifers of *complex islands* reflect complex structural and stratigraphic histories (after Stafford et al., 2004). (Vertical dimension exaggerated)

1.3 Groundwater Zones in the Freshwater Lens

Where basement rises and ridges stand above sea level, they partition the aquifer (Figure 5B-D) into semi-contiguous subterranean *groundwater basins*.[1] Within each basin are three *groundwater zones* defined by the relationships among the underlying or adjacent saltwater, bedrock-basement contact, and sea level (Figure 6). Accurate knowledge of these zones is crucial for development and management of carbonate island karst aquifers.

The *basal zone* is the portion of the lens between the coast and the flanks of basement rises and ridges that stand above sea level. *Basal groundwater*[2] is widespread and therefore easily found and developed, but quality is variable; since this portion of the lens is underlain by saltwater it presents the greatest challenges in developing and managing production wells to prevent or manage saltwater contamination.

On the headward limb of the freshwater lens, where it laps onto the flank of the rising basement slope, the lens reaches its thickest at the *saltwater toe* (Figure 6). The lens thins upslope of the saltwater toe, where it is underlain by basement rock rather than saltwater. This portion of the lens that overlies basement from the saltwater toe to mean sea level is termed the *para-basal zone* (CDM, 1982; Mink and Vacher, 1997). Since the saltwater toe can migrate either seaward or inland with changes in the freshwater mass balance or changes in sea level, this boundary between the basal and para-basal zones is transient.

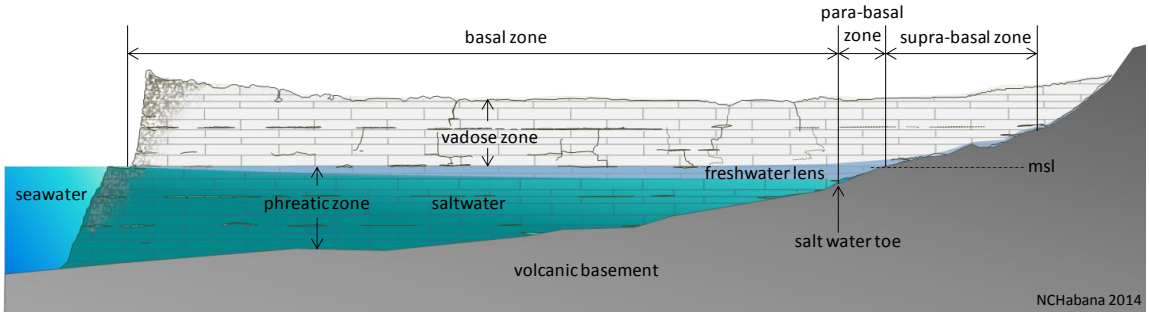

Figure 6. The three groundwater zones in carbonate island karst aquifers (not to scale): 1) the *basal zone*, in which the freshwater lens is underlain by seawater, 2) the *para-basal* zone, where the freshwater is underlain by basement rock below sea level, and 3) the *supra-basal* zone, in which freshwater lies above sea level, on the flanks of the basement rises and ridges.

Water that is underlain by nonproductive basement rock *above* sea level is termed *supra-basal water* (AECOM Technical Services Inc., 2011). (There may be occasional locations where basement rock is sufficiently permeable to produce water to wells.) Supra-basal water moving down slope likely converges along the axes of basement valleys, and may accumulate behind subterranean impoundments or restrictions in conduits before it eventually reaches the para-basal zone.

---

[1] **Groundwater basin** (a) A subsurface structure having the character of a basin with respect to the collection, retention, and outflow of water. (b) An aquifer or system of aquifers, whether basin-shaped or not, that has reasonably well-defined boundaries and more-or-less definite areas of recharge and discharge (Neuendorf et al., 2011).

[2] **Basal groundwater**. A term that originated in Hawaii and refers to a major body of groundwater floating on and in hydrodynamic equilibrium with saltwater (Neuendorf et al., 2011).

Supra-basal water tends to be the freshest water in the aquifer, and because it is not in contact with saltwater, is invulnerable to contamination by it. Supra-basal water does not form a continuous sheet of water along the limestone-volcanic interface, but flows along the interface mainly through dissolution-widened bedrock fractures and cave networks.

1.3.1 Considerations for aquifer development

The basal zone occupies about 75% of the aquifer by area. Basal water is thus very accessible, although it is of variable quality and vulnerable to saltwater contamination. The para-basal zone occupies <5% of the aquifer, but it has historically been the zone of choice for development of groundwater (Figure 7) on Guam because para-basal water is fresher, somewhat thicker and much less vulnerable to salt-water contamination than the basal water downstream (Figure 6). Because this ribbon-like zone is narrow in most places, however, drillers targeting it run the risk of missing it, and thus striking either the downstream basal zone or the upstream supra-basal zone. Exploratory wells that are subsequently discovered to be in basal water, but which have been drilled to the relatively deep maximum recommended depths (CDM, 1982) for para-basal water, 40-50 ft (12-15 m) below mean sea level, may thus be set too deep to deliver optimal water quality in the basal zone. Boreholes inadvertently drilled on the upslope side of the para-basal zone, on the other hand, frequently produce "dry holes" where they have intercepted basement rock above sea level but missed the discrete pathways and localized subterranean impoundments in which supra-basal water resides.

Figure 7. Drilling exploratory well AECOM-11, 21 May 2010. Sites for new water wells should be selected where geologic conditions favor both high water quality and high rates of production.

The supra-basal zone, although it occupies some 20% of the aquifer, presents even greater challenges to drillers and developers than the para-basal zone. Historically, most attempts to find productive sites in it have been unsuccessful. On the other hand, when successful, wells installed in the supra-basal zone are, as noted above, invulnerable to saltwater contamination, and include some of the aquifer's most productive sources of high-quality water. (See Section 1.4.4.) Continuing improvements in our understanding of basement geology and flow routes of water along the interface with the basement will increase prospects for success in the supra-basal zone.

1.4 Historical Groundwater Studies and Development on Guam

Prior to western colonization most people on Guam lived in the south, where they obtained water from the many streams that form in the volcanic highlands. Habitable sites on northern Guam were confined mainly to coastal sites, where water was available from springs or shallow dug wells. The northern plateau has no inland sources of freshwater except for the modest spring flow issuing from the weathered volcanic rock of Mataguac Hill. With the advent of corrugated steel roofs, residents of Guam came to rely primarily

on rooftop rainwater catchments for household water needs. Electrification following World War II, however, made it possible to install wells on the northern plateau, which now produces 80% of the island's drinking water and supports the vast majority of its population. Today there are some 150 active water production wells in the NGLA being operated by Guam Waterworks Authority (GWA), the Navy, the Air Force, and private businesses (Bendixson, 2013).

1.4.1 Early studies and exploration

Exploration and installation of inland wells were first considered in the late 1930s when the US Navy funded an initial hydrogeologic survey of the island, conducted by H.T. Stearns (1937) of the US Geological Survey (USGS). Stearns' map (Figure 8), showing his estimate of the water table and a subsurface zone of basement from the Mataguac Hill to Mount Santa Rosa areas partitioning the northeastern and the central-eastern portions of the aquifer was the first attempt to describe a relationship between the basement and the water table. Development was forestalled, however, by the Japanese occupation during World War II. The first military wells developed in the north were the early Marianas-Bonin Island Command (MARBO) series in Yigo, the first being drilled in late 1944 following the liberation of the island by US forces.

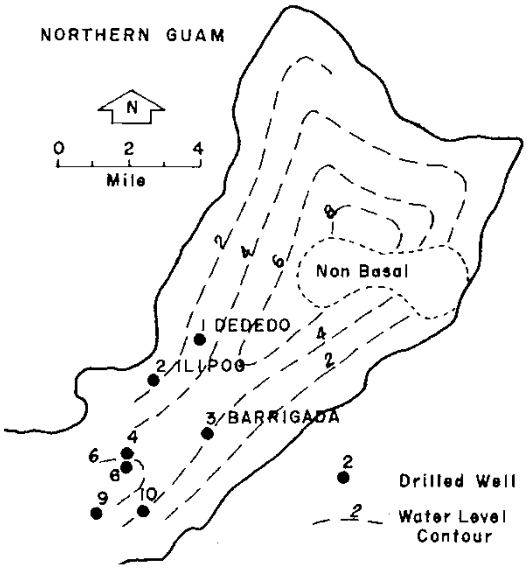

Figure 8. Early estimates of the water table and boundary of the Santa Rosa-Mataguac basement rise by Stearns (1937). Contour elevations in feet.

1.4.2 Post-war development

Following the war, Pacific Island Engineers (1950) investigated the possibility of developing water production wells in southern Guam (i.e., south of the Pago-Adelup Fault) but abandoned the effort because of inadequate production from the volcanic bedrock. In another early post-war study, Cloud (1951) concluded that the northern aquifer could be developed but expressed reservations about possible contamination from military and community sources. After some successful exploratory drilling, however, it was verified that economical amounts of potable groundwater could be produced in northern Guam. Concurrent with the comprehensive US Army-sponsored post-war study of the geology of Guam by Tracey et al. (1964), Ward and Brookhart (1962) and Ward et al. (1965) built on the previous works by Stearns and Cloud to produce more detailed reports on Guam's hydrology. Their preliminary map of the water table (Figure 9) shows a somewhat expanded estimate of the area of the basement rock standing above sea level.

As military installations were added or expanded over the northern half of the island, and as the local population increased, it became evident that additional resources would need to be developed. The government of Guam therefore undertook to develop the aquifer to

ultimately serve as the primary source of drinking water for the island. From the surviving drilling records, it appears that the first production well was completed in 1965, and that within five years 33 wells had been installed in the Hagåtña, Dededo, Mangilao, and Finegayan areas. During the early stages of development, well sites were selected primarily by their proximity to successful exploratory wells and established production wells. Expansion of the well fields was based primarily on the availability of government-owned land as well as proximity to roads and successful wells.

1.4.3 1982 Northern Guam Lens Study

In 1975, the Public Utility Agency of Guam (PUAG)[3] retained J.F. Mink to prepare a comprehensive report on the groundwater resources of Guam. Subsequently published as *Water and Environmental Research Institute of the Western Pacific*[4] *(WERI) Technical Report #1, Groundwater Resources on Guam: Occurrence and Development* (Mink, 1976), the report recommended prerequisites for successful exploration and proper management of the aquifer. For the reasons described above (Section 1.3.1) Mink noted that the single most important consideration for well siting was accurate knowledge of the topography of the volcanic basement.

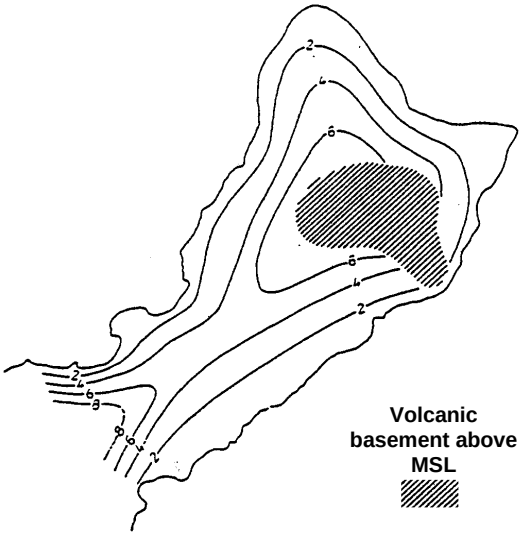

Figure 9. Subsequent estimates of the water table and boundary of the Santa Rosa-Mataguac basement rise by Ward and Brookhart (1962) and Ward et al. (1965). Contour elevations in feet.

Shortly thereafter, the Guam Environmental Protection Agency (GEPA), with federal support, commissioned the $1.2M *Northern Guam Lens Study* (NGLS). Directed by Mink, it was the first study to include broad-ranging, systematic, exploratory drilling and geophysical studies of aquifer hydrogeology. It remains the pivotal study, central reference, and starting point for aquifer research and development to this day. Among its products was the first detailed and state-of-the-art map of the basement topography, prepared by ECOsystems Management Associates from seismic refraction and gravity anomaly surveys, supplemented by lithologic and stratigraphic data from exploratory well logs and surface geology. Published as part of the NGLS report in 1982, it has served as the primary exploration tool for the past three decades (Figure 10, from Figure 3-3, Aquifer Yield Report, Plate 1, CDM, 1982). In a follow-up report made a decade later, Mink (BCG, 1992) made some revisions to the 1982 basement contours based on Time Domain Electromagnetic (TDEM) surveys performed on selected areas by Blackhawk Inc. (Hild et al., 1996). (See Section 3.2.6.)

[3] In 1997, PUAG was made an autonomous agency and renamed the Guam Waterworks Authority, GWA (Public Law 23-119, 31 July 1996).

[4] Previously *Water and Energy Research Institute of the Western Pacific.* The name was changed in 2000.

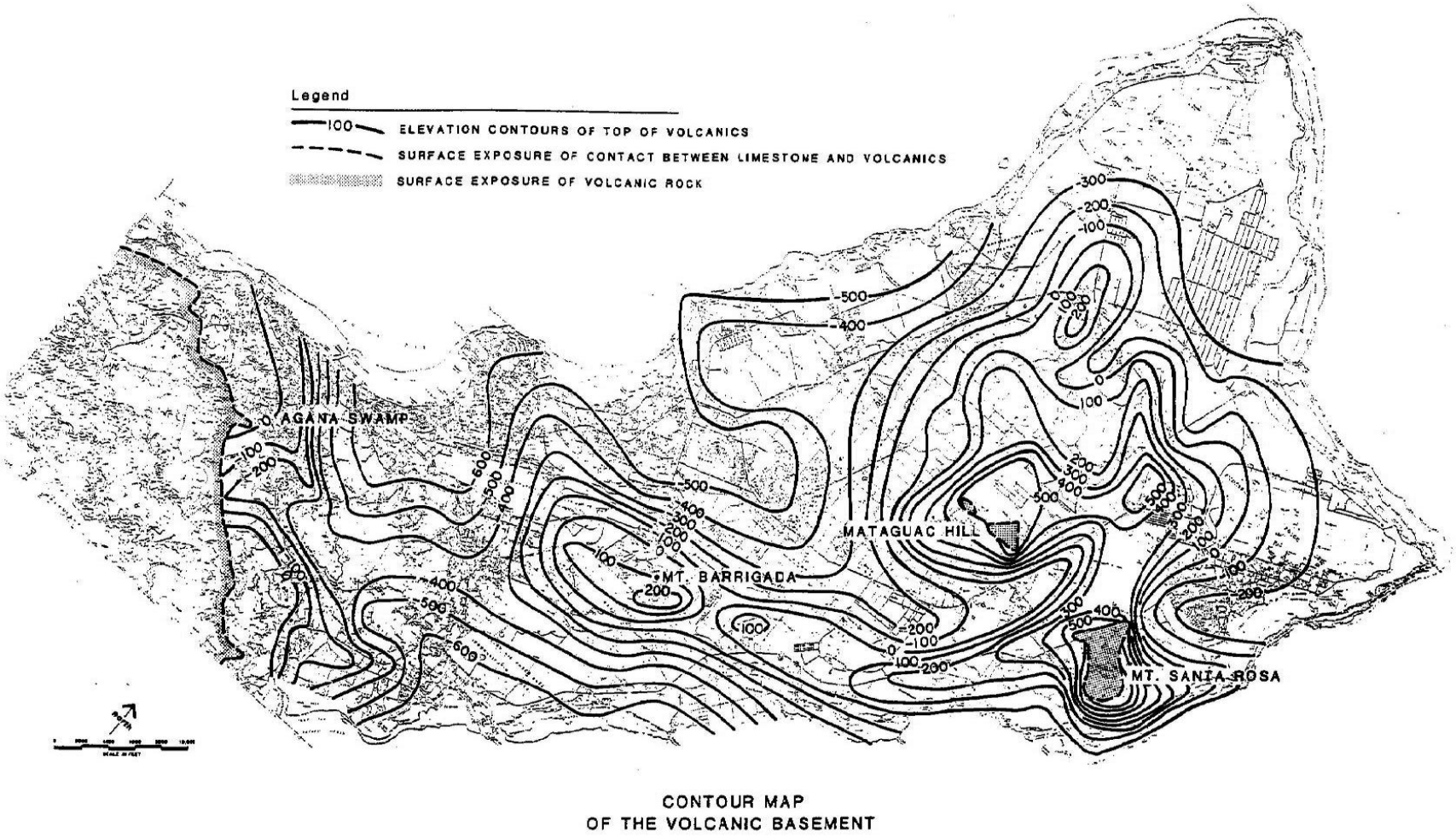

Figure 10. 1982 basement contour map from Figure 3-3, Aquifer Yield Report of the *NGLS*, based on Plate 1 of the report (CDM 1982). Contours in feet.

1.4.4 Applications of the 1982 Northern Guam Lens Study basement map

The 1982 basement map (Figure 10) provided planners, for the first time, with an empirical tool to support methodical development of groundwater in the NGLA. Equipped with the new map, developers subsequently made systematic attempts to exploit the para-basal zone in hopes of maximizing the prospect of finding high-yield, high-quality wells. From 1992 through 2000, some 68 boreholes were drilled, many of which were deliberately placed close to the sea-level volcanic contour of the 1982 map, targeting para-basal water (Appendix A). Twenty-six (~40%) of the boreholes drilled during this time, however, were "dry holes," i.e., boreholes that intercepted unproductive basement rock without encountering freshwater in the limestone bedrock. Some of these exploratory wells were deliberately drilled in the Yigo area (the "Y-series") well inside the 1982 sea-level contour line (Figure 11), in what is now called the supra-basal zone (AECOM Technical Services Inc., 2011). Most were unsuccessful, but the spectacular success in summer 1994 of well Y-15—which has produced very high quality water (<40 mg/l chloride) at 550-600 gallons per minute (gpm) (35-38 liters per second (lps)) ever since—prompted further attempts to develop more wells in this area. These attempts met with limited success, however. Five wells drilled to the southeast of Y-15 in the spring and summer of 1998 were dry. However, two successful wells—Y-17 and Y-23—were drilled in 1999, and continue to produce high-quality water.

By the late 1990s, limitations of the 1982 map were apparent—and new data were available to improve it. The 1982 map had relied primarily on geophysical surveys, with some verification and adjustments from a subset of the exploratory boreholes installed for the study. The NGLS, however, had been confined to non-military lands; hence the basement topography within military lands was poorly constrained. Drilling data obtained on the military installations in the 1990s from the *Installation Restoration Program* (IRP), along with new borehole data from the aggressive exploration by PUAG in the 1990s, prompted WERI in 1998-2000 to produce an updated map (Vann, 2000). Exploration and development slowed during the subsequent decade, however, and the map thus saw only intermittent use until interest in groundwater exploration was rekindled in 2010 by the US Naval Facilities Engineering Command Pacific (NAVFACPAC), which launched a new round of exploration in support of the anticipated military buildup on Guam (Joint Guam Program Office, 2010). The renewal of intensive exploration (AECOM Technical Services Inc., 2011), which was focused exclusively on military lands, has provided important new data precisely where the previous map had been least reliable and where new data were thus needed most. In support of the 2010 drilling program and concurrent USGS *Groundwater Availability Study* (Gingerich and Jenson, 2010), Vann (2010) prepared a preliminary revision of the sea-level contour, based on data available up to 2010 (Figure 11).

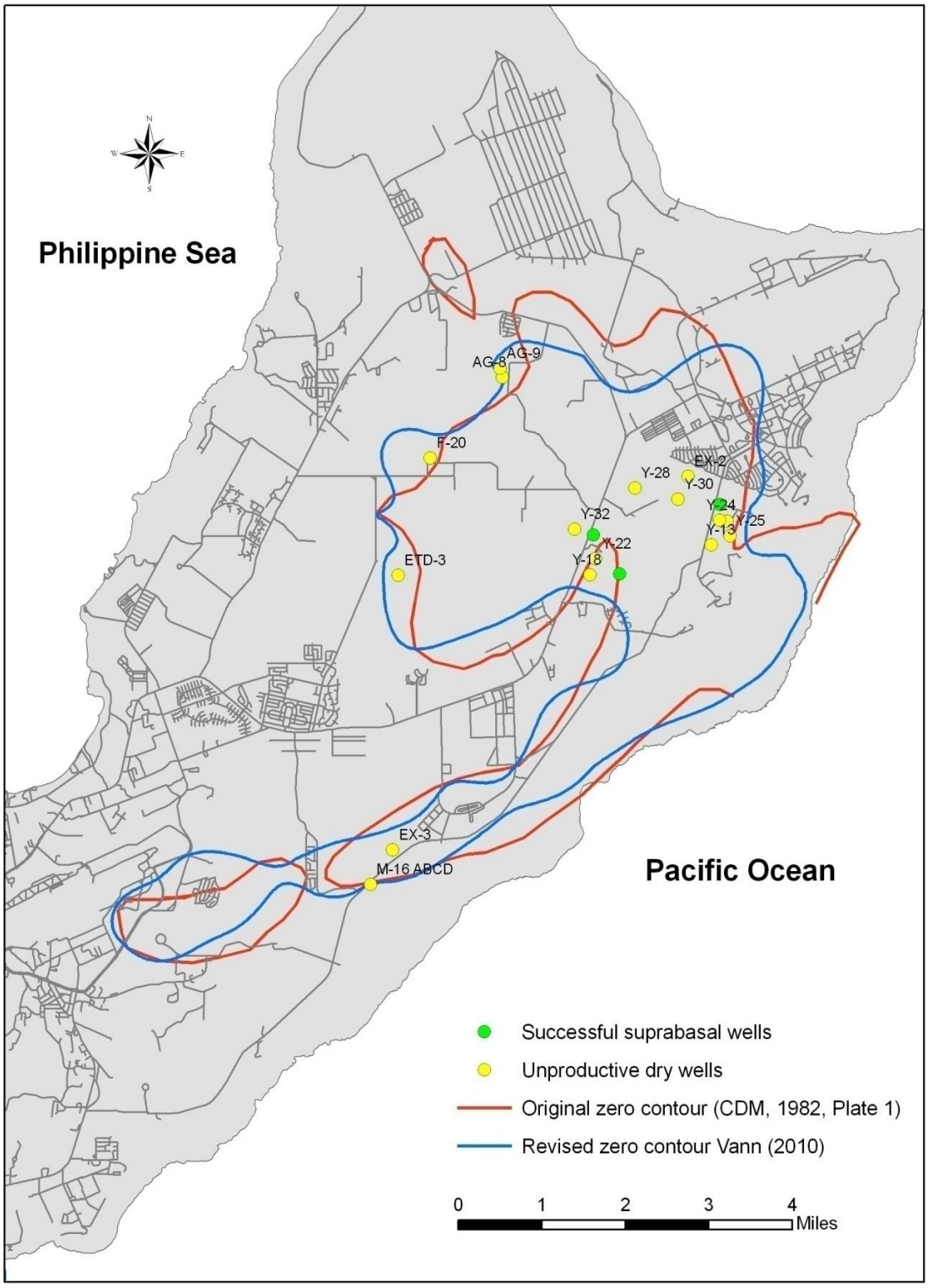

Figure 11. Revision of sea-level contours (Vann, 2010) to support the USGS Groundwater Availability Study (Gingerich and Jenson, 2010), based on 2010 data. Unproductive ("dry") wells (yellow) drilled in search of para-basal and supra-basal water, and successful supra-basal wells (green) drilled in the 1990s are shown, along with their proximities to the 1982 NGLS sea-level contour line (Figure 10, shown here in red) and the revised sea-level contour line (blue).

2 SCOPE & OBJECTIVES

We note below the scope of work and precise purpose of the map development project as well as the purposes of the map itself:

1. The purpose of this project was to produce an up-to-date, state-of-the-art map of the NGLA basement topography using all the relevant historical data that could be located, including the data associated with the 1982 NGLS and subsequent studies, and incorporating the latest data and insights on aquifer geology, up through those acquired most recently from the 2010 NAVFACPAC Exploratory Drilling Program.
2. The primary purposes of the map are to support and enhance 1) the success of groundwater exploration and development and 2) aquifer research, management, and protection. Meeting these objectives required, first, assembling a comprehensive, up-to-date database of the contact between the basement volcanic rock and the overlying limestone (Bendixson, 2013). Data sources included the historical data described above, with additional historical and new data obtained from the Navy Public Works Center (PWC), US Air Force 36th Civil Engineering Squadron (36 CES), GWA, USGS, and the Earth Tech Inc. (subsequently AECOM Technical Services Inc.) office in Tamuning, Guam (now closed). Geographical coordinates, surface elevations, and reported depths to non-carbonate materials, along with other relevant parameters, were extracted and consolidated into a single database, which also contains related data on the wells and the aquifer (Appendix B). The ultimate step was to generate digital Geographic Information System (GIS) coverages of the basement topography using state-of-the-art tools and methods.

3 METHODOLOGY

To build the new map we employed a systematic six-step process of comparative analysis building on Hunter's (1992) recommended systematic methodology for inferring surfaces for environmental applications from geospatial data (Figure 12):

1. Rigorously define the problem and develop a suitable conceptual model that incorporates practical definitions of its components and other relevant entities.
2. Select and consolidate useful data from the available sources classifying the data according to the types and quality of the data that are useable, and looking for clues as to which interpolation method may be most appropriate.
3. Assemble the data set that establishes the boundary conditions and internal control points for the interpolator.
4. Apply candidate interpolation methods that seem most promising for both the data set and the phenomenon being modeled.
5. Evaluate the interpolation results using descriptive statistics and professional judgment to select the most reliable model.
6. Edit the interpolated surface based on professional judgment and additional data that cannot be accommodated by the interpolator but which can help to more accurately and precisely constrain the final (modeled) surface.

3.1 Step 1—Definitions and Conceptual Model

To achieve a meaningful estimate of the basement surface from the available data requires first establishing an explicit and useful definition of what is to be mapped—in this case the bedrock-basement contact. The definition must thus be built on terms that serve the purpose of the project—in this case identifying the effective bottom of the aquifer, where the rock changes from permeable to practically impermeable, or in hydrogeologic terms, from aquifer to aquiclude. The next task is to develop a conceptual model (Figure 13) of the three operative components of the system—in this case the limestone bedrock, the volcanic basement, and the contact between them. The conceptual

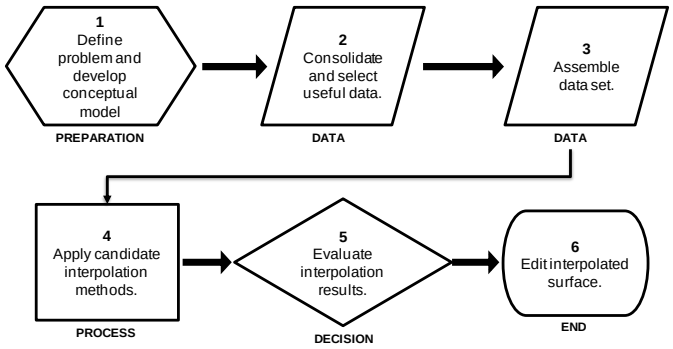

Figure 12. Six-step comparative analysis process (built from Hunter, 1992).

model provides the framework for organizing the data to estimate the spatial locations and properties of the components of interest—in this case the elevation of the bedrock-basement contact across the entire aquifer. The success of the analysis is dependent on both the accuracy of the conceptual model and the quality of the data set—where quality is defined in terms of accuracy and completeness of coverage (see Bendixson, 2013).

3.1.1 Defining and identifying the depth to the bedrock-basement contact

Experienced drillers know that ascertaining the depth to basement rock is not always straightforward. There have been no systematic geological studies of the contact between the bedrock and basement of the NGLA. Given what is known or can be inferred about the conditions of limestone deposition (Tracey et al., 1964; Siegrist and Randall, 1992) however, it is reasonable to assume that the non-carbonate material at the contact may vary from bare, unaltered "hard" volcanic rock, to altered, soft, saprolitic rock, to soft sediment covering either hard or soft rock. Observations and reports of the recovery of clay-like material clinging to drill bits, and blue-, gray-, or brown- colored drilling foam suggest that the contact is complex—layers of "dirty" limestone may be interlayered with volcanic rock fragments or sediment in some places (Figure 14). Occasionally, cuttings consisting of chips of hard volcanic rock indicate that the drill bit has unequivocally encountered relatively unaltered volcanic basement (although chips could also be derived from volcanic rip-ups above the contact). Such cuttings are usually only obtained when the drilling objective is actually to reach "hard" volcanic rock, as was done for a few exploratory wells of the NGLS (CDM, 1982). More often, when exploring for groundwater, drilling is terminated when the cuttings or foam recovered contain anything other than clean limestone. The depth to hard basement rock and thickness of the transition zone are thus rarely precisely known.

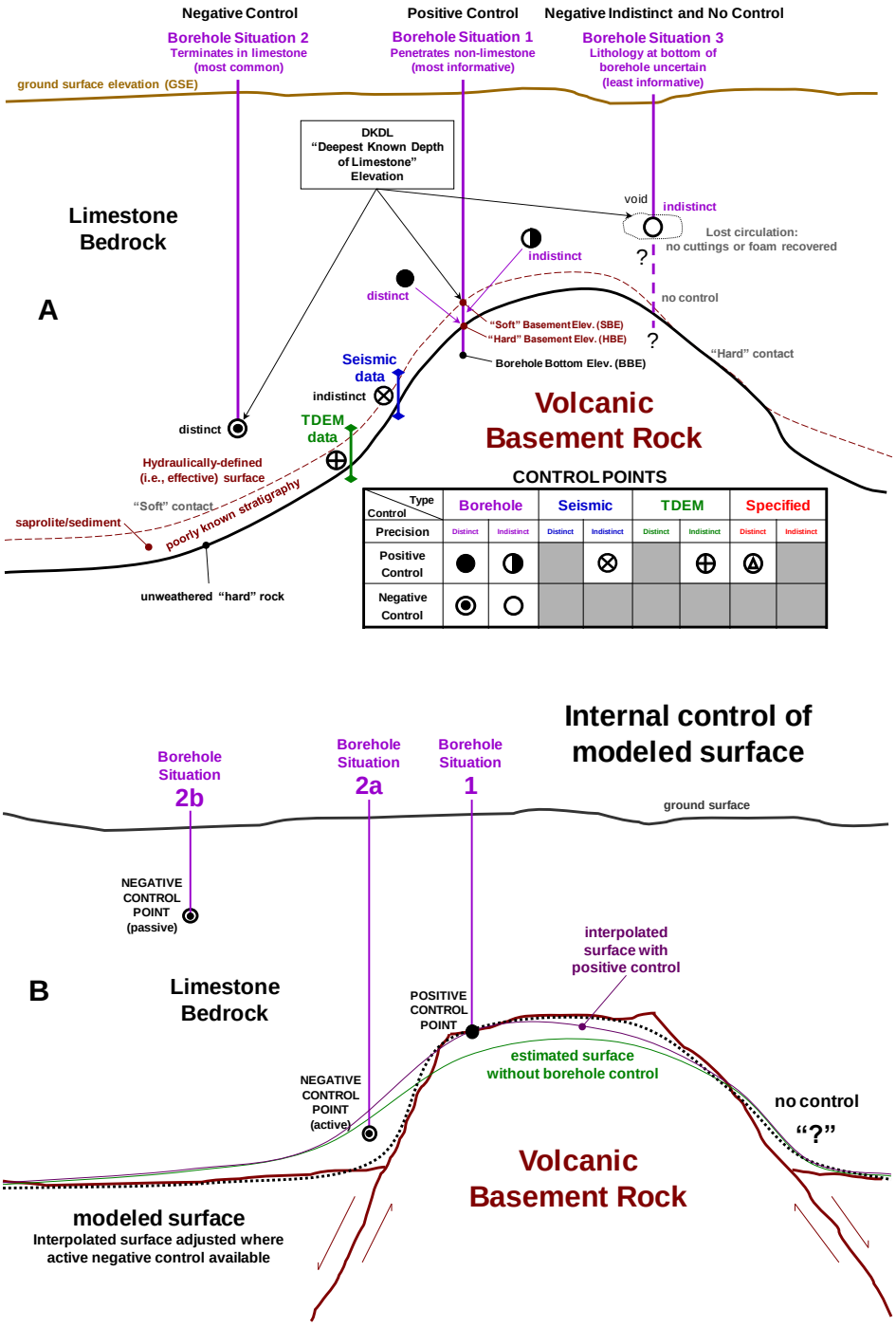

Figure 13. Concepts and terminology for modeling the bedrock-basement interface. A) Conceptual model showing 1) the kinds of contacts, 2) the types of internal data (i.e., data used inside the domain, as distinct from boundary conditions) used to constrain interpolations of the basement topography, and 3) symbols for the kinds of control and relative precision provided by each type of data. Distinct control points provide precise locations; indistinct control points provide approximate locations. The modeled (mapped) surface lies between the soft and hard contacts, given that the depth to basement for any given borehole may lie on or between either the soft or hard contact and cannot be precisely determined by geophysical methods. B) Positive and negative control concepts. The diagram illustrates how a surface originally estimated for a structural block exclusively from geophysical data might be adjusted to meet positive control constraints (situation 1) and then further refined where active negative control points are available (situation 2a). Passive negative control (situation 2b) refers to control points that provide certainty of minimum depths of limestone but do not contribute to modifying the interpolated surface.

3.1.2 Defining the basement surface

Given these uncertainties, the term *basement surface*[5] has meaning only if the geologic conditions used to define it are clearly specified—and there are of necessity some arbitrary aspects of any such definition:

- We define the basement surface as the contact marking the change from either solid limestone or unlithified carbonate sediment to *any* kind of non-carbonate material.

Given that the hydraulic properties of the contact itself and the rocks immediately above and beneath it may be spatially variable, we note that the stratigraphic boundary may only approximate the *hydrogeologic* boundary, i.e., the *effective* bottom of the aquifer, where the permeability of the rock, regardless of its composition, changes from very high to very low.[6] For clarity in discussion, we thus define *the basement surface* as the *hydraulically-defined surface*. We note that the hydraulically-defined surface is likely comprised of a complex patchwork of gradual, "soft" contacts and abrupt, "hard" contacts between carbonate rock or sediment and volcanic rock (Figure 13A).

Figure 14. Evidence of contact with basement. Saprolitic material clinging to the drill bit, recovered from bottom of AECOM-3, which was drilled to the basement contact. Photograph taken 6 December 2010.

It is important to keep in mind that buried geologic surfaces can only be estimated to various degrees of accuracy, given that actual positional data are only available at a limited number of *control points* (Figure 13A), from which the entire surface must be estimated. Between the control points, the surface can only be inferred or estimated, normally by some scheme of systematic interpolation. The reliability of the *estimated* or *interpolated surface* at any given point decreases in proportion to its distance from the nearest control points. Our objective in modeling the NGLA basement surface then, is to produce, from the necessarily limited, and less-than-ideal, data set an interpolated surface that matches the hydraulically-defined surface (i.e., the effective bottom boundary of the aquifer) as closely as current data and techniques allow.

[5] We also note here that in this context we are using the term "surface" in its mathematical sense, as "the boundary or portion of the boundary of a three-dimensional region. *Webster's Third New International Dictionary*, Unabridged. Merriam-Webster, 2002. http://unabridged.merriam-webster.com.

[6] Meso-scale geology and hydraulic properties at the contact are poorly known. Observations and results from drilling and geophysical studies (CDM, 1982), along with theoretical conjectures, however, suggest that the contact varies from sharp to gradational, and that limestone above the contact may in some places grade from pure, low-density, high-permeability limestone to argillaceous, high-density, low-permeability limestone. Locally, the contact itself may contain relict solution cavities and even contact cave networks. Although in general, the permeability of the volcanic basement is orders of magnitude lower than that of the limestone bedrock, it is conceivable that there could be some localities where the conductivity of higher-conductivity volcanic rock facies might approach that of lower-conductivity limestone.

The final step in modeling the basement surface, as noted above, is to manually adjust those portions of the interpolated surface that are inconsistent with data. The interpolated surface thus adjusted is the *modeled surface*. We note that the accuracy of the modeled surface can only be evaluated after the fact, by field testing—most precisely by drilling—which is expensive, and therefore seldom done. Use of the map must therefore be informed by a full understanding of the nature and limitations of the conceptual model, as discussed above, as well as the quality of the data and the techniques of interpolation. The types of surface defined above are summarized in Table 1.

Type of Surface*	Definition
Basement surface	A lithologically-defined imaginary or abstract surface constituting the contact between limestone bedrock above and basement volcanic rock below, which would presumably be marked in field sampling by a change from limestone or carbonate sediment to any kind of non-carbonate material, whether sedimentary or volcanic rock, soft or hard, fresh or weathered. It may also be marked by a discontinuity in geophysical parameters, such as seismic velocity, which is assumed to correspond to the lithologic boundary, but which may not be precisely contiguous with it.
Hydraulically-defined surface	The effective bottom boundary of the aquifer, where permeability changes by orders of magnitude from very high to very low. It must be inferred from the basement surface, and is expected to follow it, but need not be identical to it. The basement surface, drawn from lithologic data, should thus be regarded as a proxy for the hydraulically-defined surface.
Estimated or Interpolated surface	The surface drawn by the interpolation program using data that provide control points for the basement surface. It can only approximate the actual basement surface, which is positively identified only at certain control points. The terms "estimated" and "interpolated" refer to the same entity, but the former term is invoked to emphasize that the surface is approximate. The latter term is used to emphasize the process by which the surface is approximated.
Modeled surface	The final map, obtained after editing the interpolated surface to correct for discrepancies between the interpolated surface and known control points, and to incorporate additional control that could not be incorporated into the interpolation program.
*The term "surface" is used in two senses in this report: The first is with reference to the surface of the earth, as opposed to subsurface or subterranean entities. The second is with reference to surfaces in the mathematical sense, as "the boundary or portion of the boundary of a three-dimensional region."	

Table 1. Summary of definitions: terminology associated with the term "surface." See text for detailed definitions and explanations.

3.2 Step 2—Selection and Consolidation of Useful Data

Interpolated surfaces are built from a combination of *boundary conditions* and *internal control points* that pin the periphery and the surface inside, respectively, to known three-dimensional coordinates. Reliability of the estimated or interpolated surface is a function of the number, density, distribution, and reliability of boundary conditions and internal control points. We selected *four types of data* that we deemed reliable for the construction of the map:

1) Boundary conditions taken from our own field observations or other maps, including LiDAR (Light Detection and Ranging)-based digital elevation models (DEM)

2) Historical borehole data from municipal and military records

3) Seismic refraction data from the 1982 study (CDM, 1982)

4) TDEM data from the 1992 study (BCG, 1992)

Borehole data are the most accurate and precise data for internal control. It should be noted that although the more than thirty-year accumulation of borehole data since 1982 provided more than 120 points that had not been available for the NGLS map, borehole data—in contrast to geophysical data are typically "lumpy," or unevenly distributed. This follows from the fact that borehole data on basement topography are an incidental product of exploration, which tends to be targeted, rather than a deliberate product of systematic, broad-coverage, uniformly-distributed surveying. Geophysical data, on the other hand, while less accurate and precise, are obtained exclusively from systematic surveys with the express purpose of locating the bedrock-basement contact. Where borehole data are available they can provide ground truth for nearby geophysical data, and thereby "trump" geophysical data at or near the same location. Where borehole data are not available, however, geophysical data are the sole means of control. As explained in detail, below, where elevations of surface exposures of the basement rock could be taken or inferred from independent sources, such as elevations from LiDAR-based DEM, or depths from bathymetric maps, we utilized them as boundary conditions to provide additional control. Where no data were available to provide boundary conditions, we specified estimated basement elevations. For internal control, we gave priority to borehole data where available, but we retained the seismic data from the 1982 map and the TDEM data from the 1992 revision (Hild et al., 1996) to fill spatial gaps in the borehole data.

3.2.1 Data collection, screening, and evaluation

The new map is built from 24 boundary conditions and 148 internal control points selected from 529 borehole data records (Bendixson, 2013), 81 seismic points on the 1982 NGLS map, and 87 points on the 1992 TDEM survey (Table 2, Table 3, and Appendix B). Screening the data involved not only some preparatory steps such as converting and standardizing units or coordinate systems, but also required subjective judgments regarding the origin, accuracy, and utility of historical source documents. Such judgments included 1) interpretation of marginally legible, ambiguous, or contradictory documents, annotations, or comments; 2) selecting from among separate documents with conflicting or uncertain information; and 3) resolving apparent or suspected changes in well names or deviations from naming conventions. Among the source documents, we found records for different wells having the same or similar names, and records for the same well having different names, sometimes with the same date and sometimes with different dates. Prioritizing our work on the more difficult cases required assessing the relative value added for each unit of effort. Some of the more difficult records were therefore temporarily set aside and revisited after simpler questions were resolved; some were permanently set aside as unresolvable.

The sections below describe in detail the classifications and priorities assigned to the data used to build the map (Appendix B). Each type of data has its own quality criteria considerations. Although borehole data are in general the most definitive, the interpretation of field samples—much less of historical drilling records—is not always clear cut. Moreover, as explained above (Section 3.1) borehole data can place the defined surface for the basement at any depth from the top to the bottom of the "soft" basement layer (i.e., between the dashed and solid lines in Figure 13). The "surface" as defined by borehole data must therefore be thought of as actually a rind-like zone of variable

thickness. It is also apparent that the "soft" surface defined by borehole data, i.e., the shallowest depth at which the lithology differs from limestone—which is the borehole data criterion for the modeled surface—may be different from the depths of the discontinuities that define the "depth to basement" for seismic and TDEM techniques.

Thus, the different types of data can provide different elevations for control at a given point. Where more than one type of data are available for a given area, some judgment is required to select the most reliable data for that area. It should also be noted that even for each type of data, reliability may vary from one location to another. In the case of borehole data, it is sometimes impossible to determine the lithology of the materials reported on the log, especially the older logs. Some logs provide precise coordinates and depths; others do not. Moreover, while the most useful data provide positive information for the elevation at which the surface is likely to be located, other data only provide negative information as to where it is *not located*. Across the four selected types of data, we therefore apply two cross-classifications: one to designate the *kind of control* provided by it, and one to designate the *precision of the data* (Figure 13):

1. Classifications by the kind of control:

   a. Positive control. Data that provide positive empirical evidence for the location of the basement contact, regardless of the type and whether relatively precise (distinct) or imprecise (indistinct) are said to provide positive control (Figure 13A, Borehole Situation 1). Positive control points are the "pinning points" from which the rest of the modeled surface is interpolated (Figure 13B). Ironically, most of the most reliable positive control points are the result of unsuccessful exploratory attempts to locate para-basal or supra-basal water, in which the borehole encountered non-carbonate rock above sea level, without first intercepting economical water.

   b. Negative control. More commonly, wells set successfully in the para-basal or basal zones terminate in limestone, mostly at depths of 50 ft (15 m) or shallower. Although such wells do not provide information on where the basement contact is, they do provide limited information as to where it is *not*. Borehole data that establish with certainty an elevation above which the basement cannot be present can be said to provide negative control for the basement surface by providing a minimum depth (thus, maximum elevation) to constrain the estimated surface (Figure 13B).

2. Classifications by the precision of the data:

   a. Distinct points are those for which the source records indicated a sharp and distinct boundary, which we defined as having been measured to a precision within a few feet:

      1) Wells or boreholes terminating in non-limestone material where the terminus elevation can be determined to be within a few feet provide distinct positive control.

2) Wells or boreholes terminating in limestone where the terminus elevation can be determined to be within a few feet provide distinct negative control (Figure 13A, Borehole Situation 2).

b. Indistinct (low-precision) points are those which define an order-of-magnitude less precise range of possible values (i.e., a few 10s of feet). These include depths defined by geophysical techniques (i.e., seismic and TDEM), and depths defined by boreholes in which the onset of the contact was too gradual to be determined within a few feet, or where the lithology at the bottom of the borehole could not be determined because no cuttings were returned.

1) Wells or boreholes terminating in non-limestone material where the terminus elevation can only be measured to precision within a few tens of feet provide indistinct positive control.

2) Wells or boreholes that encounter bedrock voids large enough to intercept all of the drilling fluid, so that no foam or cuttings rise to the surface, are said by drillers to have "lost circulation." Such wells can only provide indistinct negative control at the depth of the void; even if the depth to the ultimate bottom of the borehole (beneath the void) can measured precisely, the lack of recovered cuttings or foam precludes identification of the lithology beyond the depth of the void (Figure 13A). When circulation is lost, drillers and geologists may have to rely on secondary—and uncertain—clues such as penetration rate and rig chatter to estimate the depth of the contact.

3. Active vs. passive negative control. Finally, within the classification of negative control, we distinguish between *active* and *passive negative control* for the interpolated basement surface:

a. Active control. Where the initial interpolated surface is at a higher elevation than a negative control point, and therefore must be adjusted in the vicinity of the point to eliminate the inconsistency, the negative control point is said to provide *active* control.

b. Passive control. Negative control points with elevations higher than the initial interpolated surface do not mandate adjustment of the interpolated surface, and are therefore said to provide *passive* negative control for the surface.

The table at the bottom of Figure 13A shows the map symbols that have been developed to identify the various types of data and control points. Users of the map and database can thus make informed judgments regarding the reliability of the map and considerations that may apply to its use for a given project in a given area.

3.2.2 Additional data quality considerations: measurement error in borehole data

Anyone experienced with drilling and with interpretation of historical drilling logs is aware that determining the depth to any given feature (whether water table, cave, or any other geologic feature) is fraught with a number of possible errors and uncertainties. The most familiar source of error is in the survey measurements of ground surface elevation, the identification of the measurement point (i.e., starting point) for down-hole measurements (e.g., whether the top of a constructed well head or the concrete apron around the well), and mismeasurements due to stretching or misreading of down-hole measuring tapes and probes. These kinds of errors are difficult to detect and correct, especially in historical records. Moreover, depths reported by drillers are often actually estimated by the length of the drill rod above the ground surface and the number of drill rods in the hole—precision is inherently limited.

For obvious errors to which corrections could confidently be made, we made the corrections and noted them in the *NGLA Database* (Bendixson, 2013). Data which were suspect (and for which there was no reliable basis for correction) were set aside and excluded from the data set used to build the map (Appendix B). Given these considerations, users of the map should also bear in mind that there could still be some undiscovered errors in assigned basement elevations arising from inaccuracies or errors in surveyed reference points, reported wellhead elevations, or logged depth measurements. If high precision is needed or apparent discrepancies arise at any particular location, the source documents (see the *NGLA Database*) should be examined—and the age, technology, and other factors that may bear on reliability of the documents taken into account.

3.2.3 Data Type 1: Boundary conditions

Boundary condition information was mainly gleaned from other maps and data sets. Bathymetric depths from the geologic map (Siegrist and Regan, 2008) provided approximate control beyond the perimeter. LiDAR data provided elevations with ±1 m (3.28 ft) control for the surface expression of the basement unit (Alutom Formation). Where there are insufficient data to provide control for the interpolated surface, it was necessary to apply specified boundary conditions to provide at least a realistic "best guess" for local basement elevation. Boundary conditions were thus employed as follows:

1. *Bathymetry*. Seventeen bathymetry points were used from the nearby ocean floor around northern Guam (USGS, 1978) to provide the interpolator with first-order regional-scale boundary conditions.[7] (See Section, 4.1.2(4).) Such points, of course, provide only rough approximations for actual elevations for the basement rock (Alutom Formation). However, given their relatively large distance from the coast compared to the scale of vertical interpolation along and inside the coast, the approximation provides suitable boundary control for the interpolation algorithm.

[7] Only 15 are shown on the map, however; two are south of the area shown on the map.

2. *LiDAR data*. The summits of Mount Santa Rosa and Mataguac Hill were taken from a DEM derived from LiDAR data.

3. *Specified boundary conditions—Central east coast and Pago-Adelup Fault*. Due to the absence of basement topographic data along the central east coast, interpolators tend to unrealistically extend the zero-contour seaward beyond the base of the coastal cliffs. The cliffs along this eastern flank and the relatively narrow carbonate terrace at the base help provide natural constraints on this boundary, and there are reliable anecdotal reports (Richard H. Randall, personal communication to Jenson, December 2012) that volcanic rock is actually exposed in small caverns at sea level within this segment of the eastern coast of northern Guam. These are too small to map, however, and are accessible only rarely, when the trade winds are weak and surf from the Pacific Ocean is calm. Five points were specified along this coast to realistically, if approximately, constrain the interpolation. A sixth point (MS Springs) was also used south of the Pago-Adelup Fault.

Type of boundary condition	Number	Sources
LiDAR-based DEM	2	LiDAR summits of Mount Santa Rosa and Mataguac Hill
Bathymetric soundings	17	Geologic maps: Tracey et al. (1964); Siegrist & Reagan (2008)
Specified boundary conditions	5	Inspection and personal field reports (see text)
TOTAL	24	

Table 2. Summary of boundary conditions and sources.

3.2.4 Data Type 2: Well log borehole data

The ideal technique for determining the precise depth and characteristics of the bedrock-basement contact would be to cut and extract continuous, intact rock cores through the contact. For obvious reasons, such work is extremely expensive and therefore done only for highly specialized and well-funded research projects. The next best technique is ordinary drilling in which descriptions of drilling cuttings arriving at the surface are recorded and correlated with the depth of the drill bit as the cuttings arrive. Such drilling logs provide a means of estimating the maximum depth (or equivalently, minimum elevation) from which the cuttings were obtained. Because the drill bit descends much more slowly than the rate at which drilling foam (carrying the cuttings) ascends to the surface, however, it is usually assumed that the difference between the measured (logged) depth and the actual depth from which the cuttings came is no more than a few feet. As noted above (Section 3.2.2), however, even this degree of precision in estimating the depth of the contact can be further limited by additional uncertainties, including especially the driller's interpretation of the cuttings, or the subsequent reader's interpretation of the drilling log. Nevertheless, drilling logs, despite these limitations, provide the only direct—and the most reliable—data from which to infer the depth to the contact. We therefore invested substantial effort in finding and consolidating all of the historical and current drilling data that could be acquired.

From 1998 to 2000, WERI collected copies of over 170 well logs for historical and active wells from various sources on Guam (Table 2) with the objective of updating the 1982 basement map (Vann, 2000) (Section 1.4.4.). Recently, these and over 350 more well descriptions have been assembled, digitized (scanned), and consolidated into the *NGLA Database* (Bendixson, 2013):

1. From this dataset, we identified logs from 65 sites at which we could confidently infer that the boreholes reached non-carbonate material and which also contained sufficient information to reliably locate the boreholes with sufficient accuracy to be useful for the map.

2. Three drilling logs contained reports of non-carbonate materials having been recovered, but could not be used because the depth of recovery or the location of the borehole could not be determined.

3. Most recently, in 2010, AECOM Technical Services Inc. drilled 11 new exploratory wells (summary at Appendix C). One of them (AECOM 3), in the Agafa Gumas Basin, was purposely drilled to basement, as the well was planned to be an observation well.

4. A second exploratory well, AECOM 8, in the MARBO area, encountered volcanic rock where the earlier map estimated it would be considerably deeper. As noted earlier, the exploratory drilling program provided new data in areas where it was most needed for improving the accuracy of our knowledge of the topography of the bedrock-basement contact.

Given that most drilling is done to install production wells, the vast majority of drilling logs contain no information regarding the location of the basement contact because production wells are purposely drilled only to relatively shallow depths (generally less than 50 ft or 15 m) below the water table, and the drillers seek to avoid basement rises and ridges, where they are known. While for mapping the basement the value of knowing the depths of boreholes terminating in limestone is limited to verifying only that the basement surface does *not* reach the given elevation at the given location, such information can be of high value where there are no other data to test or verify the accuracy of the interpolated surface. In this revision of the map, we applied 136 boreholes that terminated in limestone and revised the interpolated surface around 16 points at which the bottom of the borehole terminated in limestone *below* the initial interpolated surface. (The applications of negative control points are described in Sections 3.5.3, 4.1.2(6), and 4.1.2(12).)

3.2.5 Data Type 3: 1982 Seismic refraction data

The primary data set for the 1982 map was the seismic refraction data obtained from the survey conducted by ECOsystems Management Associates (Section 1.4.3). Mink (1982) reported that 56 refraction profile lines were run. Some 51 of the seismic profile lines appear on the 1982 map. However, Mink reported that 18 to 27 of the 56 lines (depending on interpretation) did not refract from basement; where depth to basement was greater

than about 500 ft (150 m), the survey could not discriminate the volcanic rock. Mink also noted some important discrepancies discovered in the application of the seismic data to the 1982 map. Specifically,

> "…in several instances, the higher range of velocity in the limestone overlaps the lower velocity range of the volcanics so that judgment based on other factors must be exercised in selecting depth to basement. This is particularly the case in the Dededo well field area where the depth to basement rocks, as determined from the seismic survey, does not coincide with well data. Here seismic profiles indicate an elevation of volcanics on the order of 200 to 250 feet above sea level where several wells in the area penetrate limestones to the elevation in excess of 50 feet below sea level. This inconsistency can be explained in two ways: the subsurface topography of the volcanics is extremely rugged, or what has been interpreted as volcanics is actually a third layer of limestone with a seismic velocity equivalent to that of volcanics."

Accordingly, the map at Appendix D shows (red circles) where the seismically-determined values are substantially different from observed elevations based on nearby borehole data, as noted by Mink. Of the four sites shown in Appendix D, seismically-derived basement elevations were off by 130 ft (40 m) to almost 500 ft (150 m).

We therefore employed geospatial tools to compare basement elevations inferred from 1982 seismic data against elevations determined from subsequent borehole data. From the 81 control points that Mink derived from the 1982 seismic lines, we excluded 38 points shown to be unreliable by the subsequent borehole data, retaining 43 of the 1982 seismic points. We note that the seismic profiles, though better distributed than the boreholes, were of necessity collected only where roads provided access, and that coverage of the military reservations was excluded (except along the perimeters). Nevertheless, seismic data from the 1982 map continue to provide the only elevation data for basement rock in areas where borehole data are lacking. This is generally along the perimeter of the plateau, where drilling data are most sparse—and, it should also be noted, where the basement is the deepest and the seismic data consequently least accurate.

3.2.6 Data Type 4: 1992 TDEM data

A decade after the 1982 study, PUAG retained Blackhawk, Inc. to conduct a TDEM survey of areas targeted for exploration (Hild et al., 1996) (Appendix E). TDEM surveying is based on detection of induced currents in subsurface materials of varying resistivity. The altered volcanic rock at the top of the basement contains large amounts of conductive clays, which promote low resistivity. Freshwater-saturated limestone has higher resistivity than the volcanic rock, but saltwater-saturated limestone, on the other hand, tends to have lower resistivity than the volcanic rock. There is thus some overlap between the resistivity of saltwater-saturated limestone and altered volcanic rock, so TDEM cannot always discriminate between them. As noted in the Blackhawk report, however, saltwater-saturated rocks do not occur above sea level, so reliable discrimination can thus be made between freshwater-saturated limestone and altered volcanic rock above the bottom of the freshwater lens.

The TDEM data were collected to prospect for water in four zones of interest over northern Guam (Appendix E): the west flank and northwest flank of the Mataguac Rise (Swamp Road and Machananao), the head of the Yigo Trough (north Yigo), and the north

flank of the Santa Rosa Rise (Lupog). For the present study, we compared the 1992 TDEM elevations against nearby data from boreholes drilled during the past two decades and accordingly selected 23 TDEM data points for positive control over these four areas. Where there were substantial differences between the borehole and TDEM values, we removed the TDEM values from our dataset. Table 3 summarizes the sources and disposition of the data as discussed above. Table 4 summarizes the types and quality of data selected and applied as control points.

Data Type	Data Source	Disposition of screened data							Total screened each source
		Positive control			Negative control				
		Applied Active	*Set aside	Total screened	Applied		*Set aside	Total screened	
					Active	Passive			
Borehole data from *NGLA Database* (Bendixson, 2013)	PUAG EarthTech GWA	**32**	2	35	**9**	96	36	140	175
	Navy (including AECOM)	**2**	0	2	**3**	7	24	34	36
	AF (including IRP)	**16**	0	16	**0**	10	191	201	217
	Guam Hydrologic Survey	**2**	0	2	**4**	6	12	23	25
	Private	**3**	0	3	**0**	0	32	32	35
	Unknown	**9**	1	10	**0**	0	31	31	41
	Total	**65**	3	68	**15**	120	326	461	529
Seismic	1982 Map	**45**	36	81					81
TDEM	1992 Map	**23**	64	87					87
TOTAL	All sources	**132**	103	236	**16**	120	326	461	697
					136				

*Reasons for setting aside data include missing attributes, missing drilling log, lithology not discernible, data-rich area in which additional data are redundant or unnecessary, or data disagree with borehole data (the last reason is applicable to seismic and TDEM only). Bold underlined numbers are active internal control points applied to construct the mapped surface. (See Tables Table 1 and Table 4.)

Table 3. Summary of internal control data: sources and disposition of all data screened.

Control \ Type	Boundary Conditions		*Internal Control						Total
			Borehole		Seismic		TDEM		
Precision	Distinct	Indistinct	Distinct	Indistinct	Distinct	Indistinct	Distinct	Indistinct	
Positive Control	24		46	19		45		23	157
Negative Control			15						15
Total	24		61	19		45		23	172

*All internal control data, whether positive or negative, disinct or indistinct, are applied, active (see Table 3).

Table 4. Summary of active applied control points.

3.3 Step 3—Assembly of the Dataset

With reliable data thus selected and classified, the next step was to *assemble the dataset* to be used for interpolation of the basement surface, and then *prioritize* the various components of the dataset according to the expected value-added that each might contribute toward achieving a reliable model of the basement surface, (i.e., its expected contribution to the reliability of the product for each unit of effort expended in its implementation). "Hard cases" were set aside for later attention. Dataset assembly, as discussed in detail below, is necessarily iterative: *preliminary interpolations* must be undertaken on *provisional datasets* to identify gaps or uncertainties, which then dictate which of the set-aside "hard cases" warrant additional pursuit, or whether some other approach might better be taken to resolve or accommodate important uncertainties. The data selection and assembly processes and their outcomes are summarized in Figure 15.

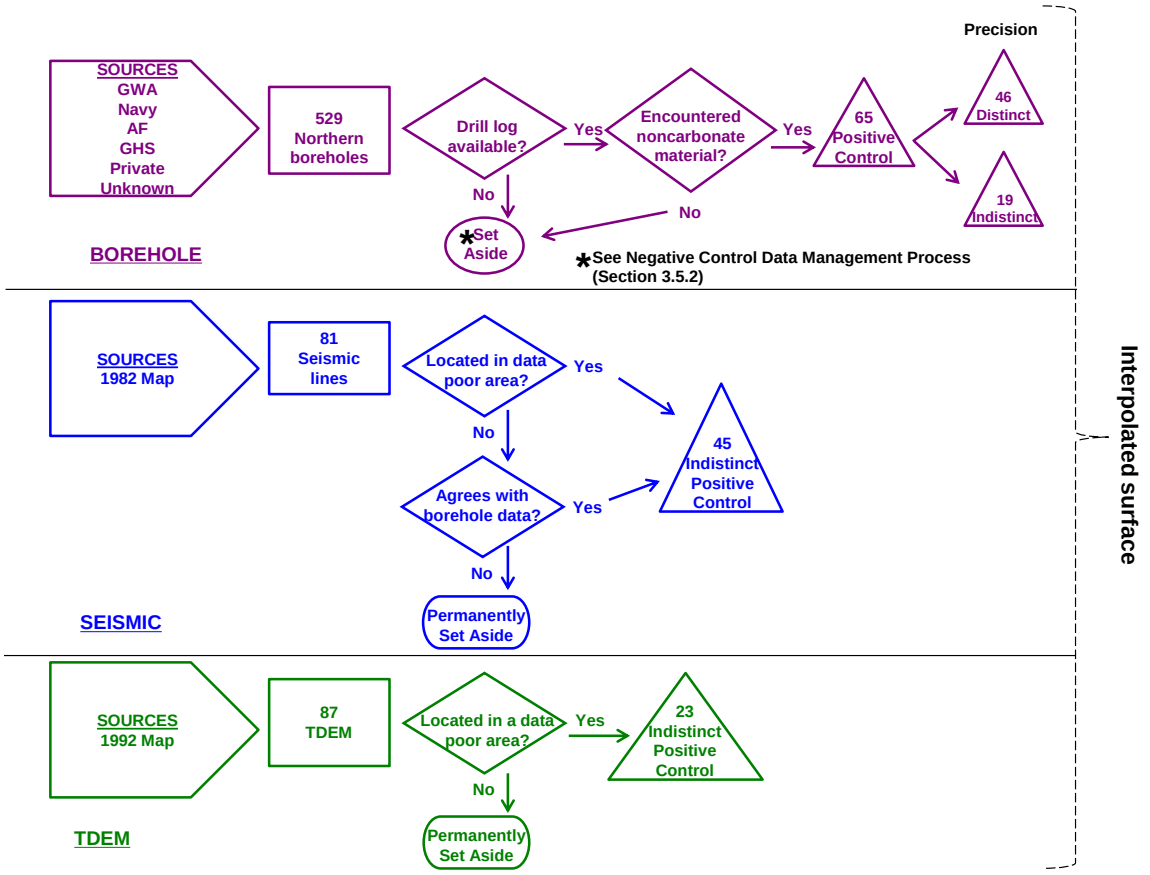

Figure 15. Data selection and application processes for positive control points.

3.3.1 Provisional boundary conditions and internal positive control points

Whether boundary conditions are sufficient at any given sector of the boundary cannot always be determined before running the interpolator. In certain cases, it is only after the first interpolated surface is produced that it is possible to discern where the interpolated surface is insufficiently constrained. It is thus necessary to specify *provisional boundary conditions*, run the interpolator, evaluate the surface produced by the model, and then specify additional boundary conditions as needed or, where the boundary is complex, manually modify local basement topography to conform with the available boundary data

and other geologic features (e.g., faults or surface morphology) that provide clues for more precise or realistic placement of the boundary. (See Section 3.5.)

In assembling the dataset, first and second priorities are given, respectively, to provisional boundary conditions and distinct internal positive control points (Figure 13 and Section 3.2). Selection of provisional boundary conditions usually requires some subjective judgments. Typically, boundary data are available only in limited areas, as noted above in Section 3.2.3. Moreover, in some of the places where they are known, the details may be too fine or complex to incorporate in the initial run for an interpolator. Application of the boundary conditions is therefore necessarily iterative: Where sufficient but nevertheless simple boundary conditions are available, they are incorporated in the initial data set to provide positive control at or near the boundary.

As noted in Section 3.2.4 (and shown in Figure 13A) *the only data that can provide distinct internal positive control are from drilled wells with reliable drilling logs.* Reliable logs are defined as those from which one can reliably discern surface elevation, total drilled depth, and depth at which non-carbonate materials (defined as the surface of the basement; see Section 3.1.2) were encountered. The elevation at which non-carbonate material was encountered was based on our own interpretation of the drilling log and the surface elevation reported on the drilling log. (Resurveying of well sites to obtain missing data or evaluate suspect data was beyond the scope of this project.) For sites where a measured surface elevation was not reported on the drilling log or other reliable historical documents, we assigned a surface elevation taken from a LiDAR-based DEM, and validated it by checking for consistency with reported elevations for surrounding sites. (See Section 4.1.2.)

The next priority is given to *indistinct positive control points* (Figure 13A). These include, in priority order, 1) drilling logs with indistinct reported depth to non-carbonate materials, 2) seismic lines, and 3) TDEM data. Where any of these three types of data conflicted with one another, seismic values were employed over TDEM, and borehole values were employed over either of the other two. Where interpretation of a drilling log was not straightforward, a subjective judgment was made of the most likely depth to the defined surface, and noted in the *NGLA Database* (Bendixson, 2013). In cases where such judgments could not be made with reasonable confidence, the data point was set aside. The positive control points were the principal means of spatial control for interpolation. Once the full set of positive control points, both distinct and indistinct, was selected, a set of *candidate estimated basement surfaces* was generated by the selected interpolation methods.

3.4 Steps 4 & 5—Application and Selection of Interpolation Methods

To generate a continuous surface for a spatially-distributed property (basement elevation, in this case), an appropriate interpolation method must be selected to estimate surface elevations between the control points. Selection of the most suitable interpolation method depends on the study objectives and on how the property represented by the control points varies between them (Mitasova and Hofierka, 1993). Factors that should be considered include the texture of the surface (e.g., whether smoothly or discontinuously

varying, and the scale of variance, or "ruggedness"), the distribution of control points (i.e., whether systematic and uniform, or random and "lumped"), the accuracy of the data, and the magnitude of error inherent in the various types of data (Hu, 1995). For this study, the lead author (Vann) rigorously evaluated three different interpolation algorithms to model the basement surface, 1) spline with tension, 2) kriging, and 3) inverse distance weighting (IDW).

Spline algorithms estimate values using a mathematical function that minimizes overall surface curvature, resulting in a smooth surface that passes exactly through the positive control points. This method is generally regarded as most appropriate for smoothly varying properties such as topographic elevation, water-table depths, or dissolved contaminant plumes (Childs, 2004). Kriging and IDW are similar in that they weight the surrounding measured values to derive a prediction not only according to the distance between the measured points but also considering the overall spatial arrangement among the measured points. IDW assumes that things that are close to one another are more alike than those that are farther apart. To predict a value for any unmeasured location, IDW will use the measured values surrounding the prediction location. Those measured values closest to the prediction location will have more influence on the predicted value than those farther away. These techniques are thus more suitable for modeling properties that inherently have sharp or discontinuous gradients.

To compare the three interpolators and provide a basis for selection, *cross-validation* (ESRI, 2003) was performed using identical data sets and equivalent modeling parameters for each. Cross-validation sequentially omits a point, predicts its value using the rest of the data, and then compares the measured and predicted values. The objective of cross-validation is to help the modeler make an informed decision about which model provides the most accurate predictions. For a model that provides accurate predictions, the mean error should be close to zero and the Root Mean Square Error (RMSE) should be minimized. Figure 16 shows the comparative results between the three interpolators. Based on the results using ESRI Geospatial Analyst, spline with tension was chosen over the other interpolators to generate the contour lines and surfaces for this study. ESRI Spatial Analyst was used to generate the raster surfaces.

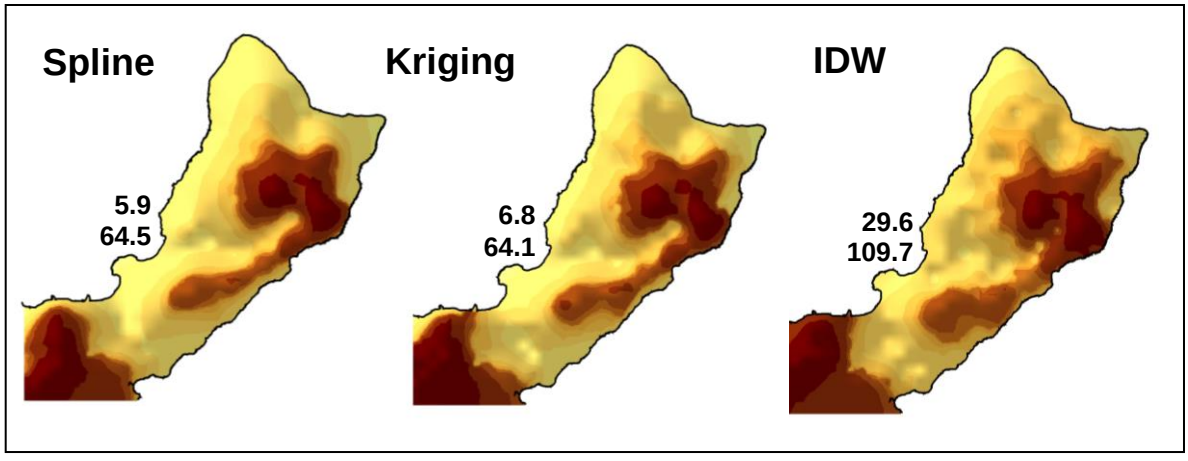

Figure 16. Interpolated surfaces, with mean error (top) and root-mean-square error (bottom) in meters for each.

3.4.1 Limitations and considerations in modeling the basement surface

The relatively large 65-m RMSE (Figure 16) reflects the fact that the most poorly controlled elevations of the basement surface are the deepest. This mainly reflects the gaps and clustering of the control points and most especially the paucity of positive control points along the perimeter of the plateau. The interpolator must predict depths everywhere within the 102-mi.^{2} (264 km^2) plateau from only 173 non-uniformly distributed points and over depths that reach more than 3,300 ft (1000 m). The great majority of control points are concentrated around the relatively shallow and spatially confined sea-level flanks of the basement rises and ridges. There is thus reason to place higher confidence in the interpolated surface within the shallower contour lines (down to ~60 m) than is implied by the 65-m RMSE calculated from the entire dataset. Fortunately, for most applications of the map, it is these shallowest and most well-controlled areas that are of greatest interest.

It will not be possible to improve substantially on the RMSE or any other statistical measures of accuracy and reliability of interpolation without a broader, more uniform, and higher density network of positive control points acquired by systematic drilling or geophysical exploration. The most comprehensive exploration program to date (the 1982 NGLS) is now over 30 years old, and included only sparse coverage of the military installations, which occupy a large portion of the plateau and contain an even larger proportion of the undeveloped groundwater reserve. The military IRP drilling and PUAG exploratory drilling programs of the 1990s were focused on specific and limited areas, and although the data provided are useful, they do not provide full coverage of the aquifer. The present study has the additional benefit of new data from the 2010 Navy-funded exploratory drilling program (AECOM Technical Services Inc., 2011), which fortunately was focused on military lands, where exploration was most needed, but which nevertheless covered only parts of the data-poor areas of the aquifer.

3.5 Step 6— Editing the Interpolated Surface: Corrections and Refinements

After a suitable computer-generated surface has been selected as described above, it is proofed and checked for errors or anomalies. The entire interpolation is systematically re-examined and validated against the control data (i.e., control-point type, coordinates, and DKDLE elevations), as well as against maps and images of surface terrain, geology, and infrastructure. Where unrealistic results or obvious anomalies have occurred, the associated data are checked, and either verified or corrected. Field verifications may be required in some cases. If a portion of the computer-generated interpolation is discovered to have been incorrectly or inadequately constrained, the interpolation program may be re-run after making corrections or additions to the relevant control points (e.g., correcting or adding boundary conditions, control points, or elevation-offsets from negative control points). Even if the computer-generated interpolation is generally valid, however, it may still be improved by manual refinements in locations where additional data allow more accurate or precise interpretations. Where sufficient control points are available to justify a specific, and presumably more reliable, re-interpretation, manual refinements are indicated by *yellow* highlights on the basement elevation contours. Where too few controls points are available to support computer-generated interpolation, we have made manual refinements to provide provisional hypotheses for basement topography. These

remain poorly constrained, however, and are thus marked on the map with dashed-line contours and a question mark ("?"). (See Section 4.1.2.) *The edited (i.e., corrected and refined) topography constitutes the final, modeled, surface* (Table 1).

The following sub-sections describe the three basic types of manual refinements: 1) application of control terrains, 2) addition of new control points, and 3) application of negative control points. Refinements include 1) introduction of higher-resolution controls (which may not have been accommodated by the interpolator; 2) parsimonious application and selection of reasonable or most probable interpretations; 3) consistent application of interpolation rules governing the effects of neighboring control data; and 4) smooth and reasonable integration into adjacent computer-interpolated surfaces. Interpretations incorporated by manual editing thus reflect not only the judicious application of new or more finely resolved data, but also professional judgment, intuition, and common sense.

3.5.1 Application of control terrains at surficial basement-bedrock boundaries

Weathered outcrops of basement rock (Alutom Formation) inside the plateau (at Mount Santa Rosa, Mataguac Hill, and Palii Hill; northeast of Janum Spring; and along the Pago-Adelup Fault) provide positive control for basement elevations along the basement-bedrock contacts, and are thus designated as *positive control terrains* (Figure 17). The plateau surfaces of the adjacent bedrock provide negative control, and are thus termed *negative control terrains* (Figure 17). The boundaries along the bedrock-basement contacts are taken from the geologic map (Siegrist and Reagan, 2008), and surface elevation contours of the terrains were obtained from LiDAR-derived DEM (BSP, 2007). As shown in Figure 17, positive control terrains replace the crude, under-constrained, initial interpolations on and around basement outcrops with the actual surface topography of the outcrop, and closer approximation of boundary conditions. *Positive control terrains are highlighted with bold black elevation contours on the map* (Plate 1). Positive control terrains adjacent to (i.e., outside) the domain boundaries (e.g., Alutom Formation on the southwest side of Pago-Adelup Fault) are also instrumental to refinements, but have been clipped off in the rendering of the final map (Plate 1). Negative control terrains (plateau surface contours) are not highlighted in the final map. The accuracy of the subsurface basement topography around the positive control terrains (and beneath the surrounding negative control terrains) is improved by manually editing the basement elevation contours to achieve relationships consistent with the terrain boundaries, geologic features, nearby control points, and adjacent basement topography.

Relevant geologic features inside or around control terrains include mapped or suspected faults (Figure 17). In the situation depicted in Figure 17A, a relatively smooth topographic gradient is assigned in the absence of additional data or knowledge of local geological structure. In Figure 17B, the presence of a mapped fault provides a basis for inferring a steeper gradient near the fault, although the actual depth to basement along the hanging wall of the fault is not known. The accuracy of the interpretation is enhanced in either case by fixing the boundary to the surface contact rather than the top or center of the outcrop. It should be noted, however, that fixing the boundary for the basement topography to the *surface* elevation of the limestone unit along the fault, rather than to the

base of the limestone unit at the fault, retains some upward bias in the inferred (yellow highlight) basement elevation near the boundary. The bias is greatest near the boundary, but diminishes with proximity to nearby control points. As shown in the schematic diagrams, this kind of discrepancy is likely more pronounced along fault boundaries (situation B) than non-faulted (situation A) boundaries. In the absence of proximal controls on basement elevation *at the base* of the limestone unit, however, there is no basis for a more accurate estimate. Exploration for groundwater in the vicinity of positive-control boundaries should be conducted with these limitations in mind.

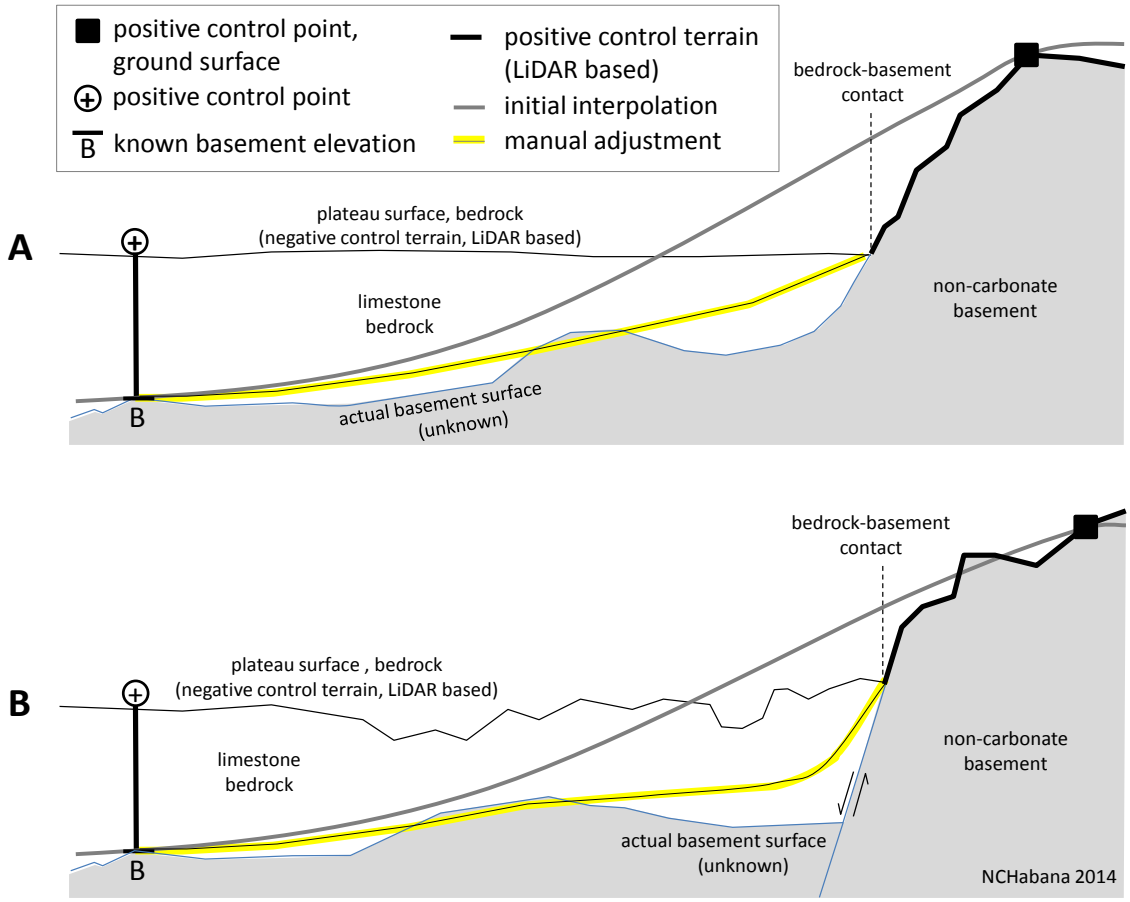

Figure 17. Application of control terrains. A) Outcrop in which the adjacent limestone laps onto the flank of a high-standing basement outcrop. B) Outcrop in which the contact occurs along a normal fault. In both cases, the initial spline-interpolated basement surface (dark gray line) is anchored at the boundary by a single positive control point (black square) on the basement outcrop. Such a boundary condition enables only a crude approximation of the surrounding subsurface basement topography. Note that as it approaches the boundary, the interpolation is actually drawn above the known (mapped) surface of the adjacent limestone plateau. In both cases, the fit is improved by manually repositioning the boundary control point to the surface contact between the limestone plateau and the non-carbonate outcrop. The inferred basement topography thus is placed everywhere beneath the plateau surface (i.e., the negative control terrain). The yellow-highlighted line depicts the inferred subsurface basement topography anchored to nearby control points and merging smoothly to the adjacent interpolated topography.

3.5.2 Application of additional positive control points

Elsewhere, where additional (newly-discovered or relocated) positive control points became available after the final interpolation is completed, refinements to the original spline interpolation are made accordingly (Figure 18). Such editing was applied to seven

areas (described in detail in Section 4.1.2): Andersen AFB landfill, Swamp Road area along Y-Sengsong Road, Anao Valley, Sasayan Valley, and the Mangilao Golf Course. *Positive control points that were applied for such manual editing are shown on the map in yellow*. As explained above, manual interpretations derived from such editing are integrated smoothly with the surrounding control points, in accordance with the applicable rules of interpolation.

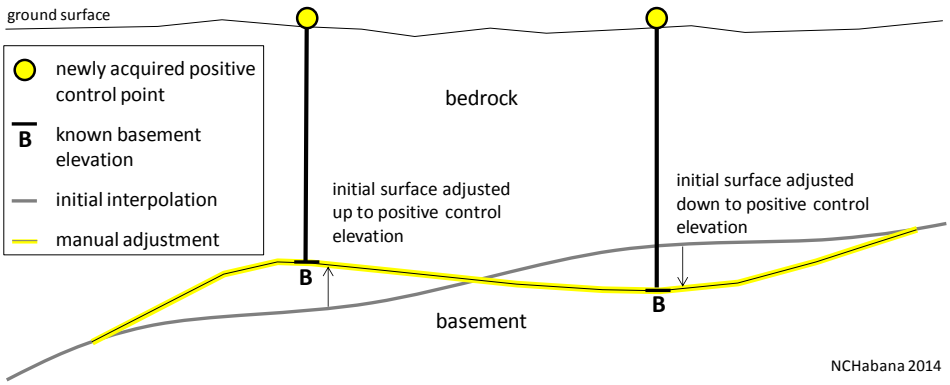

Figure 18. Application of additional control points. The spline- interpolated basement surface (dark gray line) is reshaped (yellow highlighted line) to conform to additional post-interpolation positive control (B).

3.5.3 Application of negative control points

As noted above, spline interpolators pin the interpolated surface to the positive control points (as illustrated in Figure 13B) in the initial dataset. The reliability of the interpolated surface is thus highest near positive control points; with increasing distance from them the probability of error increases. At other locations, especially where positive control is sparse, the depths of boreholes that terminate in limestone (which is the vast majority) provide a very limited, but nevertheless useful, check on the accuracy of the interpolated surface. If the interpolated basement surface intercepts such a borehole above its terminus, the interpolated surface is certainly too high. To test the interpolated surface for consistency with *all* the available data, then, it is useful to define the set of *Deepest Known Depths of Limestone Elevations* or *DKDLE* (Figure 13A). The DKDLE is thus *the total set of control points, positive and negative,* which provide a *maximum limit for the elevation of the basement surface*. Where the interpolated basement surface stands above the DKDLE, the interpolated surface must be adjusted so that the entire modeled surface lies at or below the DKDLE. Points on the DKDLE that have been used to make such refinements are referred to as *active negative control points*. Those which have not induced adjustment (but nevertheless provide some confidence that the local interpolated basement surface at least is consistent with the DKDLE) are called *passive negative control points* (Figure 19).

In the NGLA, the vast majority of wells that terminate in limestone are GWA production wells. The GWA dataset was thus the first to be screened and applied for negative control, with first priority given to areas where positive control points were distant or sparse. Other potential sources of negative control may eventually be incorporated, which may drive some additional adjustments to the map. Out of the 136 applied negative control points examined, 16 induced adjustments (i.e., provided *active* negative control). (See Tables 3 and 4, Section 4.1, and Appendix B.)

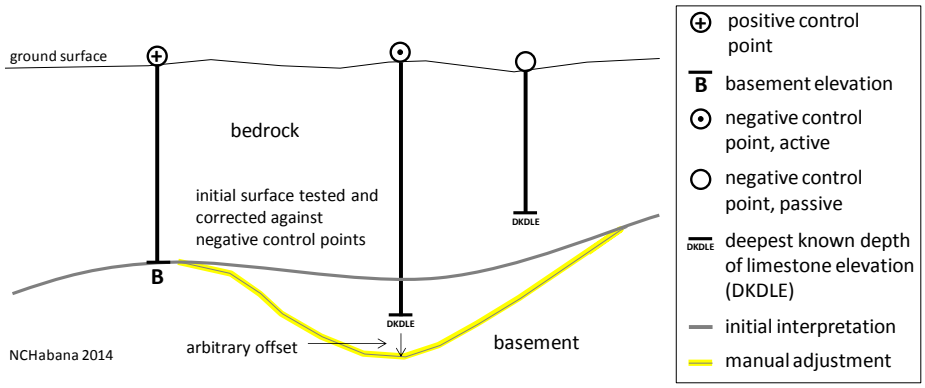

Figure 19. Application of negative control points. Active negative control (open circle with "bulls-eye"), where the original interpolation (dark gray line) is shown to have been too shallow. The adjusted surface remains tied to the nearest positive control points (B), while being placed at some (necessarily) arbitrary depth beneath the DKDLE. Elsewhere, passive negative control points (i.e., where the associated DKDLE lies above the original interpolated surface) provide some additional confidence that the interpolated surface at least lies below the minimum know depth of limestone at that point.

4 RESULTS: THE BASEMENT MAP

We note that this version of the basement topography (Plate 1) incorporates the most recent additions to our empirical knowledge of bedrock-basement relations and aquifer properties, as gained from the US Navy's 2010 Exploratory Drilling Program (AECOM Technical Services Inc., 2011). Eleven new wells were drilled in summer and fall 2010 to ascertain potential capacity and quality for new wells that might be needed to support additional production. From the study, some 58 candidate sites were selected and evaluated for potential development. (The estimated future production requirement has since been substantially reduced and planning and needs assessment are still ongoing at the time of this writing.) Besides supporting future development of the aquifer, whether for military or civilian needs, the basement map also provides fundamental boundary conditions for the numerical model built as part of the USGS-WERI *Groundwater Availability Study* funded by the US Marine Corps (Gingerich, 2013; Gingerich and Jenson, 2010). It should be kept in mind that results and interpretations of the numerical model are sensitive to the accuracy of the basement map. Work should continue to check, correct, update, and improve the basement map, especially in areas of interest for management, regulation, development, and modeling. (See Section 5.2.)

4.1 Additions and Innovations on the Map (Plate 1)

The map incorporates the following new attributes and innovations.

4.1.1 Display of control points and contour lines

The 1982 map displays the seismic lines and borehole information from which the topography was interpolated at that time. Similarly, the map displays each of the control points used in its construction, using the map symbols shown in Figure 13A and data types described in Section 3.1:

1. Positive control. Borehole data that provide positive control are shown with a *solid black circular dot* for distinct control, *or* a circle containing a "*half-moon*," for indistinct control.

2. Negative control. Borehole data that provide negative control are marked with an open circle containing a "*bulls-eye*" for distinct control, *or* an open, *empty circle* for indistinct control.

3. Seismic data. Seismic control points retained from the 1982 map are shown as *circles containing the symbol* "×". We note that even the most reliable geophysical data (seismic and TDEM) are inherently less precise than the best borehole data, thus all geophysical control points are regarded as indistinct.

4. TDEM data. The TDEM control points used from the 1992 study are shown with an open *circle containing the symbol "+"*. Like seismic data, TDEM data also inherently indistinct.

5. Specified data. Where no data are available to constrain interpolation and the interpolator produced unrealistic or impossible results (e.g., extending the surface of the basement beyond the seaward edge of the plateau), provisional, specified points representing the current "best guess" for pinning the sea-level contours in the absence of field data (Section 3.2.3 and Table 2) are shown with an *open circle containing an open triangle*.

6. New data applied for post-interpolator refinements. Additional control data discovered or verified after the interpolation provided a basis for making local refinements of the initial interpolation. *Symbols for such control points are shown in yellow.*

7. Control points with imperfectly known locations. On a few drill logs, coordinates for the wells were imprecise or otherwise uncertain, although the log may have provided unequivocal information regarding the depth of the basement contact. In some instances, research of the historical records brought into question the actual location of control points that had been adopted from previously examined records. Symbols for control points with imprecise locations are shown in *red*. Where such points were added as part of a post-interpolation refinement, they are highlighted with a yellow rim around the symbol.

8. Basement elevation contour lines. Thin black contour lines show the general interpolation, based on the assigned boundary conditions and internal control points. Where basement rock is exposed at the ground surface, the elevation contours are bolded. Contours highlighted in yellow show locations where the initial computer-generated interpolation has been refined based on additional data and/or professional judgment. Dashed contours show speculative interpretations where control data were insufficient to support reliable computer-generated interpolation or manual refinement.

4.1.2 Display of geologic and hydrogeologic features

Ongoing advances in geospatial analysis are providing powerful new means for integrating geologic data. The new map includes GIS enhancements—some of which

have become available only in the past five years—for terrain analysis and overlays of DEMs from surface LiDAR data, satellite imagery, and selected geologic features:

1. Basement topography is depicted with conventional contour lines using standard symbols, including those for closed-contour depressions. The map includes *hill-shade rendering of the topography* to assist in study and interpretation.

    - Names for topographic features. We have assigned formal names to the basement rises and ridges, and some of the interposed saddles, which have heretofore had only informal usage: *Mataguac Rise, Pati Point Rise, Santa Rosa Rise, Santa Rosa Ridge, Santa Rosa-Adacao Saddle, Adacao Rise, Adacao-Barrigada Saddle,* and *Barrigada Rise*. We have also assigned geographic names to the significant basement valleys: *Yigo Valley, Yigo Trough, Haputo Valley*, *Tarague Valley*, and *Anao Valley*.

2. Hydrologically significant geologic features. Some geologic features that are known or suspected to influence the hydrologic properties of the aquifer are incorporated:

    a. *Mapped faults are shown using long-dashed black lines*. Faults and fractures are important features in karst aquifers, as they can introduce either barriers or paths of enhanced conductivity (Ford and Williams, 2007). For this map, we have chosen to use this single generic symbol for all mapped faults rather than the standard geologic symbols that indicate fault types, displacements, and other details on geologic maps. For hydrologic applications of the map, the mere presence of the fault is the relevant feature; and to the extent that geologic details are desired for any given fault they can be obtained from the source map, i.e., Siegrist and Regan (2008).

    b. The surface exposure of the *Hagåtña Argillaceous Member of the Mariana Limestone is also shown*, given that this unit also constitutes a unique geomorphic and hydrogeologic province.

3. Infrastructure relevant to water resources management. To facilitate use of the map, we have included the following infrastructure:

    a. *Major roads and airfields* are overlain, as on the 1982 map, but updated with 2010 geographic data obtained from the Guam Bureau of Statistics and Plans.

    b. *Active GWA and other production wells*. Production wells are shown on the map for the convenience of users. Such wells, which were not otherwise used for basement topographic control, are marked on the map with an open triangle.

    c. *Hydrologic observation wells* are maintained and serviced by WERI and USGS under the *Comprehensive Water Monitoring Program (CWMP)* established by the Guam Legislature in 1998 under Public Law 24-161 (WERI website, 2013. Under a

joint agreement, technical teams from the USGS *Pacific Islands Water Science Center* in Honolulu visit Guam at least quarterly to collect hydrologic data from a network of stations. Seven *deep monitoring wells* (i.e., wells that penetrate the entire thickness of the freshwater lens) provide specific conductance data, from which chloride or salinity profiles can be estimated over the depth of the lens at these locations.[8] Profiling data are currently collected twice a year, at the transitions between the wet and dry seasons. (Profile data were collected quarterly up until about 2011.) Eight wells, including three of the deep monitoring wells, are equipped with *water-level recorders*.[9] Water-level recording wells collect continuous (10-, 15-, and 30-minute intervals) data on water-table elevations. Most of these wells (in particular, the EX-series wells) are the legacy of the 1982 *NGLS*. (See Section 1.4.) Others were originally installed as production wells but taken out of service because of performance problems, and then converted to water-level recording wells. CWMP wells are marked on the map according to the type of control they provided, and are labeled in bold. Names of active deep monitoring wells are rendered in green. Names of active water-level monitoring wells are underlined.[10] (See para. 12, below.)

d. *2010 NAVFACPAC Exploratory wells*. The 11 AECOM-series wells (AECOM Technical Services Inc., 2011) are also shown, using the applicable symbol for type of control provided by each of them. (See Appendix C for a summary of results.)

4. Bathymetric points used to provide provisional boundary conditions for the interpolator are shown on the map. These were extracted from the 15-minute quadrangle of Guam (USGS, 1978). (As noted in Section 3.2.3, 17 points were used,

[8] It should be noted that in karst aquifers, and especially in island karst aquifers which characteristically contain vertically-distributed lateral zones of enhanced conductivity, boreholes may intercept zones of variable hydraulic potential. These would induce vertical borehole flow, which would disturb the natural gradients of salinity. This is a topic of active discussion (cf., Jenson, J. W., Lander, M. A., and Randall, R. H., 2011, Vadose Flow in a Tropical Island Karst Aquifer, Guam, Mariana Islands, Carbonate Geochemistry: Reactions and Processes in Aquifers and Reservoirs: Billings, Montana, USA, Karst Waters Institute). Nevertheless, deep monitoring wells provide the best and only means of direct observation of aquifer conditions within the freshwater lens, and studies of processes within them will yield important new insights into aquifer dynamics.

[9] USGS has collected continuous water-level data for all of the deep monitor wells during various studies: EX-6 and the GUHRA-Dededo well were monitored during the GEPA 2004 study (Wuerch, H.V., Cruz, B.C. and Olsen, A.E., 2007, Analysis of the Dynamic Responses of the Northern Guam Lens Aquifer to Sea Level Change and Recharge. *WERI Technical Report No. 115*. Mangilao, Water & Environmental Research Institute of the Western Pacific, University of Guam.), and EX-1, EX-4, EX-9, and the GURHA-Dededo well were monitored during the 2010 NAVFACPAC study (AECOM Technical Services Inc., 2011, Guam Water Well Testing Study to Support US Marine Corps Relocation to Guam: Naval Facilities Engineering Command, Pacific).

[10] The seven active deep monitoring wells are EX-7, EX-10, and the GHURA-Dededo well in the Yigo-Tumon Basin; EX-1, EX-4, and EX-9 in the Hagåtña Basin; and EX-8 in the Agafa Gumas Basin. The eight active water-level monitoring wells are EX-7, EX-10, M-10A, and MW-2 in the Yigo-Tumon Basin; A-16, A-20, and BPM-1in the Hagåtña Basin; and EX-8 in the Agafa Gumas Basin. Note that EX-7, EX-8, and EX-10 belong to both categories. The Andersen and Mangilao Basins contain no CWMP monitoring wells.

although two lie outside the domain of the basement map. Only 15 therefore appear on the map. The source maps show many other soundings, but only those used for basement boundary conditions are shown on the basement map.)

5. Manual editing to incorporate additional positive-control. As described in Section 3.5.1, the basement contours generated by the spline interpolator have been edited where mapped outcrops of the basement provided control along the contact and where additional positive control points were either found or had to be specified.[11] Adjusted contours are highlighted in yellow. Additional positive control points are shown as solid yellow circles:

   a. Positive control terrains. We have edited the spline-generated basement surface (Figure 16) at 3 locations where contacts between the overlying limestone units and outcrops of basement Alutom Formation are mapped (cf., Siegrist and Reagan, 2008):

      1) Mount Santa Rosa, Mataguac Hill, and Palii Hill in the northwest

      2) The coastal exposure of Alutom Formation below the eastern flank of Mount Santa Rosa, southwest along the coast

      3) Adjacent to the Pago-Adelup Fault at the southwest end of the plateau

   b. Post-interpolation positive control points (Section 4.1.1, para. 6). We have edited the spline-generated basement surface (Figure 16) at six locations, where additional positive control data became available or certain anomalies had to be addressed. These are described below, in the order of their geographic locations, from north to south:

      1) AAFB Landfill vicinity. The numerous monitoring wells that surround the landfill provided abundant local positive control (indistinct) for interpolation. The interpolator, however, produced a curious salient extending northwestward on the northwest flank of the Mataguac Rise. We added control from IRP-11, which was discovered to have been missing from the initial data set, and re-accomplished the interpolation manually. The interpretation may be over-constrained here, but in the absence of a better hypothesis we have chosen to retain the salient, with minor adjustments.

      2) Swamp Road area. Subsequent to the interpolation from the initial dataset, we found drill log for wells D-23 (17 October 1994) and D-17X (26 Jan 1979) in this area. D-17X was apparently drilled as an exploratory well but abandoned

[11] The editing process (Section 3.5.3) also revealed two locations in which positive control points had been misplaced: IRP-5 on AAFB, and production well A-3, in Chaot (between Sinajaña and Hagåtña). After field checking and verifying the correct locations, we manually corrected the inferred basement topographies at each location.

because it struck basement rock above sea level and yielded no production. It could have thus provided positive control for the basement surface, but the precise location of the well is not recorded on the drill log. The ground surface elevation (440.3 ft (134 m)) and information regarding setback from Y-Sengsong Road sketched on the log, however, reduce the possible locations to two prospective sites, each at 440.3 ft elevation (based on LiDAR data) (BSP, 2007). Authors Habana and Jenson visited the area to search for evidence by which to determine which of the two sites is most likely to be D-17X. No such evidence was found. We therefore put *both* of the prospective sites on the map (in red) along with a provisional interpretation of the basement surface in the area, shown in dashed contours and annotated with a question mark ("?").

3) Piga Subdivision, Dededo. Subsequent discovery of the drill log for F-20, an unsuccessful attempt to install a production well (July 1998) provided an additional positive control point here.

4) Sasayan Valley area. M-16 (drilled May 1985) provided distinct positive control (solid black circle) at 52 ft (16 m) for the initial interpolation. Subsequent discovery of a drill log (July 1985) for M-16B, only 650 ft (198 m) to the east, provided additional distinct positive control (solid yellow circle) in this area at -33 ft (-10 m), revealing a sharp gradient in the basement topography and bracketing the sea-level contour here. Consequent adjustment of the adjacent basement elevation contours is shown by the yellow-highlighted contour lines. The area between the Adacao Rise, Barrigada Rise, and Mangilao Golf Course is otherwise notably lacking in control points, and the initial interpolation had only the external bathymetric data to constrain the coastal boundary. The addition of the control provided by M-16B, along with new control points obtain for the Mangilao Golf course (described below) provided a basis for refining the initial interpolation. The yellow-highlighted contours provide a refinement that is consistent with the new control points, the surrounding control points, the LiDAR surface data, and is smoothly integrated with the surrounding interpolated topography. It should be kept in mind, however, that this interpretation remains poorly constrained.

5) Mangilao Golf Course. New data supplied by golf course employees seeking advice regarding the course's water wells provided some positive control where there previously was none. Basement elevation is 79 ft (24 m) amsl at MGC-3M, and -10 ft (-3 m) at MGC-2, only 804 ft (245 m) WNW. These two data points admit a variety of interpretations; the adjacent yellow-highlighted contours and the dashed contour lines that connect to the surrounding basement topography provide a provisional interpretation.

6) Plateau Side of the Pago-Adelup Fault. As illustrated in Figure 17B, the boundary control for the inferred basement surface beneath the limestone plateau next to the fault was set at the ground surface contact of the plateau with the non-carbonate terrain on the opposite (southwest) side of the fault. At a single point,

near the Ordot Dump, seismic data provided positive control next to the fault. The closely-spaced basement elevation contours show the kind of topographic gradient expected along the fault, and may be representative of what occurs elsewhere along the fault. In the absence of positive control elsewhere along the fault, however, we adhered to the model shown in Figures 17B and 19, fixing the boundary at the ground surface along the fault, but keeping the inferred basement surface to the northeast below the ground surface and any negative control points, and tying it smoothly into the nearest positive control points. Anyone conducting exploration along the fault should keep in mind the increasing upward bias of the inferred basement elevation next to the fault (with the single exception of the area next to the positive control point by the Ordot Dump). Additional positive control is needed along the fault to more accurately characterize basement topography beneath the plateau boundary.

6. Manual editing driven by negative control points. As noted above in Section 3.2.4, the interpolated surface generated from the positive-control dataset has been adjusted at 16 points where the DKDLE was lower than it was estimated to be on the initial interpolated surface (Figure 19). It should be kept in mind that negative control points (and most positive control points, for that matter) provide only fortuitous, random, and limited control, rather than deliberate, systematic, and spatially comprehensive control. Large areas of sparse control remain, and negative control, where active, serves only to establish a poorly known limit to the elevation of the basement.

   Locations (listed from north to south) at which the interpolated surface has been adjusted to make the modeled surface consistent with negative control *are shown with contour lines highlighted in yellow*:

   a. Mataguac Rise, west flank (based on EX-7, EX-10, D-27, and F-17)

   b. Barrigada Rise, northeast flank (based on M-17A, M-17B, and M-20)

   c. Barrigada Rise, southwest flank (based on NAS-1)

   d. Barrigada Rise, south flank (based on EX-9)

   e. Adacao Rise, south flank (based on M-4 and M-8)

   f. Adacao-Santa Rosa Saddle, north flank (based on AECOM-9)

   g. Nimitz Hill (based on NRMC-1, NRMC-2, and NRMC-3)

7. Imperfectly located control points. In accordance with the convention described in Section 4.1.1, para. 7, controls points for which the coordinate are imprecisely known are rendered in red. This edition of the map includes only one such point: D-17X, above). (See paragraph 2.)

8. Water-table contours. The revised map displays *thin blue contour lines* for the water table predicted by the numerical model developed concurrently for the Guam Groundwater Availability Study (Gingerich, 2013; Gingerich and Jenson, 2010).

    a. A noteworthy "local anomaly" is the steep gradient in the water table seen on the north flank of the Mataguac Rise in the Agafa Gumas Basin. Although no direct geologic evidence for basement lithology is available at this site, coastal exposures of the rhythmically-bedded argillaceous *Janum Limestone* on the flank of the Santa Rosa Rise (Siegrist and Reagan, 2008) suggest that it may elsewhere also be mantled by Janum Limestone. This unit is laminated and includes deep-water foraminiferal turbidite sequences that grade upward. These deep-water sequences may be siliciclastic and, therefore, relatively "dirty" as contrasted with the Barrigada Limestone. Although the hydraulic properties of the Janum Limestone have not been directly studied, they might be reasonably inferred to be similar to those of the Argillaceous Member of the Mariana Limestone in the Hagåtña Basin. The hydraulic conductivity of the argillaceous limestone is well established from field testing (CDM, 1982; Rotzoll et al., 2013) to be orders of magnitude lower than that of the Barrigada Limestone (Section 1.2) which dominates the rest of the interior of the aquifer. If the north flank of the Mataguac Rise is mantled with Janum Limestone or an equivalent unit, the hydraulic gradient would be expected to be accordingly greater there. Focused study of this area would be required to answer this question.

    b. *Regional-scale karst features (e.g., dissolution-widened fractures or faults) that have yet to be identified could induce significant local-to-regional-scale perturbations* in the actual water table. The predicted water table for the aquifer, as shown on the new map, however, has been calibrated to match field observations from at least 34 inland wells, and reflects the distributions of hydraulic conductivity assigned to the model (Rotzoll et al., 2013). Karst-induced departures from the predicted water table are especially likely to be important near Haputo Bay, where the water-table contours show flow converging on a zone of very high hydraulic conductivity (Rotzoll et al., 2013). Prolific concentrated discharge is well documented in previous field studies of that include Haputo Bay, which is intersected by convergent faults, and of the adjacent coast, which exhibits several spectacular springs (Jenson et al., 1997; Jocson et al., 1999; Mylroie et al., 2001; Taborosi et al., 2013a).

9. Basement hydrologic divides are *marked with bold blue solid lines* along the axes of the topographic ridges of the modeled basement topography. Water percolating down to the bedrock-basement contact on either side of the divides is shunted down-slope as supra-basal water to the lip of the lens, where it enters the para-basal zone. *Hydrologic divides along the basement rises and ridges may be considered fixed or "hard" boundaries* for water reaching them, although it should be noted that theory and field evidence suggest that downward-moving vadose groundwater may enter transverse zones of enhanced horizontal conductivity within the limestone bedrock, which in

principle could redistribute vadose water across an adjacent subterranean basement divide beneath (Jenson et al., 2011; Mylroie et al., 2001).

10. Groundwater basins. The basement hydrologic divides, with the above qualifications kept in mind, partition the aquifer into partly contiguous groundwater basins (Wilson and Moore, 1998). (See Section 1.3.) *We have adopted for this report, and propose for future use, this standard and more accurate term "basin" in lieu of the non-standard term "sub-basin,"* which has been in use locally since at least the 1982 study (CDM, 1982). We have, however, *retained names assigned by the 1982 map, with two slight modifications*. "Agana" is now rendered "Hagåtña" to conform to Chamorro-language lexicography. The name of the "Yigo Sub-basin" has been changed to "Yigo-Tumon Basin" to better reflect the geographical extent of this large and important unit.

11. Basin boundaries. Water in the phreatic zone is assumed to generally flow perpendicular to contours of equal potentiometric head (water-table elevation), although, as noted above, regional-scale fractures could induce significant anisotropy. In demarcating the groundwater basins (called "sub-basins" at the time) J.F. Mink (CDM, 1982) noted this possibility, but in the absence of empirical knowledge of variations in regional hydraulic conductivity, regional anisotropy, or regional karst pathways, simply extended the boundaries formed by the basement hydrologic divides along the flow-lines that phreatic water would presumably follow from the end of the basement boundary in a homogeneous, isotropic medium, under natural, unperturbed (i.e., pre-development) conditions. *The new map shows revised boundaries for the six basins, based on flow-lines inferred from the newly modeled water table*, described above:

    The presumed flow-line boundaries originate where the ends of the supra-basal hydrologic divides meet the water table, and are shown for modeled pre-development conditions. They are marked with *bold blue dashed lines* because they constitute "soft" or variable boundaries *that could be shifted by local gradients induced by pumping, or could actually follow currently unknown karst pathways* that re-direct or re-distribute water on its way to the coast. It should be noted that the model currently assumes that each of the hydrogeologic units is isotropic. Flow-line boundaries thus calculated may be revised as our understanding of aquifer properties, especially the contribution of karst features, improves.

12. Saltwater toe (para-basal/basal boundary). The saltwater toe is defined here as the intersection of the 50% seawater isochlor with the bedrock-basement contact. (See Section 1.3.) The new map thus displays the saltwater toe as the depth where the 50% seawater isochlor calculated by the numerical groundwater model built for the 2013 *Guam Groundwater Availability Study* (Gingerich, 2013; Gingerich and Jenson, 2010) intercepts the basement. *Except as noted below, the calculated boundary displayed on the map has not been field checked or corrected against empirical data.* It should be noted that the position of the para-basal/basal boundary estimated by the model is sensitive not only to the calculated depth of the 50% seawater isochlor, but

also to the accuracy of the interpolated depths and topographic gradients of the basement contact.

Actual observations of salinity profiles (i.e., of how salinity varies with depth) against which to evaluate the calculated para-basal/basal boundary are very limited. Where deep monitoring wells are not available, lens thickness can in theory be estimated from water-level well data using the Dupuit-Ghyben-Herzberg (D-G-H) ratio, by which the depth to the bottom of the lens in relation to the observed water-table elevation is in principle about 40:1. This provides only the crudest of estimates, however. The D-G-H ratio assumes static (simplified) rather than dynamic (actual) conditions. It also assumes a sharp interface and thus provides no means of accounting for transition zone thickness or the gradient in salinity with depth. Moreover, Simard et al. (2013) note that the actual, observed depth-to-head ratio of the lens in the NGLA varies from 28:1 to 46:1. In the absence of profile measurements, however, the D-G-H ratio provides the only other means of making a first-order estimate of the depth to the bottom of the lens, defined here, as noted above, at the 50% seawater isochlor.

Given the dearth of deep monitoring wells by which to obtain measured depths to the 50% isochlor, we have chosen, as noted above, to map the para-basal/basal boundary exclusively according the estimate of the 50% seawater isochlor depth calculated by the groundwater model, without attempting to adjust the modeled depth, even where observational data are available. Rather, we present below a brief summary of the status of available observations for each basin, and their comparisons to the modeled estimates. Details of observed historical spatial patterns and temporal trends in the NGLA are reported in WERI Technical Report 143, *Analysis of Salinity in the Northern Guam Lens Aquifer* (Simard et al., 2013). Their study built on the previous historical study by McDonald and Jenson (2003), utilizing water-level recording well records from 1975 to 2010, and the most recent salinity profiles, from May 2005 to October 2010. Relevant observations follow:

a. The Yigo-Tumon Basin is the largest groundwater basin and contains the most monitoring wells. All are in the basal zone. There are no monitoring wells at the head of the Yigo-Tumon Trough. Historical salinity profile records are available from EX-7, EX-10, the GHURA-Dededo well, and EX-6 (not currently in service). Historical water-level records are available from M-10A and M-11 (no longer in service). During the *Guam Groundwater Availability Study,* water-level data were obtained from AECOM-9. Recently, MW-2 has been brought into service as a *CWMP* monitoring well. Salinity profiles recorded at EX-6, EX-7, EX-10, and GHURA-Dededo place the 50% seawater isochlor between -112 to -151 ft (-34 to -46 m) elevation. The modeled saltwater toe location approximating the minus 120-ft or minus 40-m volcanic basement contour is thus consistent with empirical data across the Yigo-Tumon Basin, particularly in comparison to the salinity profile data.

b. The Agafa Gumas Basin. Too few salinity profiles were available in this basin for meaningful comparison with the modeling results. The basins contains a single deep monitoring well, EX-8, which is located in the basal zone and currently also collects water-level data. EX-8 was out of service for several years, and regular data collection (semi-annual) was resumed at EX-8 only in January 2012. During the *Guam Groundwater Availability Study*, water-level data were collected from AECOM-1 and AECOM-3, both of which are in the modeled para-basal zone. Measured hydraulic head at AECOM-3 is 30 to 32 ft (9 to 10 m) above mean sea level (amsl). An explanation for the high head in this area has yet to be determined (AECOM Technical Services Inc., 2011).

c. The Finegayan Basin contains NCS-A, which was once converted from a production well to a water-level monitoring well, but is no longer active. No salinity profile data are available for this basin, nor are sufficient groundwater level data are available to estimate the saltwater toe location (Simard et al., 2013).

d. The Andersen Basin contains no monitoring wells. A few hydraulic head measurements recorded during the *Guam Groundwater Availability Study* at AECOM-7, situated in the modeled para-basal zone, range from 2.4 to 3.9 ft (0.7 to 1.2 m) amsl. A D-G-H estimate of the 50% seawater isochlor depth would thus put it at -95 to -157 ft (-29 to -48 m) elevation.

e. The Mangilao Basin, like the Andersen Basin, contains no monitoring wells. Hydraulic head measurements recorded during the *Guam Groundwater Availability Study* at AECOM-11, situated in the modeled para-basal zone, range from 2.4 to 7.9 ft amsl (0.7 to 2.4 m amsl), providing a D-G-H estimate for the 50% seawater isochlor of -95 to -315 ft (-29 to -96 m) elevation.

f. The Hagåtña Basin contains argillaceous (4-6% clay) limestone that distinguishes it from the other groundwater basins in the aquifer. The decreased permeability associated with argillaceous limestone results in a much deeper saltwater toe than areas with pure limestone. There are three distinct hydrogeologic provinces within the Hagåtña Basin: the para-basal/supra-basal region in the southwest along the Pago-Adelup Fault, the anomalously high-salinity basal region in the center and southeast, and the remaining basal region to the north:

   1) The southwest region of the Basin contains no basal monitoring wells capable of identifying the saltwater toe location. Nor are there any monitoring wells in the para-basal zone. Supra-basal monitoring well A-20 (the only supra-basal monitoring well in the NGLA) is not hydraulically connected to saltwater (and is therefore uniquely valuable for assessing aquifer response to recharge, in isolation from the lens dynamics). (See Lander et al., 2001.)

   2) The central and southeast regions of the Hagåtña Basin contain basal deep monitoring wells EX-1 and EX-4, respectively. Salinity profiles completed at these wells put the 50% seawater isochlor at -223 to -256 ft (-68 to -78 m)

elevation. Based on salinity profile data collected from EX-1 and EX-4, the modeled saltwater toe in the southwestern region should be adjusted closer to the minus 240-ft or minus 80-m basement contour.

3) The northeastern region of the Hagåtña Basin contains basal water-level recording wells A-16, BPM-1, and deep monitoring well EX-9. Hydraulic head measurements vary between 2.3 and 7.1 ft (0.7 to 2.2 m) amsl at monitoring wells A-16, BPM-1, and EX-9, which places the 50% seawater isochlor at -92 to -285 ft (-28 to -87 m) elevation. Salinity profiles completed at EX-9 put the 50% seawater isochlor at -115 to -135 ft (-35 to -41 m) elevation. Based on salinity profile data collected from EX-9 in the northeastern region near the Barrigada Rise, the modeled saltwater toe should be adjusted closer to the minus 120-ft (40-m) basement contour.

13. Santa Rosa-Adacao Saddle. One of the most noticeable revisions of the topography from the 1982 map is the deepening of the saddle at the southeastern end of the Santa Rosa Ridge, which places the bottom of the saddle below the sea-level contour, isolating the Santa Rosa Ridge from the Adacao Rise at sea level. This lowering of the saddle is driven by the introduction of an active negative control point provided by AECOM-9, which was drilled to -248 ft (76 m) amsl without encountering non-carbonate material. Since there is no other basis for adjusting the spline-interpolated topography up or down here, we have chosen to retain the spline interpolation for now, but with the following observations and caveats:

- The 1982 map, which did not place a saddle here, had fewer data points and contained some obvious incongruities elsewhere (such as extending basement contours seaward, beyond the coastline on the central southeast coast of the plateau). There is *no basis for assuming either the 1982 or 2013 interpretation to be superior to the other* at this location, especially given that we do not know whether the local basement topography changes smoothly (as it might if the surface had been modified by deposition or erosion) or abruptly (as it might if the morphology is dominated by unmodified structural discontinuities, such as fault scarps that have been neither mantled by deposition nor smoothed by erosion). Although we have therefore retained the spline-based interpolation, we have marked the saddle with a question mark (?) to note that this interpretation is uncertain.

14. Santa Rosa-Adacao-Barrigada Hydrologic Barrier. We note that the *results of Rotzoll et al. (2013) are consistent with the existence of a strong hydrologic barrier* from the Santa Rosa Rise to the Barrigada Rise, regardless of the depths of the saddles between the rises. Additional research will be required to verify and determine the nature of the barrier, but at least three hypotheses—which are not entirely exclusive of one another—might be investigated:

a. *The 2013 interpolation is incorrect*, and bottom of the saddle in the basement ridge is in fact at or slightly above sea level; or

b. Given that the entire ridge would have stood above sea level for most of the Pleistocene, *open karst pathways that can carry strong tidal signals might have evolved independently but simultaneously over geologic time from opposite sides of the ridge axis*. These are now submerged in the marine phreatic zone, such that the tidal signals propagating from either side of the island remain mostly isolated from one another; or

c. *The first few tens of meters of limestone in the vertical section above the limestone-volcanic contact have been primarily a zone of carbonate redeposition* during the large amount of geologic time when the basement ridge has stood above sea level. The *original porosity of the limestone above the axis of the saddle has thus been occluded* by carbonate cements deposited by descending saturated vadose waters, *resulting in a net decrease of permeability* in the limestone along the axis of the saddle.

5 RECOMMENDATIONS

For reasons noted throughout this report, improved accuracy and detail on the basement map improves the odds for successful site selection for new wells, and also for prevention and management of remediation of salinity and other types of contamination of groundwater. Improvements in the reliability and precision of the basement map are also essential to improving the reliability and usefulness of numerical models for groundwater flow and/or contaminant transport. We offer two categories of recommendations, the first for applications of the map, and the second for activities and research to keep the map up to date and improve its accuracy and functionality.

5.1 Applications of the Map to Future Exploration and Sustainable Development

Experience has shown that capacity and quality of well sites can vary greatly across the aquifer. Unfortunately, as in most other communities, there has been no methodical documentation or record-keeping of failed attempts at well siting and development. Precise rates and reasons for failures over the seven decades since drilling began are therefore unknown. The received wisdom among local drillers, however, is that only about one in three or four exploratory wells provides economical production. This is consistent with recent experience: Of the 11 wells drilled in the 2010 NAVFACPAC study, four (AECOM 1, 6, 10, 11) delivered water at 400 gpm (25 lps) or more; three (AECOM 2, 3 and 7) produced water at 68 to 250 gpm (4-16 lps); and four others (AECOM 4, 5, 8, 9) were insufficiently productive even to support a pump test (AECOM Technical Services Inc., 2011, summary at Appendix C). Water from one of the test wells (AECOM 6) did not meet secondary MCLs for total dissolved solids. Exploration thus poses a dual challenge: 1) selecting an appropriate area for development, and 2) finding productive sites within the selected area.

Given that most of the lowest-risk/highest-productivity areas in the aquifer have by now undergone substantial development, simply installing more wells in them—even with shallow draft and low pumping rates—will risk degradation of water quality. Developers must therefore tailor production targets according not only to the original quality of water

at the site, but to future projections of water quality as a consequence of future water pumping. The numerical groundwater model developed by the USGS Pacific Islands Water Science Center for the *Guam Groundwater Availability Study* (Gingerich, 2013; Gingerich and Jenson, 2010) will provide a useful tool for assessing possible responses and managing production to minimize degradation of water quality around the aquifer. In addition, the 2010 *NAVFACPAC Exploratory Drilling Program* (AECOM Technical Services Inc., 2011) has—besides making possible the latest improvements in the accuracy and reliability of the new basement map—provided fresh and timely new insights regarding prospects for successful exploration and development precisely in the areas most likely to undergo development. With these new tools, groundwater developers and managers seeking sites for wells that can produce high-quality water at high production rates are better prepared to invest in higher-risk exploration, in less-accessible areas, with higher startup costs.

To enhance the prospects for successful exploration and cost-effective development strategies, we offer below some specific recommendations for the application of the new basement map in each of the three groundwater zones of the NGLA—the basal, para-basal, and supra-basal zones—with reference to the results of the *NAVFACPAC Exploratory Drilling Program* (AECOM Technical Services, Inc., 2011, summarized in Appendix C).

5.1.1 Exploration for basal water

The basal zone is the most accessible of the three groundwater zones in the aquifer, in the sense that it underlies about 75% of the surface area of the plateau. (See Section 1.3.) Notably, all four of the most productive wells in the 2010 exploratory program were located in the basal zone. (See Appendix C.) Although water quality is characteristically variable in the basal zone, it can be high. All six of the basal wells installed in the 2010 exploratory program (AECOM 1, 2, 6, 7, 10, 11) produced water within the 250 mg/l US Environmental Protection Agency (USEPA) secondary standard for chloride, with the lowest concentration at 16 mg/l and the highest at 227 mg/l.

1. These recent results suggest *promising prospects for some additional development of basal water, but it should be kept in mind that the risk of saltwater contamination is highest* in this zone, where the freshwater lens is underlain by saltwater. The groundwater model will provide a useful and timely new tool for estimating the likely trade-offs between increased production and increased salinity.

2. *Where additional development of basal water is sought, developers would be best advised to seek inland sites closest to the para-basal zone, and where possible, along the axes of the three basement valleys below*:

   a. Yigo Valley and Yigo Trough of the Yigo-Tumon Basin

   b. Tarague Valley of the Agafa Gumas Basin

   c. Anao Valley of the Andersen Basin

3. In contrast, development of the Haputo Valley of the Finegayan Basin should be avoided, given the high permeability of the bedrock, the consequent thinness of the freshwater lens that can be expected, and the already manifest high incidence of higher-salinity wells in this basin (Simard et al., 2013).

4. The Mangilao Basin generally lacks basal water of substantial depth except along the southeast flank of the Barrigada Rise.

5. The Hagåtña Basin, in which the dominant aquifer rock is a "dirty limestone" (Argillaceous Member of the Mariana Limestone (Siegrist and Reagan, 2008; Tracey et al., 1964)) presents a special case. The southeastern part of this basin has historically contained high-salinity water (McDonald and Jenson, 2003). A recent WERI study of the incidence of salinity in the aquifer (Simard et al., 2012, in review, 2013) shows a strong seasonal variation in water quality, with the depth to the 250-mg/l isochlor rising and falling as much as 70 m from the wet to the dry seasons in this basin. Further development of basal water in the Hagåtña Basin is not advised.

6. Finally, it should be noted that any new wells installed in the basal zone of any of the six basins should be shallow—fewer than 25 ft (7.6 m) below sea level. More research is advisable to gain a more precise understanding of the locations and characteristics of the water-bearing zones in this complicated karst aquifer, particularly within the first 25 ft (7.6 m) above and beneath the modern water table.

5.1.2 Exploration for para-basal water

As noted above (Sections 1.3.1 and 1.4), the para-basal zone has historically been the zone of choice for exploration and development. The 2010 Exploratory Drilling Program installed only two wells that were unequivocally in the para-basal zone: AECOM 2 and AECOM 3. AECOM 3 was deliberately installed as an observation well, and thus drilled to the basement contact. (See Appendix C.) Water quality was high (16-36 mg/l chloride) but productivity was low; AECOM 3 tested to 250 gpm (16 lps), but with ~13 ft (~4 m) drawdown. Nevertheless, *the para-basal zone should continue to provide the best prospects for development of high quality water sources, particularly in the Agafa Gumas and Andersen Basins, where it remains relatively undeveloped*. It should be noted, however, that although groundwater is relatively undeveloped in these basins, the extensive existing and planned military operations and support activities within these basins places substantial restrictions on useable well sites.

1. Like the adjacent basal water, para-basal water can be expected to be thickest and freshest close to the axes of the basement valleys.

2. In contrast to the valleys, a notable feature of the para-basal zone at the northeast corner of the Mataguac Rise is the broad shallow zone that extends northwestward from the basement rise. The shallowing of the para-basal zone here suggests that this area may be relatively more vulnerable to inland migration of the saltwater toe in response to sea-level rise or thinning of the freshwater lens in response to reduced

recharge or increased local withdrawal from either of the adjacent basins. The similarly shallow zone at the head of the Yigo Trough may be similarly sensitive to changes in water budget, even though it is flanked by slopes that shunt supra-basal water into the trough. Accurate and precise knowledge of the basement depths and slopes is crucial in such areas.

3. Some potential for development of para-basal water may still exist along the flank of the Pago-Adelup Fault at the southwestern end of the Hagåtña Basin, although it may be increasingly difficult to access suitable sites.

4. It should be noted that increased development of the para-basal zone will degrade the quality of water from basal wells downstream as the downstream portion of the lens thins in response. Groundwater modeling simulations can help to evaluate the likely effects of upstream development and the consequent trade-offs between increased para-basal development and concomitant degradation of downstream basal production. Given the relative advantages of production from the para-basal zone, however, continuing investments should be made in more accurately and precisely determining the boundaries of it and in locating and developing productive sites within it.

5.1.3 Exploration for supra-basal water

As noted in Section 1.4.4, the area from Mount Santa Rosa west to Mataguac and Palii Hills was historically regarded as unproductive until the discovery in the early 1990s, during the installation of military IRP monitoring wells, of what was then called "perched" water on the flank of the basement above sea level. These discoveries were followed in the late 1990s by the spectacular success of a few new productions wells, notably Y-15, Y-17, and Y-23 (Figure 11), which have been consistent, high-quality producers to this day. New insights regarding the basement geology in this zone and prospects for future development discovered from recent work are discussed below.

1. New insights from the map. The improved resolution and detail of the updated basement map may help to explain why Y-15, in particular, has been able to consistently produce very high quality water (<40 mg/l chloride) at 550-600 gpm (35-38 lps) ever since its installation. If the topography shown on the new map is correct, Y-15 is centered on a "dimple" in the volcanic basement terrain that lies north of the Mount Santa Rosa outcrop and just west of the subterranean Anao Valley. A closed or nearly closed depression in the basement in this location would serve as a natural subterranean reservoir that could impound a sufficient portion of the supra-basal water descending from the slopes to keep Y-15 productive year round.[12] Water-table data are too sparse to construct a water-table map in the supra-basal zone, but the map is annotated with light blue patches that indicate where supra-basal groundwater may concentrate in basement valleys and depressions.

[12]This sort of topography seems a reasonable hypothesis, given that the Santa Rosa-Mataguac Rise is interpreted as a horst-and-graben province that underwent syndepositional faulting as the limestone bedrock was deposited on it (Tracey et al., 1964). The underlying basement surface, therefore, would not have developed an open drainage system such as has developed on the sub-aerially exposed terrain of the same rock unit (Alutom Formation) in the southern province of Guam.

2. Observations from the 2010 NAVFACPAC Drilling Program. In summer 2010, during the year-long exploratory drilling program undertaken to support the anticipated military build-up, supra-basal water was discovered at three wells. (See Appendix C and AECOM Technical Services Inc., 2011.)

   a. AECOM-8, in the MARBO area, on the northwest flank of the Santa Rosa Ridge, Yigo-Tumon Basin. Water-table elevation at this site was 158 ft (48 m) amsl. Color changes in drilling foam every few feet beginning at 6 ft (2m) above the water table suggest the borehole intercepted a complex contact with the basement beginning, coincidentally, at about the same elevation as the water table. We assigned an elevation of 142 ft (43 m) to the basement contact here, based on the recovery of gray-colored drilling foam from that elevation. This well thus provides a new positive control point (although indistinct) for the map. Drilling was terminated 43 ft (13 m) below the water table, placing the bottom of the borehole at 115 ft (35 m) amsl, but borehole collapse precluded inserting a pump below 131 ft (40 m) elevation, 27 ft (8 m) below the water table. The apparent coincidence of the water table with the basement contact suggests that this well marks the upper boundary of the supra-basal zone here. Not surprisingly (because of well collapse and the resulting thin saturated thickness), pump testing showed that this well cannot produce an economical yield.

   b. AECOM-4, on AAFB, east of the axis of the Tarague Valley, on the northwest flank of the Pati Point Rise, Agafa Gumas Basin. The water table was encountered at 122 ft (37 m) amsl. Drilling was terminated 56 ft (17 m) below the water table, placing the bottom of the well at 66 ft (20 m) amsl. Although this well did not intercept basement rock, it lies very close (75 ft or 23 m) to AAFB's IRP-17, which intercepted basement at about 25 ft amsl and thus provides a distinct positive control point for the basement map. Accordingly, we assigned AECOM-4 to the supra-basal zone based on its close proximity to IRP-17. (See Figure 6-6 AECOM 2011.) Pump testing showed that this well cannot produce economical yield. However, were drilling continued until the borehole intercepted basement (presumably above sea level, given its close proximity (75ft (23 m)) to IRP-17 at which the water-table elevation is 135.43 ft (41 m) amsl) (PCR Environmental Inc., 2012) it is possible in principle that it could intercept a productive zone (Jenson et al., 2011).[13] Such an experiment, however, was not considered, as the driller was concerned that GEPA regulations and guidance precluded drilling more than 40 ft (12 m) below the water table, even with the elevation of the water table at 122 ft (37 m) amsl.

[13] There is abundant, though as yet sparsely documented, evidence for transverse flow of freshwater along horizontal zones of enhanced permeability in the vadose zone. A recent example is the discovery of vadose water cascading down an open borehole from ~84 ft (~26 m) above the water table at AG-10, located in the Finegayan Basin on the northeast flank of the Mataguac Rise.

c. AECOM 5, on AAFB, on the southeast flank of the Pati Point Rise, Andersen Basin. The water table was encountered here at 208 ft (63 m) amsl. The borehole intercepted non-carbonate material at 33 ft (10 m) below the water table, i.e., at 175 ft (53 m) elevation. We therefore assigned AECOM-5 as a distinct positive control point for the basement map. Drilling was continued down to 105 ft (32 m) amsl, 70 ft (21 m) below the basement contact, and 103 ft (31 m) below the water table. AECOM-5 intercepted water at an elevation that contoured well with the supra-basal heads from Y-15 and the AAFB landfill/IRP wells. However, this well cannot produce an economical yield. It is noteworthy that this well was only 2660 ft (810 m) north of the high-yielding supra-basal GWA well, Y-15.

d. Apparent hydraulic gradients above the Santa Rosa-Mataguac complex (AECOM Technical Services, 2011, Figs. 6-2, 6-6). The hydraulic heads of the basal wells installed seaward of the Santa Rosa-Mataguac complex (AECOM 1, 2, 6, and 7) are in the 2-to-4 ft (0.75-1.3 m) amsl range, as one would expect for basal water. Heads at AECOM 3, 4, and 5, which lie a short distance further toward the south central portion of the base, are significantly higher, however. Similarly, high heads (greater than 20 ft (6 m) amsl) coinciding with the Santa Rosa and Mataguac Rises occur at GWA wells Y-15, Y-17 and Y-23 and AAFB monitoring wells IRP-5, IRP-6,[14] IRP-11, IRP-17, and IRP-59 (see AECOM, 2011, Figure 6-6; and PCR Environmental Inc., 2012). It is unclear what is producing the steep apparent hydraulic gradients that tend to mirror the underlying basement topography of the Pati Point Rise. Our interpretation of the current data (shown on the map) is consistent with the interpretation from a previous study on AAFB by ICF Technology Inc. (1995) (Appendix F). If hydraulic conductivities were similar to most other places in the Barrigada Limestone, gradients would be expected to be much gentler. Conditions that could explain these observations include lower hydraulic conductivity in the Mio-Pliocene Janum Limestone that is likely to cover basement rises in the supra-basal zone on the flanks of Mt. Santa Rosa and Mataguac Hill. (See Section 4.1.2(7).) This lower-permeability unit may be inhibiting the subterranean downslope and vertical flow of groundwater and thus locally producing steeper hydraulic gradients. Moreover, the Janum Limestone could be offset in complex patterns along the flanks of the Mount Santa Rosa-Mataguac Rise.

e. Apparent continuity of supra-basal water above the Santa Rosa-Mataguac complex. While the high-capacity wells (e.g., Y-15, Y-17, and Y-23) in this area have been seen as spatial and temporal anomalies in the past, the apparent continuity of groundwater head contours in the several wells across this area, along with decades of above-average production from the successful wells, suggests that groundwater above the volcanic rock may be laterally continuous, rather than isolated. (See AECOM Technical Services, Inc., 2011, Figure 6-6; and PCR Environmental, 2012,

[14] Based on the IRP-6 drill log (18 February 1987) the water table (h = 6.8 m) appears to lie within the volcanic basement rock (basement elevation = 24.7 m), indicating that at this site the basement rock is sufficiently permeable to constitute part of the supra-basal aquifer.

Figure 3-5.) On the other hand, as noted in Section 1.4.4, many attempts at exploration in this area in the 1990s (Figure 11), as well as recent attempts at AECOM-4 and AECOM-5 yielded poorly producing wells. Such "dry holes" likely reflect a poor connection between water transmitted in secondary fissures and conduits and water stored in the surrounding low-permeability matrix. Although static water level at any given site will reflect the general regional hydraulic head, the site may not have sufficient local hydraulic connectivity and transmissivity to produce economical well yields. Wells that intercept the network of secondary features, however, will tend to be high producers. To determine the actual degree of continuity of the phreatic water will require focused field research (e.g., drilling, aquifer testing, and/or geophysical exploration) to identify discontinuities wrought by karst features in the bedrock and constraints imposed by structural or topographic features in the basement.

3. Hydrogeologic considerations regarding development of supra-basal water. While AECOM 4 and AECOM 5 did not encounter significant hydraulically-connected conduits or fractures, it is possible that good-producing wells (similar to Y-15, Y-17 and Y-23) could be located in this general area, especially if hydraulically-interconnected zones are penetrated by advancing these and other supra-basal wells all the way down to the volcanic rock contact. Because supra-basal wells can be drilled all the way through the freshwater phreatic zone down to the basement, they have a significant chance of intercepting networks of former phreatic (water table) caves from previous sea-level stillstands, bedding planes, and contact caves along the limestone/volcanic rock interface, all of which could contribute to high production. Additionally, since they can be screened along the entire phreatic depth down to the volcanic contact they would have relatively high transmissivity (i.e., hydraulic conductivity times saturated thickness) even in relatively-low-permeability, diffuse-flow-dominated limestone. It should be kept in mind, however, that development of new wells in the supra-basal zone could lower the yields of nearby wells that could have close hydrologic connections. Moreover, development of the supra-basal zone will draw water from it that currently recharges down-gradient portions of the surrounding para-basal zone. Care must be taken to identify undeveloped areas that will have minimal effect on already-developed areas. As noted, an accurate and detailed basement map is essential for this purpose.

4. Reasons for pursuing development on the supra-basal zone. The relatively high density of positive control points and consequent higher resolution of the new basement map in this area improves the odds for successful prospecting for supra-basal water in the NGLA. Keeping in mind the considerations cited above, there are at least five positive reasons for pursing development of supra-basal water:

    a. Given that the Santa Rosa-Mataguac-Pati Point complex occupies about 20% of the transverse area of the aquifer, and nearly half of the Andersen Basin, which remains only sparsely developed but adjacent to a substantial military activity, it may be cost-effective to judiciously pursue development in this zone.

b. Supra-basal water is invulnerable to saltwater up-coning and lateral migration, since the base of the unit is above sea level.

c. It lies upstream of most of the possible sources of surface contamination, at the headwaters of the groundwater basin, even above the para-basal zone.

d. The newly-updated map shows dimples in other locations, similar to the one that may provide the consistent water supply to Y-15. These may provide promising sites for future exploration.

e. Besides targeting such dimples, it might also be productive to install supra-basal wells along the axes of the basement valleys, i.e., Yigo Valley, Tarague Valley, and Anao Valley, where vadose waters descending down-slope are likely to have converged and, over geologic time, dissolved conduits along the limestone-volcanic contact that carry concentrated flow along the axes to para-basal zone.

5. Well design considerations for the supra-basal zone. As noted above, wells drilled anywhere in the supra-basal zone should as a matter of practice be extended all the way to the basement contact, which will not only maximize their chances of being productive, but will also continue to enhance our working knowledge of this high-risk/high-value zone. (Local environmental regulations and/or regulatory interpretations and practices may need to be adjusted accordingly.) As with the para-basal zone, extraction of water from the supra-basal zone will reduce the flow to downstream production wells, which may cause salinity to rise in adjacent para-basal wells.

6. Limitations on mapping and modeling of the supra-basal zone. It should be noted that the karst pathways and other hydrogeologic features of the supra-basal zone are both too complex and poorly known at this time to be incorporated in the map or in numerical groundwater models, including the one built for the 2013 Guam Groundwater Availability Study (Gingerich, 2013; Gingerich and Jenson, 2010). The model could, nevertheless, be applied to help evaluate the effects of supra-basal extraction on the para-basal and basal zones, to the extent that the water budget (cf. Johnson, 2012) for this area can be accurately determined. Continued improvements in the accuracy and precision of the basement map would nevertheless be fruitful for exploration and development of the supra-basal zone.

5.1.4 Other applications: aquifer protection, etc.

Finally, we note that the basement topography indicates how the aquifer is partitioned and provides a basis for predicting karst flow paths that might form along the bedrock-basement contacts, particularly along the axes of the basement valleys. This provides an additional tool to assist planners and regulators in assessing the potential threats from surface contaminants that might reach the bedrock-basement contact. Taboroši et al. (2013) have suggested that mapped concentrations of coastal discharge may be correlated with the axes of the basement valleys. If so, this would also provide an additional clue to the potential pathways and residence times for contaminants in the aquifer.

5.2 Improvements and Updates of the Map

The map provides developers, managers, and regulators with a singularly important tool for groundwater exploration, development, and management. More accurate and detailed maps will become increasingly important and cost-effective as greater demands are placed on already-developed areas, and as development extends into new areas of the aquifer. The latest applications of the USGS model (Gingerich, 2013; Gingerich and Jenson, 2010) suggest, for example, that gentle topographic gradient of the basement at the head of the Yigo-Tumon Trough may make the location of the saltwater toe very sensitive to changes in freshwater lens thickness. To support sustainable management of the aquifer, the map must be kept up to date as new data are acquired, whether incidentally from ongoing exploration for new wells or systematically from targeted research projects, including exploratory drilling.

5.2.1 Regular updates and revisions of the map

Development and production of a sophisticated scientific resource such as this map is a major project that requires a sizeable commitment of scientific expertise and technical skills. In addition to the investments in the 1982 and 1992 geophysical studies, this most recent revision required three-and-a-half years, a budget of about $100,000, and a team of seven researchers (co-authors of this report) to conduct the data search, assemble the database, and prepare the map and accompanying technical report. Keeping the database and map up to date will not only preserve this investment, but will also increase the return on investment as new data are acquired and as geophysical tools and spatial analysis technology continue to improve. More accurate and detailed maps will become increasingly important and cost-effective as sites for new wells are sought in already densely-developed areas and as development is extended into the less-developed, higher-risk frontier locations. We therefore recommend the following:

1. Ongoing update and maintenance of the *NGLA Database*. Under Public Law 24-247, drillers must notify WERI prior to drilling and provide copies of down-hole or geophysical data to be archived at WERI in the Guam Hydrologic Survey (GHS) database. This information should be entered into the *NGLA Database* (Bendixson, 2013) as soon as it is received, along with any other new information, updates, or corrections to existing data that might affect the current model of the basement. The database should be maintained by technical staff at WERI.

2. Annual updates of the map. By the end of each calendar year, the additions and changes to the database should be assessed and brief addenda and/or minor revisions made to the map, with notifications posted on-line in HydroGuam.net (Taboroši et al., 2013b).

3. Five-year revisions of the map and technical report. Every fifth year (beginning 2018), the existing map should be systematically revised utilizing the latest GIS and graphics tools to give it maximum utility for interpretation and application. The attendant report (this one) should be updated accordingly. The five-year revision should incorporate not only the new data collected in the database over the previous five years, but also

new theoretical insights, and new discoveries or revisions of the geology and hydrology of northern Guam, especially from such studies as recommended below.

5.2.2 Development of a comprehensive hydrogeologic map of northern Guam

The production of the updated basement map provides a propitious starting point for a comprehensive hydrogeologic map that would integrate and overlay additional geologic features that are of crucial importance for more accurate and detailed understanding of aquifer properties and processes, including recharge, storage, transport, and discharge, including:

1. The locations and sizes of faults and fractures (some of which are already on the current map); sinkholes, shafts, and caves

2. Coastal seeps, springs, and discharging fractures and caves

3. Rock units and facies, and

4. Infrastructure, including the municipal water and sewage systems, and locations of septic tanks and other potential sources of contamination.

Much of this information is already available, so that GIS coverages containing these features need only to be assembled and overlain on the new basement map.

5.2.3 Coastal discharge evaluation

Field studies of coastal discharge suggest that concentrations of coastal springs may correlate with structural features, such as faults and fractures, and with geomorphic features, such as the subterranean valleys between the basement rises and ridges (Taboroši et al., 2013a). Recent results by Rotzoll et al. (2013) confirm the presence of a zone of lower permeability around the periphery of the plateau (Ayers and Clayshulte, 1984) which may serve to concentrate and focus flow into seeps and springs along the coast. The very high hydraulic conductivities deduced for other areas from the modeling results of Rotzoll et al. (2013) are most likely explained by the presence of some as yet unidentified types of karst conduits.

An important next step toward understanding and explaining the distribution of flow and discharge would be a field study to more precisely locate and quantify the discharge from the major springs and seeps already located and mapped, and to search for undiscovered discharge features that may also provide important clues regarding aquifer properties, dynamics, and evolution. Candidate technologies include thermal infrared (e.g., airborne thermal mapping of the coastal ocean water surface) and electrical resistivity surveys of the coastal zone at selected locations, especially Tumon and Haputo Bay.

5.2.4 Strategic planning and new evaluations of basement topography

Given the improvements in geophysical techniques in the 30 years since publication of the original map, a new comprehensive survey could certainly achieve more accurate and detailed measurements of basement topography. As increasing development puts a premium on more precise targeting of groundwater resources and perhaps the retirement and relocation of some of the more poorly placed or over-deep existing wells, investment in more accurate and detailed resolution of the basement topography will become more and more cost-effective.

Strategic planning for development should evaluate the cost-savings likely to be made by a new comprehensive geophysical study combined with systematic drilling to gain precise control at selected locations—especially in high-risk/high-return areas, such as the supra-basal zone. Optimally, this would be done in conjunction with continued refinements and improvements in modeling. Modern hydrological research tools are best employed in an iterative process whereby updates to maps made with new and better field techniques are then used to update conceptual and numerical models, and output from the models, along with the new and improved maps are used to guide new geologic field studies, geophysical surveys, and exploratory drilling (Schwartz et al., 1990).

Together, these considerations suggest that continued investment in the accuracy and precision of the basement map, along with prudent planning and carefully targeted exploration, will provide a basis for sound continued development and management of Guam's groundwater resources.

REFERENCES

AECOM Technical Services Inc., 2011, Guam Water Well Testing Study to Support US Marine Corps Relocation to Guam: Naval Facilities Engineering Command, Pacific.

Ayers, J. F., and Clayshulte, R. N., 1984, A preliminary study of the hydrogeology of northern Guam: WERI Technical Report No. 56, 77 pp.

BCG, 1992, Groundwater in Northern Guam: Sustainable Yield and Groundwater Development Final Engineering Report: Barrett Consulting Group [now AECOM Technical Services, Inc. in association with John F. Mink for Public Utility Agency of Guam.

Bendixson, V. M., 2013, The Northern Guam Lens Aquifer Database: WERI Technical Report No. 141, 45 pp.

BSP, 2007, Guam 2007 LiDAR survey by Joint Airborne LiDAR Bathymetric Center of Expertise (JALBTCX). Bureau of Statistics and Plans (BPS), Government of Guam

CDM, 1982, Final Report, Northern Guam Lens Study, Groundwater Management Program, Aquifer Yield Report: Camp, Dresser and McKee, Inc. in assoc. with Barrett, Harris & Associates *for* Guam Environmental Protection Agency.

Childs, C., 2004, Interpolating surfaces in ArcGIS Spatial Analyst: ArcUser, v. July-Sept, p. 32-35.

Cloud, P. E. J., 1951, Reconnaissance Geology of Guam and Problems of Water Supply and Fuel Storage, U.S. Geol. Survey, Military Geology Branch.

ESRI, 2003, Using ArcGIS Geostatistical Analyst: ESRI User's Manual, 300 pp.

Fetter, C. W., 2001, Applied Hydrogeology, Upper Saddle River, NJ, Prentice Hall, 598 pp.

Ford, D. C., and Williams, P. W., 2007, Karst Hydrogeology and Geomorphology, West Sussex, England, John Wiley & Sons, Ltd., 562 pp.

Gingerich, S. B., 2013, The effects of withdrawals and drought on groundwater availability in the Northern Guam Lens Aquifer, Guam: U.S. Geological Survey Scientific Investigations Report v. 2013–5216, 76 pp.

Gingerich, S. B., and Jenson, J. W., 2010, Groundwater availability study for Guam; goals, approach, products, and schedule of activities: U.S. Geological Survey Fact Sheet 2010–3084, 4 pp.

Hild, J., Blohm, R., Lahti, R., and Blohm, M., Geophysical Surveys for Ground Water Exploration in Northern Guam, *in* Proceedings 25th Symposium on the Application of Geophysics to Engineering and Environmental Problems, Keystone, Colorado, April 28-May 2 1996, p. 331-341.

Hu, J., 1995, Methods of Generating Surfaces in Environmental GIS Applications, Proceedings, ESRI User Conference.

Hunter, G. J., 1992, Techniques for Assessing the Effect of Processing Errors in Spatial Databases: URISA Proceedings.

ICF Technology, Inc., 1995. Final Report: Groundwater dye trace program and well cluster proposal for the landfill area, Andersen Air Force Base, Guam. Archived at University of Guam Library, Mangilao, Guam.

Jenson, J. W., Jocson, J. M. U., and Siegrist, H. G., Groundwater discharge styles from an uplifted Pleistocene island karst aquifer, Guam, Mariana Islands, *in* Proceedings The Engineering Geology and Hydrology of Karst Terranes, Springfield, Missouri, 1997, Balkema, p. 15-20.

Jenson, J. W., Lander, M. A., and Randall, R. H., 2011, Vadose Flow in a Tropical Island Karst Aquifer, Guam, Mariana Islands, Carbonate Geochemistry: Reactions and Processes in Aquifers and Reservoirs: Billings, Montana, USA, Karst Waters Institute.

Jenson, J. W., Roff, D., Bendixson, V. M., Simard, C. A., and Hylton, T., 2012, 2010 Exploratory Drilling in the Northern Guam Lens Aquifer: New Insights and Questions, *in* Savarese, M., and Glumac, B., eds., 16th Symposium on the Geology of the Bahamas and Similar Regions, Abstracts & Program: San Salvador Island, Bahamas.

Jocson, J. M. U., Jenson, J. W., and Contractor, D. N., 1999, Numerical Modeling and Field Investigation of Infiltration, Recharge, and Discharge in the Northern Guam Lens Aquifer: WERI Technical Report No. 88, 22 pp.

Johnson, A. G., 2012, A water-budget model and estimates of groundwater recharge for Guam: U.S. Geological Survey Scientific Investigations Report 2012–5028, 53 pp.

Joint Guam Program Office, 2010, Relocating Marines from Okinawa; Visiting Aircraft Carrier Berthing, and Army Air and Missile Defense Task Force: Guam Program Management Office (ed.) Final Environmental Impact Statement: Guam and CNMI Military Relocation: Naval Facilities Engineering Command, Pacific, 322 pp.

Lander, M. A., Jenson, J. W., and Beausoliel, C., 2001, Responses of well water levels on northern Guam to variations in rainfall and sea level: WERI Technical Report No. 94, 36 pp.

McDonald, M. Q., and Jenson, J. W., 2003, Chloride history and trends of water in production wells in the Northern Guam Lens Aquifer: WERI Technical Report No. 98, 70 p.

Mink, J. F., 1976, Groundwater resources on Guam: Occurrence and Development: WERI Technical Report No. 1, 276 pp.

-, 1982, Appendix B1: Description of geophysical exploration methods, Final Report, Northern Guam Lens Study, Groundwater Management Program, Aquifer Yield Report: Camp, Dresser and McKee, Inc. in assoc. with Barrett, Harris & Associates *for* Guam Environmental Protection Agency.

Mink, J. F., and Vacher, H. L., 1997, Hydrogeology of northern Guam, *in* Vacher, H. L., and Quinn, T., eds., Geology and Hydrogeology of Carbonate Islands. Developments in Sedimentology 54: Amsterdam, Elsevier Science, p. 743-761.

Mitasova, H., and Hofierka, J., 1993, Interpolation by Regularized Spline with Tension: II. Application to Terrain Modeling and Surface Geometry Analysis: Mathematical Geology, v. 25, no. 6, p. 657-669.

Mylroie, J. E., and Carew, J. L., 2000, Speleogenesis in young limestones in coastal and oceanic settings, *in* Klimchouk, A. B., Ford, D. C., Palmer, A. N., and Dreybrodt, W., eds., Speleogenesis: Evolution of Karst Aquifers: Huntsville, AL, National Speleological Society, p 225-233.

Mylroie, J. E., and Jenson, J. W., 2000, The Carbonate Island Karst Model applied to Guam: Theoretical and Applied Karstology, v. 13-14, p. 51-56.

Mylroie, J. E., Jenson, J. W., Taborosi, D., Jocson, J. M. U., Vann, D. T., and Wexel, C., 2001, Karst features on Guam in terms of a general model of carbonate island karst: Journal of Cave and Karst Studies, v. 63, no. 1, p. 9-22.

Neuendorf, K. K. E., Mehl, J. P., Jr., and Jackson, J. A., 2011, Glossary of Geology, 5th Edition, American Geological Institute, 800 p.

Pacific Island Engineers (PIE), 1950, The Geology of Middle Guam, Island of Guam, Mariana Islands: Prepared for the Department of the Navy, Bureau of Yards and Docks.

PCR Environmental Inc., 2012, Spring 2012 Long Term Groundwater Monitoring Report: Main Base and MARBO Annex Operable Units, Andersen Air Force Base, Guam: Naval Facilities Engineering Command, Marianas, v. October 2012, 99 pp.

Rotzoll, K., Gingerich, S. B., Jenson, J. W., and El-Kadi, A. I., 2013, Estimating hydraulic properties from tidal attenuation in the Northern Guam Lens Aquifer, Territory of Guam, USA: Hydrogeology Journal, v. 21, no. 3, p. 643-654.

Schlanger, S. O., 1964, Petrology of the Limestones of Guam: U.S. Geological Survey, 403-D, 52 pp.

Schwartz, F. W., Andrews, C. B., Freyberg, D. L., Kincaid, C. T., Konikow, L. F., McKee, C. R., McLaughlin, D. B., Mercer, J. W., Quinn, E. J., Rao, P. S. C., Rittman, B. E., Runnels, D. D., van der Heijde, P. K. M., and Walsh, W. J., 1990, Ground Water Models: Scientific and Regulatory Applications, Washington, D.C., National Academy Press, 55 pp.

Siegrist, H. G., and Randall, R. H., Carbonate geology of Guam, *in* Proceedings Proceedings of the Seventh International Coral Reef Symposium, Mangilao, Guam, June 22-26 June, 1992 1992a, Volume 2, University of Guam Marine Laboratory & Water & Energy Research Institute of the Western Pacific, p. 1195-1216.

Siegrist, H. G., and Reagan, M. K., 2008, Geologic Map and Sections of Guam, Mariana Islands (1:50,000), Revision of original map from USGS Professional Report 403A, 1964, by Tracey, J.I., Jr., Schlanger, S.O., Stark, J.T., Doan, D.B. & May, H.G. Field interpretations for 2008 revision assisted by Randall, R.H. and Jenson, J.W., Water & Environmental Research Institute of the Western Pacific, University of Guam, Mangilao, Guam.

Simard, C. A., Jenson, J. W., and Lander, M. A., Analysis of Salinity in the Northern Guam Lens Aquifer, *in* Proceedings 16th Symposium on the Geology of the Bahamas and Similar Regions, Gerace Research Center, San Salvador Island, Bahamas, June 14-18, 2012 2012, in review.

-, 2013, Analysis of Salinity in the Northern Guam Lens Aquifer: WERI Technical Report No. 143, 65 pp.

Stafford, K. W., Mylroie, J. E., and Jenson, J. W., 2004, Karst geology of Aguijan and Tinian, CNMI cave inventory and structural analysis of development: WERI Technical Report No. 106, 239 pp.
Stearns, H. T., 1937, Geology and Water Resources of the Island of Guam, Mariana Islands, US Navy Manuscript.
Taborosi, D., Jenson, J. W., and Mylroie, J. E., 2013a, Field observations of coastal discharge from an uplifted carbonate island aquifer, northern Guam, Mariana Islands: A descriptive geomorphic and hydrogeologic perspective Journal of Coastal Research, v. 29, no. 4, p. 926 – 943.
Taboroši, D., Khosrowpanah, S., Kottermair, M., and Jenson, J. W., 2013b, Hydrologic Atlas of Northern Guam: Mangilao, Guam, Water & Environmental Research Institute of the Western Pacific, University of Guam.
Tracey, J. I., Jr., Schlanger, S. O., Stark, J. T., Doan, D. B., and May, H. G., 1964, General Geology of Guam: U.S. Geological Survey Professional Paper, 403-A, 104 pp.
U.S. Environmental Protection Agency, 1978, Guam—Sole or Principal Source Aquifer Designation: Federal Register, v. 43 FR 17888 no. April 26, 1978.
USGS, 1978, Topographic Map of Guam, Mariana Islands (15-minute quadrangle).
Vacher, H. L., and Mylroie, J. E., 2002, Eogenetic karst from the perspective of an equivalent karst medium: Carbonates and Evaporites, v. 17, p. 182-196.
Vann, D. T., 2000, Unpublished manuscript: revision of Northern Guam Lens basement volcanic contours: Water & Environmental Research Institute, University of Guam.
-, 2010, Unpublished initial revision of basement map for USGS Groundwater Availability Study
Ward, P. E., and Brookhart, J. W., 1962, Military Geology of Guam: Water Resources Supplement: U.S. Army. Chief Eng., Intellig. Div., Headq. U.S. Army Pacific, Tokyo.
Ward, P. E., Hoffard, S. H., and Davis, D. A., 1965, Hydrology of Guam: U.S. Geological Survey Professional Paper 403-H, 28 pp.
WERI website, 2013, Locally Sponsored Research: Guam Comprehensive Monitoring Program.

APPENDICES

Appendix A

Productive and unproductive exploratory wells drilled during the 1990s

Unproductive Wells	Date drilled	Productive Wells	Date Drilled
***A-33	9/16/98	AG-7	4/26/1994
*AG-3	8/11/92	AG-10	3/17/1994
*AG-4	9/2/92	D-22A	3/29/1995
**AG-5	12/10/92	D-23	10/20/1994
**AG-8	5/31/94	D-24	9/23/1994
**AG-9	5/2/94	D-25	2/10/1994
**M-16A	5/10/98	ETF-1	7/21/1998
**M-16B	5/10/98	ETF-2	7/15/1998
**M-16C	5/10/98	ETD-1	7/25/1998
**M-16D	5/10/98	ETD-1A	1/6/1999
**Y-13	8/3/94	ETD-2	8/17/1998
**Y-18	5/8/98	ETD-4	1/21/1999
**Y-19	4/5/94	ETD-5	9/10/1998
**Y-20A	8/2/95	ETD-6	9/25/1998
**Y-22	4/29/98	ETD-7	9/20/1998
**Y-24	5/7/98	ETD-8	9/17/1998
**Y-25	4/27/98	ETF-3	9/13/1998
**Y-28	4/28/98	ETY-1	12/10/1998
**Y-30	5/8/98	ETY-2	12/17/1998
**Y-32	6/16/98	ETY-3	12/21/1998
**ETD-3	8/29/98	ETY-5	10/4/1999
**F-20	7/30/98	ETY-5A	12/13/1999
		Y-21A	12/13/1999
		F-13	7/23/1992
		F-15	7/27/1992
		F-16	7/28/1992
		F-17	1/17/1994
		F-18	1/22/1994
		F-23	5/23/2000
		F-25	4/13/2000
		M-18	4/20/1993
		M-20	2/16/1994
		M-20A	7/13/1994
		M-23	6/17/1998
		Y-10	9/14/1994
		Y-11	8/16/1994
		Y-12	8/10/1994
		Y-14	7/7/1994
		Y-15	6/15/1994
		Y-16	5/4/1998
		Y-27	5/11/1998

*marginal
**dry
***unknown

Appendix B

Map control points

"Spline interpolation data points," below, are those used in the initial spline interpolation (Section 3.4).

Spline interpolation control points

ID	Information class	Basement elevation (m)	Longitude [4]	Latitude [4]	Notes
AG-2	Borehole distinct	-22.2	144.873629	13.584447	borehole distinct - drill log depth records that provide specific depth or within a five feet range (e.g., 205-255') note of non-carbonate transition
AG-3	Borehole distinct	-14.9	144.872741	13.581742	
AG-4	Borehole distinct	-18.3	144.87274	13.579799	
AG-5	Borehole distinct	-22.9	144.874062	13.581778	
AG-7	Borehole distinct	3.9	144.87504	13.577854	
AG-8	Borehole distinct	-2.0	144.876859	13.576407	
AG-9	Borehole distinct	7.6	144.876472	13.577926	
D-22A	Borehole distinct	2.7	144.856619	13.552516	
D-24	Borehole distinct	-31.7	144.854737	13.556513	
Y-13	Borehole distinct	90.5	144.914334	13.548176	
Y-15	Borehole distinct	40.8	144.915794	13.555072	
Y-17	Borehole distinct	63.7	144.893331	13.549659	
Y-20A	Borehole distinct	68.0	144.917062	13.552223	
Y-22A	Borehole distinct	103.0	144.893768	13.545639	
Y-23	Borehole distinct	53.0	144.898021	13.54312	
Y-24	Borehole distinct	49.7	144.915751	13.552432	
Y-25	Borehole distinct	75.3	144.917624	13.549719	
Y-28	Borehole distinct	72.8	144.900658	13.557747	
Y-30	Borehole distinct	123.7	144.908353	13.555926	
Y-32	Borehole distinct	84.1	144.889946	13.550649	
IRP-17	Borehole distinct	7.6	144.902997	13.574259	
IRP-41	Borehole distinct	-37.8	144.911375	13.584377	
IRP-59	Borehole distinct	51.5	144.898773	13.571632	
EX-3	Borehole distinct	8.2	144.857983	13.495755	
EX-11	Borehole distinct	-15.2	144.841289	13.485545	
ETD-3	Borehole distinct	16.8	144.85854	13.54253	
ETD-2	Borehole distinct	-15.8	144.854726	13.545406	
HGC-1	Borehole distinct	-76.8	144.861355	13.576153	
M-16	Borehole distinct	15.5	144.854091	13.489782	
M-5	Borehole distinct	-65.8	144.843605	13.500579	
M-2	Borehole distinct	-2.7	144.843008	13.485374	
A-5	Borehole distinct	-56.7	144.760791	13.45759	
A-11	Borehole distinct	-43.3	144.756619	13.445062	
AECOM-5	Borehole distinct	53.0	144.916693	13.562105	
MGG-21	Borehole indistinct	14	144.778852	13.411571	borehole indistinct - drill log depth records that have a wide range of non-carbonate transition
MGG-34	Borehole indistinct	75	144.909304	13.569646	
MGG-55	Borehole indistinct	0	144.879995	13.582371	
MGG-120	Borehole indistinct	-77	144.76083	13.455673	
MGG-130	Borehole indistinct	63	144.871668	13.561749	
MGG-129	Borehole indistinct	6	144.860306	13.547166	
MGG-147	Borehole indistinct	-32	144.754394	13.466095	
B-2	Borehole indistinct	-46	144.899044	13.576567	
B-3	Borehole indistinct	-37	144.902435	13.577161	
B-4	Borehole indistinct	-38	144.900486	13.578699	
B-5	Borehole indistinct	-83	144.900277	13.583698	
B-6	Borehole indistinct	-27	144.8978	13.582054	
B-7	Borehole indistinct	-82	144.894833	13.581242	
B-8	Borehole indistinct	-74	144.893272	13.581713	
B-9	Borehole indistinct	-45	144.892838	13.581361	
B-10	Borehole indistinct	-81	144.890861	13.583477	
B-11	Borehole indistinct	-121	144.890421	13.589271	
AECOM-8	Borehole indistinct	43	144.879642	13.510075	
A-1a	Seismic, all from [2]	-64	144.752001	13.442865	Seismic coordinates all approximated from [2]
A-2a	Seismic	-70	144.759279	13.450205	
A-2b	Seismic	-61	144.760877	13.455212	
A-3a	Seismic	-85	144.762012	13.44743	
A-3b	Seismic	-64	144.766897	13.444085	
A-4a	Seismic	-49	144.774857	13.442087	
A-4b	Seismic	-6	144.778264	13.435407	
A-6a	Seismic	-162	144.773945	13.460888	
A-7a	Seismic	-67	144.785993	13.436409	
A-7b	Seismic	-49	144.792928	13.437854	
A-8a	Seismic	-76	144.790065	13.437186	
A-8b	Seismic	-152	144.792246	13.443422	
B-1a	Seismic	0	144.810669	13.478905	
B-1b	Seismic	30	144.812831	13.482574	
B-2b	Seismic	-24	144.831014	13.475229	
B-3a	Seismic	-165	144.811016	13.50283	
C-1a	Seismic	9	144.819426	13.485916	
C-1b	Seismic	12	144.821811	13.492695	
C-2a	Seismic	21	144.827379	13.487243	
C-3b	Seismic	-9	144.841255	13.495581	
C-4a	Seismic	34	144.85001	13.493019	
D-1b	Seismic	-134	144.852861	13.506594	
D-4b	Seismic	-134	144.858886	13.512105	
D-6a	Seismic	-61	144.879699	13.515593	
D-8a	Seismic	-122	144.826702	13.507499	

Spline interpolation control points (continued)

ID	Information class	Basement elevation (m)	Longitude [4]	Latitude [4]	Notes
S-2b	Seismic, all from [2]	49	144.864515	13.55755	
S-4a	Seismic	-101	144.833541	13.542142	
S-7a	Seismic	82	144.869395	13.560277	
S-7b	Seismic	101	144.875806	13.560003	
E-5a	Seismic	-122	144.832855	13.563022	
E-6b	Seismic	61	144.860471	13.562604	
E-7b	Seismic	-70	144.85476	13.580892	
E-10a	Seismic	77	144.88461	13.574596	
E-12a	Seismic	49	144.895195	13.553168	
E-12b	Seismic	110	144.897573	13.558626	
E-15a	Seismic	-40	144.889884	13.539658	
E-18b	Seismic	85	144.914559	13.525452	
E-19a	Seismic	79	144.886801	13.512507	
E-19b	Seismic	76	144.890573	13.517694	
E-20a	Seismic	-107	144.815521	13.52482	
E-21a	Seismic	76	144.881668	13.567637	
E-21b	Seismic	58	144.887948	13.563268	
F-4b	Seismic	-73	144.866908	13.613082	
BONG-1	Seismic	-53	144.85029	13.563901	
BONG-3	Seismic	-43	144.852193	13.563349	
TDEM7-13	Time Domain Electromagnetic (TDEM) detection, all from [2]	-149	144.929955	13.546402	TDEM coordinates all approximated from [2]
TDEM7-14	TDEM	-64	144.929373	13.546448	
TDEM7-12	TDEM	-137	144.928703	13.552088	
TDEM7-6	TDEM	-137	144.926328	13.551421	
TDEM7-8	TDEM	11	144.92129	13.546698	
TDEM-7	TDEM	-2	144.92129	13.547403	
TDEM-2	TDEM	-46	144.922216	13.54996	
TDEM-1	TDEM	-68	144.922559	13.550954	
TDEM-10	TDEM	-44	144.923189	13.554117	
TDEM-9	TDEM	-81	144.9228	13.553223	
TDEMW42	TDEM	-21	144.922116	13.551569	
TDEMW41	TDEM	7	144.920471	13.551615	
TDEMW31	TDEM	84	144.919123	13.552475	
TDEM7-3	TDEM	91	144.911911	13.557116	
TDEM7-4	TDEM	103	144.911089	13.557542	
TDEM7-15	TDEM	-76	144.92652	13.547923	
TDEM3-6	TDEM	-33	144.849722	13.553145	
TDEM1-10	TDEM	-31	144.870543	13.583452	
TDEM1-23	TDEM	-33	144.865313	13.58293	
TDEM1-22	TDEM	-41	144.864167	13.583138	
TDEM2-6	TDEM	-41	144.859389	13.581794	
TDEM2-4	TDEM	-44	144.862141	13.578267	
TDEM9-2	TDEM	68	144.894478	13.54488	
CLvolc-1	Specified Basement Boundary Conditions (SBBC)	0	144.894097	13.510153	Sea level boundary conditions along the Mangilao Basin rise, used to control spline interpolation with bathimetry
CLvolc-2	SBBC	0	144.906812	13.517467	
CLvolc-4	SBBC	0	144.929253	13.534038	
CLvolc-5	SBBC	0	144.930756	13.542569	
CLvolc-6	SBBC	0	144.8913	13.506504	
Bathrit-1	Bathymetry, Coarse, USGS quadrangle map?	-357	144.830005	13.659384	All resulting contours (in sea) were clipped at shoreline in final map
Bathrit-2	Bathymetry, Coarse, USGS quadrangle map	-457	144.811324	13.620885	
Bathrit-3	Bathymetry, Coarse, USGS quadrangle map	-521	144.80411	13.59594	
Bathrit-4	Bathymetry, Coarse, USGS quadrangle map	-402	144.803182	13.575151	
Bathrit-5	Bathymetry, Coarse, USGS quadrangle map	-311	144.897663	13.659443	
Bathtum-1	Bathymetry, Coarse, USGS quadrangle map	-338	144.782569	13.516583	
Bathtum-2	Bathymetry, Coarse, USGS quadrangle map	-485	144.747467	13.505287	
Bathtum-3	Bathymetry, Coarse, USGS quadrangle map	-572	144.708489	13.494437	
Bathnor-1	Bathymetry, Coarse, USGS quadrangle map	-311	144.939778	13.61874	
Bathnor-2	Bathymetry, Coarse, USGS quadrangle map	-512	144.991715	13.619057	
Bathnor-3	Bathymetry, Coarse, USGS quadrangle map	-695	144.990317	13.607127	
Bathnor-4	Bathymetry, Coarse, USGS quadrangle map	-622	144.977345	13.570714	
Bathnor-5	Bathymetry, Coarse, USGS quadrangle map	-622	144.956611	13.527888	
Bathnor-6	Bathymetry, Coarse, USGS quadrangle map	-384	144.939873	13.505667	
Bathnor-7	Bathymetry, Coarse, USGS quadrangle map	-530	144.896073	13.479032	
Bathnor-8	Bathymetry, Coarse, USGS quadrangle map	-549	144.855138	13.432683	
Bathnor-9	Bathymetry, Coarse, USGS quadrangle map	-457	144.825307	13.418774	

Spline interpolation points that were refined in the final map

ID	Information class	Basement elevation (m)	Longitude [4]	Latitude [4]	Contour refinement and edit notes
D-17, Swamp Road (D-17X)	Borehole distinct	30.6	144.831648	13.521972	Coordinates were unreliable in Spline interpolation. Later estimated with drill log information and contours were manually adjusted in the Swamp Road area, red coded in final map
F-20 Piga subdivision (F-20X)	Borehole distinct	26.2	144.864083	13.562548	Coordinates corrected to drill log in final map
IRP-5	Borehole distinct	5.5	144.911011	13.565442	Site field checked and placed using satellite imagery, manual contour edits in final map
IRP-6	Borehole distinct	25.0	144.918901	13.578018	Coordinates corrected to USGS coordinates in final map
MGC-2	Borehole distinct	-63.1	144.840514	13.464506	Coordinates conflicting in drill log, two sites. Only the metric NE coordinate matches the drill log elevation.

Spline interpolation points that were refined in the final map (continued)

ID	Information class	Basement elevation (m)	Longitude [4]	Latitude [4]	Contour refinement and edit notes
Y-7, Yigo Elementary School next to entrance (Y-7X)	Borehole distinct	-50.6	144.895457	13.535268	Site field checked and placed using satellite imagery, manual contour edits in final map
Y-18 north Yigo (Y-18X)	Borehole distinct	80.2	144.892768	13.54291	Coordinates corrected to drill log in final map
A-3	Borehole indistinct	-78	144.757367	13.452121	Site field checked and placed using satellite imagery, manual contour edits in final map
AECOM-3	Borehole indistinct	-54	144.888142	13.583539	Coordinates corrected to USGS, manual contour edits in final map
Msprings	SBBC, distinct point, non borehole	79.2	144.736034	13.464133	Replaced with positive control terrain in final map
CLvolc-3	SBBC	0	144.920026	13.52355	Removed and replaced with positive control terrain, manual contour editing in final map
AECOM-9	Negative Control, active, spline interpolated	-75	144.866957	13.507926	Elevation control replaced with manual edit of contour to negative control. Coordinates corrected to USGS coordinates in final map
M-4	Negative Control, active, spline interpolated	-20	144.847929	13.48703	Elevation control replaced with manual edit of contour to negative control active in final map
M-8	Negative Control, active, spline interpolated	-20	144.850868	13.487069	Elevation control replaced with manual edit of contour to negative control active in final map
M-20 (M-20A)	Negative Control, active, spline interpolated	-20	144.827804	13.493291	Elevation control replaced with manual edit of contour to negative control active in final map
MAT	SBBC, Coarse estimation	183	144.882571	13.546495	Replaced by geologic area in Mataguac Alutom formation outcrop [1], 20m contours [3], and one peak DEM raster cell point [3]
MAT	SBBC, Coarse estimation	183	144.883116	13.545727	
MAT	SBBC, Coarse estimation	183	144.882294	13.546369	
MAT	SBBC, Coarse estimation	183	144.883115	13.545392	
ROSA	SBBC, Coarse estimation	244	144.915157	13.536126	Replaced by geologic area in Santa Rosa Alutom formation outcrop [1], 20m contours [3], and one peak DEM raster cell-point [3]
ROSA	SBBC, Coarse estimation	183	144.911153	13.54317	
ROSA	SBBC, Coarse estimation	183	144.909379	13.542494	
ROSA	SBBC, Coarse estimation	183	144.911591	13.53499	
ROSA	SBBC, Coarse estimation	183	144.911969	13.533806	
ROSA	SBBC, Coarse estimation	183	144.912605	13.532377	
ROSA	SBBC, Coarse estimation	213	144.917858	13.539849	
ROSA	SBBC, Coarse estimation	213	144.916094	13.540663	
ROSA	SBBC, Coarse estimation	213	144.914071	13.540945	
ROSA	SBBC, Coarse estimation	213	144.912091	13.537141	
ROSA	SBBC, Coarse estimation	213	144.913911	13.537266	
ROSA	SBBC, Coarse estimation	213	144.912275	13.535966	
ROSA	SBBC, Coarse estimation	213	144.912948	13.534374	
ROSA	SBBC, Coarse estimation	213	144.914406	13.532304	
PAF-1	SBBC, Coarse DEM or quadrangle map	122	144.730418	13.468435	Replaced by geologic area, Alutom formation area south of Pago-Adelup Fault [1], and 20m contour [3] . Final map clipped out resulting contours, south of fault
PAF-2	SBBC, Coarse DEM or quadrangle map	61	144.737835	13.461512	
PAF-3	SBBC, Coarse DEM or quadrangle map	91	144.740218	13.458511	
PAF-5	SBBC, Coarse DEM or quadrangle map	61	144.743709	13.452175	
PAF-6	SBBC, Coarse DEM or quadrangle map	61	144.746101	13.447331	
PAF-4	SBBC, Coarse DEM or quadrangle map	91	144.741834	13.456089	
PAF-7	SBBC, Coarse DEM or quadrangle map	61	144.749767	13.443751	
PAF-8	SBBC, Coarse DEM or quadrangle map	61	144.754873	13.438491	
PAF-9	SBBC, Coarse DEM or quadrangle map	30	144.755132	13.438075	
PAF-10	SBBC, Coarse DEM or quadrangle map	30	144.761697	13.430563	
PAF-11	SBBC, Coarse DEM or quadrangle map	30	144.765954	13.425311	
PAF-12	SBBC, Coarse DEM or quadrangle map	61	144.762888	13.420386	
PAF-13	SBBC, Coarse DEM or quadrangle map	61	144.75769	13.430319	
PAF-14	SBBC, Coarse DEM or quadrangle map	61	144.755732	13.433736	
PAF-15	SBBC, Coarse DEM or quadrangle map	61	144.751641	13.437994	
PAF-16	SBBC, Coarse DEM or quadrangle map	91	144.746525	13.442079	
PAF-17	SBBC, Coarse DEM or quadrangle map	91	144.743459	13.444501	
PAF-18	SBBC, Coarse DEM or quadrangle map	122	144.742693	13.449834	
PAF-19	SBBC, Coarse DEM or quadrangle map	183	144.741067	13.452591	
PAF-20	SBBC, Coarse DEM or quadrangle map	183	144.738934	13.455764	
PAF-21	SBBC, Coarse DEM or quadrangle map	122	144.735526	13.455095	
PAF-22	SBBC, Coarse DEM or quadrangle map	122	144.730585	13.458592	

[1] Tracey et al (1964) Geologic Map Sections of Guam, Mariana Islands, Professional Paper 403, USGS; Siegrist et al. (2008) Geologic Map Sections of Guam, Mariana Islands, WERI, UOG

[2] Mink (1982) - Seismic, Plate-1; Mink (1992) - TDEM

[3] BSP (2007) LiDAR based bare earth DEM (1 m raster resolution), converted to 20 m contour

[4] Prepared in Geographic Coordinate System: GCS_WGS_1984, Datum: D_WGS_1984, Prime Meridian: Greenwich, Angular Unit: Decimal Degrees

"Final map positive control points," below, are the positive control points used to build the final map.

Final map positive control points

ID	Name	Alias and notes	Information class	Basement elevation (m)	Longitude [4]	Latitude [4]
A-003	A-3	Site field checked, along roadside of Route 4 by Chaot River, contours in the area was manually edited	Borehole distinct	-78	144.758609	13.450708
A-005	A-5	Original spline interpolation point, checked with USGS coordinates	Borehole distinct	-56.7	144.760829	13.457572
A-011	A-11	Original spline interpolation point	Borehole distinct	-43.3	144.756619	13.445062
AECOM-003	AECOM-3	Coordinates corrected to USGS, required manual editing of contours	Borehole distinct	-53.7	144.888115	13.583529
AECOM-005	AECOM-5	Original spline interpolation point, area was manually edited	Borehole distinct	53.4	144.9168	13.56236
AG-002	AG-2		Borehole distinct	-22.2	144.87356	13.584392
AG-003	AG-3		Borehole distinct	-14.9	144.872741	13.581742
AG-004	AG-4		Borehole distinct	-18.3	144.87274	13.579799
AG-005	AG-5		Borehole distinct	-22.9	144.874062	13.581778
AG-007	AG-7	Original spline interpolation point	Borehole distinct	3.9	144.874716	13.578127
AG-008	AG-8	Original spline interpolation point	Borehole distinct	-2	144.876607	13.576593
AG-009	AG-9		Borehole distinct	7.6	144.876472	13.577926
D-022A	D-22A		Borehole distinct	2.7	144.85669	13.552576
D-024	D-24		Borehole distinct	-31.7	144.854795	13.556595
ETD-002	ETD-2		Borehole distinct	-15.8	144.854726	13.545406
ETD-003	ETD-3		Borehole distinct	16.8	144.85854	13.54253
EX-003	EX-3		Borehole distinct	8.2	144.857983	13.495755
EX-011	EX-11	Original spline interpolation point	Borehole distinct	-15.2	144.841299	13.485514
F-020	F-20	F-20X, Piga Subdivision, coordinates based on drill log	Borehole distinct	26.2	144.863844	13.562695
HGC-001	HGC-1		Borehole distinct	-76.8	144.861355	13.576153
IRP-005	IRP-5	Site field checked, located on main street corner entrance of Auto Care in AAFB, Yigo. Manual editing of contours in the area	Borehole distinct	5	144.919975	13.565598
IRP-006	IRP-6		Borehole distinct	25	144.91865	13.578203
IRP-017	IRP-17	Original spline interpolation point	Borehole distinct	7.6	144.888656	13.574451
IRP-041	IRP-41	Original spline interpolation point	Borehole distinct	-37.8	144.91112	13.584559
IRP-059	IRP-59	Original spline interpolation point	Borehole distinct	51.5	144.89852	13.571818
M-002	M-2	Original spline interpolation point	Borehole distinct	-18	144.843039	13.485351
M-005	M-5		Borehole distinct	-65.8	144.843605	13.500579
M-016	M-16		Borehole distinct	15.5	144.854091	13.489782
MGC-002M	MGC-2 (M)	Drill log, MD Inc. (1991), Well M-2, Mangilao Golf Corse, Pagat Mangilao. Conflicting coordinates in drill log, however, the metric northing easting matches the recorded elevation 61 m. MGC-002M is the new ID in the borehole database	Borehole distinct	-63	144.8402569	13.463307
Y-013	Y-13	Original spline interpolation point	Borehole distinct	90.5	144.914079	13.548363
Y-015	Y-15	Alias Y-23 or Y-13 in borehole database	Borehole distinct	40.8	144.915802	13.555125
Y-017	Y-17	Alias Y-14 in borehole database	Borehole distinct	63.7	144.893331	13.549659
Y-018	Y-18	Y-18(X), not to be confused with Marbo Area Y-18, located along Chalan Paharu, north Yigo - based on drill log NE coordinates	Borehole distinct	110	144.892508	13.543097
Y-023	Y-23	Alias Y-15 in borehole database	Borehole distinct	53	144.898021	13.54312
Y-024	Y-24		Borehole distinct	49.7	144.915499	13.552613
Y-025	Y-25		Borehole distinct	75.3	144.917624	13.549719
Y-028	Y-28	Original spline interpolation point	Borehole distinct	72.8	144.900402	13.557936
Y-030	Y-30	Original spline interpolation point	Borehole distinct	123.7	144.908095	13.556109
Y-022	Y-22		Borehole distinct	103	144.893768	13.545639
Y-032	Y-32		Borehole distinct	84.1	144.889946	13.550649
Y-020A	Y-20A		Borehole distinct	68	144.917062	13.552223
B-002	B-2		Borehole indistinct	-46	144.899044	13.576567
B-003	B-3		Borehole indistinct	-36.6	144.902435	13.577161
B-004	B-4		Borehole indistinct	-38.4	144.900486	13.578699
B-005	B-5		Borehole indistinct	-83.2	144.900277	13.583698
B-006	B-6		Borehole indistinct	-27.1	144.896969	13.582222
B-007	B-7		Borehole indistinct	-82.3	144.894833	13.581242
B-008	B-8		Borehole indistinct	-74.1	144.893272	13.581713
B-009	B-9		Borehole indistinct	-45.4	144.892838	13.581361
B-010	B-10		Borehole indistinct	-81.1	144.890861	13.583477
B-011	B-11		Borehole indistinct	-1.2	144.890421	13.589271
MGG-021	MGG-21		Borehole indistinct	14.3	144.778852	13.411571
MGG-034	MGG-34		Borehole indistinct	75	144.909304	13.569646
MGG-055	MGG-55		Borehole indistinct	0	144.879995	13.582371
MGG-120	MGG-120		Borehole indistinct	-76.8	144.76083	13.455673
MGG-129	MGG-129		Borehole indistinct	6.1	144.860306	13.547166
MGG-130	MGG-130		Borehole indistinct	62.8	144.871668	13.561749
MGG-147	MGG-147		Borehole indistinct	-32.3	144.754394	13.466095
AECOM-008	AECOM-8		Borehole indistinct	43	144.879643	13.510062
MAT	Mataguac DEM	Mataguac DEM 1	SBBC, DEM 1m cell raster-point [3]	190.6	144.88236	13.545579
ROSA-1	ROSA-1	Mt Santa Rosa DEM 1	SBBC, DEM 1m cell raster-point [3]	253.1	144.914178	13.535542
A-001a	A-1a	all seismic points here are from the original spline interpolation points	Seismic	-64	144.752001	13.442865
A-002a	A-2a		Seismic	-70.1	144.759279	13.450205
A-002b	A-2b		Seismic	-61	144.760877	13.455212
A-003a	A-3a		Seismic	-85.3	144.762012	13.44743
A-003b	A-3b		Seismic	-64	144.766897	13.444085
A-004a	A-4a		Seismic	-48.8	144.774857	13.442087
A-004b	A-4b		Seismic	-6.1	144.778264	13.435407
A-006a	A-6a		Seismic	-1.6	144.773945	13.460888
A-007a	A-7a		Seismic	-67.1	144.785993	13.436409
A-007b	A-8b		Seismic	-48.8	144.792928	13.437854

Final map positive control points (continued)

ID	Name	Alias and notes	Information class	Basement elevation (m)	Longitude [5]	Latitude [5]
A-008a	A-8a		Seismic	-76.2	144.790065	13.437186
A-008b	A-8b		Seismic	-1.5	144.792246	13.443422
B-001a	B-1a		Seismic	0	144.810669	13.478905
B-001b	B-1b		Seismic	30.5	144.812831	13.482574
B-002b	B-2b		Seismic	-24.4	144.831014	13.475229
B-003a	B-3a		Seismic	-1.6	144.811016	13.50283
C-001a	C-1a		Seismic	9.1	144.819426	13.485916
C-001b	C-1b		Seismic	12.2	144.821811	13.492695
C-002a	C-2a		Seismic	21.3	144.827379	13.487243
C-003b	C-3b		Seismic	-9.1	144.841255	13.495581
C-004a	C-4a		Seismic	33.5	144.85001	13.493019
D-001b	D-1b		Seismic	-1.3	144.852861	13.506594
D-004b	D-4b		Seismic	-1.3	144.858886	13.512105
D-006a	D-6a		Seismic	-61	144.879699	13.515593
D-008a	D-8a		Seismic	-1.2	144.826702	13.507499
S-002b	S-2b		Seismic	48.8	144.864515	13.55755
S-004a	S-4a		Seismic	-1	144.833011	13.542428
S-007a	S-7a		Seismic	82.3	144.869395	13.560277
S-007b	S-7b		Seismic	100.6	144.875806	13.560003
E-005a	E-5a		Seismic	-1.2	144.832855	13.563022
E-006b	E-6b		Seismic	61	144.860471	13.562604
E-007b	E-7b		Seismic	-70.1	144.855274	13.580777
E-010a	E-10a		Seismic	76.5	144.88461	13.574596
E-012a	E-12a		Seismic	48.8	144.895195	13.553168
E-012b	E-12b		Seismic	109.7	144.897573	13.558626
E-015a	E-15a		Seismic	-39.6	144.889884	13.539658
E-018b	E-18b		Seismic	85.3	144.914559	13.525452
E-019a	E-19a		Seismic	79.2	144.886801	13.512507
E-019b	E-19b		Seismic	76.2	144.890573	13.517694
E-020a	E-20a		Seismic	-1.1	144.815521	13.52482
E-021a	E-21a		Seismic	76.2	144.881668	13.567637
E-021b	E-21b		Seismic	57.9	144.887948	13.563268
F-004b	F-4b		Seismic	-73.1	144.866908	13.613082
BONG-001	BONG-1		Seismic	-52.7	144.85029	13.563901
BONG-003	BONG-3		Seismic	-43	144.852193	13.563349
TDEM7-013	TDEM-13	All TDEM points here are from the original spline interpolation points	TDEM	-1.5	144.929955	13.546402
TDEM7-014	TDEM-14		TDEM	-64	144.929373	13.546448
TDEM7-012	TDEM-12		TDEM	-1.4	144.928703	13.552088
TDEM7-006	TDEM-6		TDEM	-1.4	144.926328	13.551421
TDEM7-008	TDEM-8		TDEM	11	144.92129	13.546698
TDEM-007	TDEM-7		TDEM	-2.1	144.92129	13.547403
TDEM-002	TDEM-2		TDEM	-46.3	144.922216	13.54996
TDEM-001	TDEM-1		TDEM	-68	144.922559	13.550954
TDEM-010	TDEM-10		TDEM	-44.5	144.923189	13.554117
TDEM-009	TDEM-9		TDEM	-81.1	144.9228	13.553223
TDEMW42	TDEMW42		TDEM	-21.3	144.922116	13.551569
TDEMW41	TDEMW41		TDEM	6.7	144.920471	13.551615
TDEMW31	TDEMW31		TDEM	83.5	144.919123	13.552475
TDEM7-003	TDEM7-3		TDEM	90.8	144.911911	13.557116
TDEM7-004	TDEM7-4		TDEM	102.7	144.911089	13.557542
TDEM7-015	TDEM7-15		TDEM	-76.2	144.92652	13.547923
TDEM3-006	TDEM3-6		TDEM	-33.2	144.849722	13.553145
TDEM1-010	TDEM1-10		TDEM	-31.1	144.870543	13.583452
TDEM1-023	TDEM1-23		TDEM	-32.9	144.865313	13.58293
TDEM1-022	TDEM1-22		TDEM	-41.1	144.864167	13.583138
TDEM2-006	TDEM2-6		TDEM	-40.5	144.859389	13.581794
TDEM2-004	TDEM2-4		TDEM	-44.5	144.862141	13.578267
TDEM9-002	TDEM9-2		TDEM	68.3	144.894478	13.54488
CLvolc-001	CLvolc-1	Sea Level Volcanic - 1, all sea-level volcanic boundary condistions here are from the original spline interpolation points	SBBC	0	144.894097	13.510153
CLvolc-002	CLvolc-2	Sea Level Volcanic - 2	SBBC	0	144.906812	13.517467
CLvolc-004	CLvolc-4	Sea Level Volcanic - 4	SBBC	0	144.929253	13.534038
CLvolc-005	CLvolc-5	Sea Level Volcanic - 5	SBBC	0	144.930756	13.542569
CLvolc-006	CLvolc-6	Sea Level Volcanic - 6	SBBC	0	144.8913	13.506504
Bathrit-001	Bathrit-1	Bathymetry, Ritidian - 1, all bathymetric points here are from the original spline interpolation points	Bathymetry, Coarse, USGS Quadrangle map	-357	144.830005	13.659384
Bathrit-002	Bathrit-2	Bathymetry, Ritidian - 2	Bathymetry, Coarse, USGS Quadrangle map	-457	144.811324	13.620885
Bathrit-003	Bathrit-3	Bathymetry, Ritidian - 3	Bathymetry, Coarse, USGS Quadrangle map	-521	144.80411	13.59594
Bathrit-004	Bathrit-4	Bathymetry, Ritidian - 4	Bathymetry, Coarse, USGS Quadrangle map	-402	144.803182	13.575151
Bathrit-005	Bathrit-5	Bathymetry, Ritidian - 5	Bathymetry, Coarse, USGS Quadrangle map	-311	144.897663	13.659443
Bathtum-001	Bathtum-1	Bathymetry, Tumon - 1	Bathymetry, Coarse, USGS Quadrangle map	-338	144.782569	13.516583
Bathtum-002	Bathtum-2	Bathymetry, Tumon - 2	Bathymetry, Coarse, USGS Quadrangle map	-485	144.747467	13.505287
Bathtum-003	Bathtum-3	Bathymetry, Tumon - 3	Bathymetry, Coarse, USGS Quadrangle map	-572	144.708489	13.494437
Bathnor-001	Bathnor-1	Bathymentry, North - 1	Bathymetry, Coarse, USGS Quadrangle map	-311	144.939778	13.61874
Bathnor-002	Bathnor-2	Bathymentry, North - 2	Bathymetry, Coarse, USGS Quadrangle map	-512	144.991715	13.619057
Bathnor-003	Bathnor-3	Bathymentry, North - 3	Bathymetry, Coarse, USGS Quadrangle map	-695	144.990317	13.607127
Bathnor-004	Bathnor-4	Bathymentry, North - 4	Bathymetry, Coarse, USGS Quadrangle map	-622	144.977345	13.570714
Bathnor-005	Bathnor-5	Bathymentry, North - 5	Bathymetry, Coarse, USGS Quadrangle map	-622	144.956611	13.527888
Bathnor-006	Bathnor-6	Bathymentry, North - 6	Bathymetry, Coarse, USGS Quadrangle map	-384	144.939873	13.505667
Bathnor-007	Bathnor-7	Bathymentry, North - 7	Bathymetry, Coarse, USGS Quadrangle map	-530	144.896073	13.479032
Bathnor-008	Bathnor-8	Bathymentry, North - 8	Bathymetry, Coarse, USGS Quadrangle map	-549	144.855138	13.432683
Bathnor-009	Bathnor-9	Bathymentry, North - 9	Bathymetry, Coarse, USGS Quadrangle map	-457	144.825307	13.418774

Final map positive control points (continued), yellow and red coded positive control

ID	Name	Alias and notes	Information class	Basement elevation (m)	Longitude [4]	Latitude [4]
D-022	D-22		Borehole distinct (yellow)	2	144.856701	13.552481
IRP-011	IRP-11		Borehole distinct (yellow)	-16	144.904402	13.576427
M-016B	M-16B		Borehole distinct (yellow)	-14	144.855804	13.490113
MGC-003M	MGC-3M	Drill log in BCA Report (1989) of "Test Well," MD Inc. (1992), Well No. M-3, Mangilao Golf Club, Pagat Mangilao. Coordinates estimated to report map and placed using satellite image	Borehole distinct (yellow)	24	144.845909	13.468074
Y-019	Y-19	Y-19, Lupog Area, W.B. Flores (1995) well coordinates	Borehole distinct (yellow)	-17	144.920937	13.548147
Y-020	Y-20	Y-20, Lupog Area, W.B. Flores 1995 well coordinates	Borehole distinct (yellow)	-21	144.919186	13.547302
D-017X	D-17X	Field checked, well not located. Location based on drill log map and surface elevation information in the Swamp Road Area, resulting in two possible points along the road	Borehole distinct (red)	31	144.854913, np* 144.854871, sp*	13.551556 np 13.549011, sp

Note: the use of geologic area information and corrective data to manually edit contours may have influenced adjustment to neighboring contours. Yellow positive control points are post interpolation (additional) points. Red positive control points are crude approximate and/or possible locations.

* np, north point; sp, south point

[1] Tracey et al (1964) Geologic Map Sections of Guam, Mariana Islands, Professional Paper 403, USGS; Siegrist et al. (2008) Geologic Map Sections of Guam, Mariana Islands, WERI, UOG

[2] Mink (1982) - Seismic, Plate-1; Mink (1992) - TDEM

[3] BSP (2007) LiDAR based bare earth DEM (1 m raster resolution), converted to 20 m contour

[4] Prepared in Geographic Coordinate System: GCS_WGS_1984, Datum: D_WGS_1984, Prime Meridian: Greenwich, Angular Unit: Decimal Degrees

"Final map negative control points," below, are the negative control points used to build the final map.

Final map negative control points active

ID	Name	Alias and notes	Information class	BBE (m)	Interpolated Basement (m)	Longitude [4]	Latitude [4]
AECOM-009	AECOM-9	was used in spline interpolation. Coordinates matched to USGS' records, then manually adjusted in final map.	active	-73	-80.1	144.866681	13.505879
D-027	D-27		active	-20	-23.3	144.855808	13.540851
EX-007	EX-7		active	-126	-125.2	144.82397	13.52333
EX-009	EX-9		active	-84	-89.0	144.80753	13.46967
EX-010	EX-10		active	-108	-97.7	144.83389	13.54183
F-017	F-17	CT-4	active	-19	-17.9	144.863585	13.568118
M-004	M-4	was used in spline interpolation, then manually adjusted in final map	active	0	-21.2	144.847924	13.487022
M-008	M-8	2950-05A, was used in spline interpolation, then manually adjusted in final map	active	-12	-21.3	144.850869	13.487082
M-017A	M-17A		active	-18	-15.7	144.826292	13.493742
M-017B	M-17B		active	-14	-7.3	144.826703	13.492471
M-020A	M-20A	was used in spline interpolation, then manually adjusted in final map	active	-11	-19.2	144.827789	13.493289
NAS-001	NAS-1		active	-21	-27.5	144.807829	13.479362
NRMC-001	NRMC-1	NH-001, all NRMC wells initiated first application of manual adjustment methods	active	-12	-19.3	144.737856	13.473012
NRMC-002	NRMC-2	NH-002	active	-12	-27.0	144.740371	13.472528
NRMC-003	NRMC-3	NH-003	active	-13	-29.9	144.742606	13.472109
Y-007	Y-7	Field checked, located next to entrance gate of Yigo Elementary School, and mapped using satellite image	active	-16	-28.2	144.895471	13.535259

Note: the use of geologic area information and corrective data to manually edit contours may have influenced adjustment to neighboring contours.

Appendix C

Table C-1. Summary of Exploratory Drilling Program results (AECOM Technical Services, 2011; Jenson et al., 2012)

	Guam Water Well Study Results										
Date: 14 December 2010	Test Borehole Location										
Updated: 24 April 2014/1625 PDT By Schumann	Northwest Field			North Field/Main Base				Andersen South		Navy Barrigada	
Well	AECOM 1	AECOM 2	AECOM 3*	AECOM 4	AECOM 5	AECOM 6	AECOM 7	AECOM 8	AECOM 9*	AECOM 10	AECOM 11
Surface Elevation (ft)	475.8	485.4	567.1	532.1	555.2	531.5	523.8	475.0	361.7	382.2	352.7
Well bottom elevation (ft)	-37	-38	-193	66	105	-41	-31	115	-248	-40	-37
Groundwater Elev (ft, msl)	4.4	4.3	29.5	121.6	207.8	2.4	3.2	158.3	4.1	2.7	2.4
Draft: Depth of borehole below w.t. (ft)	42	42	223	56	103	44	34	43	252	43	40
Borehole reached basement	no	no	yes	no	no	no	no	yes	yes	no	no
Elevation of basement (ft) blue = measured, black = estimated from map (Tables 6-1, 6-2, 6-5, 6-4)	-130	-130	-178	25	175	-60	-60	142	deeper than -248	-60	deeper than -37
Inferred groundwater zone (based on modeled w.t.)	Para-basal	Para-basal	Para-basal	Supra-basal	Supra-basal	Basal	Basal	Supra-basal?	Para-basal	Para-basal	Para-basal
Chloride at final pump test step (mg/l)	33	16	16	23	33	227	131	no test	36	55	97
Chloride trend during 72-hr pump test	increase	no trend	no trend	no 72-hr test	no 72-hr test	no trend	increase	no pump test	no 72-hr test	no trend	no trend
pH	7.77	7.8	ND	ND	ND	7.75	ND	7.75	ND	5.39	7.65
Q at final pump test step (gpm)	410	80	250	<20	<40	430	68	<500	<30	500	500
Specific Capacity (Q/s) @ 72 hrs	1708	23	19	<0.6	< 1.1	1387	49	no test	< 1.9	1563	1613
*Intended to be observation well											

Appendix C

AECOM Wells, profiles (to scale).

Note: As reflected in Table C-1, field geology and engineering were done in English units. The profiles below, however, are rendered in meters, as the basement map and modeling projects were done in metric units. (See page viii.)

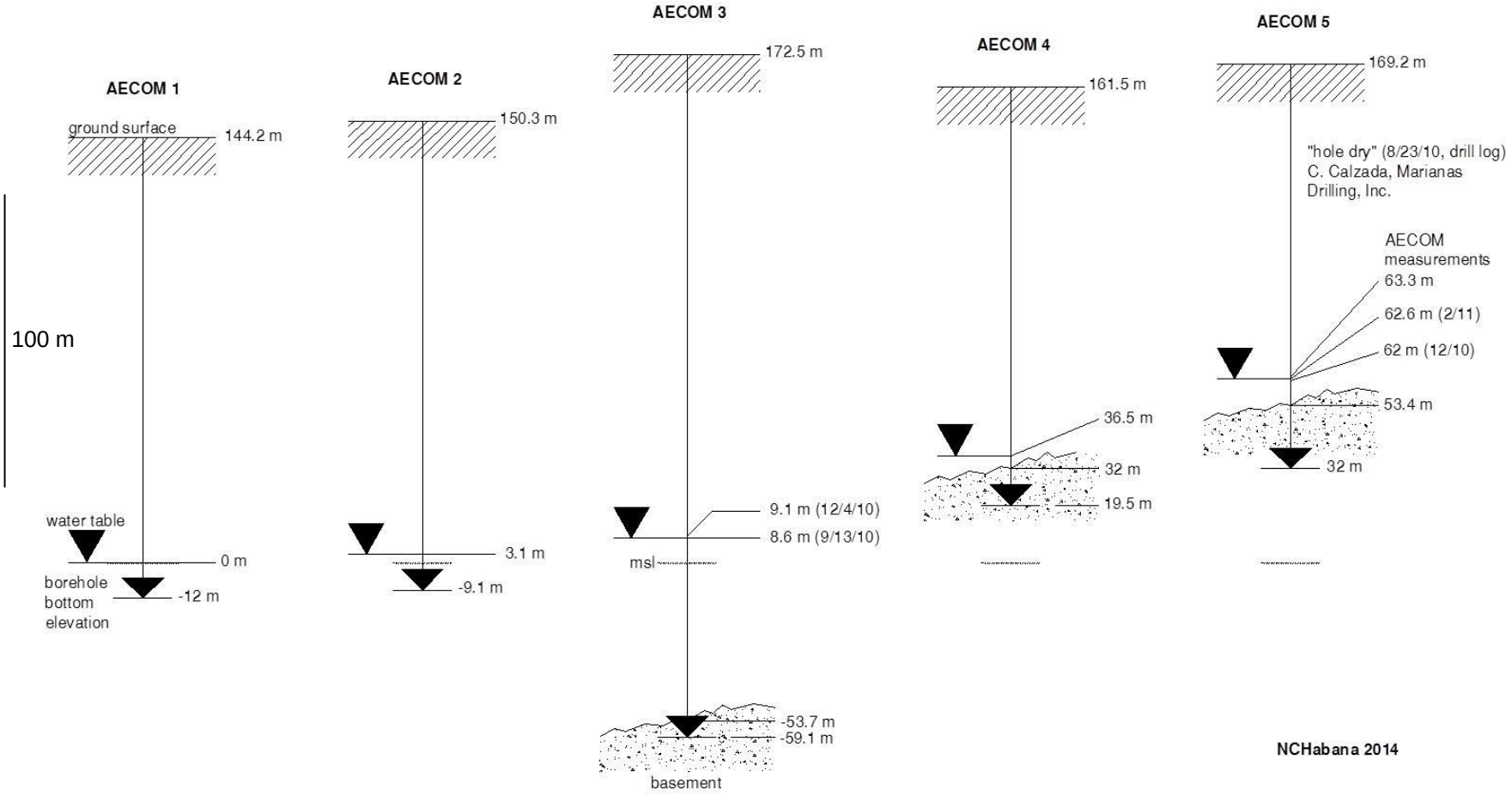

This page intentionally left blank.

AECOM Wells, profiles (continued)

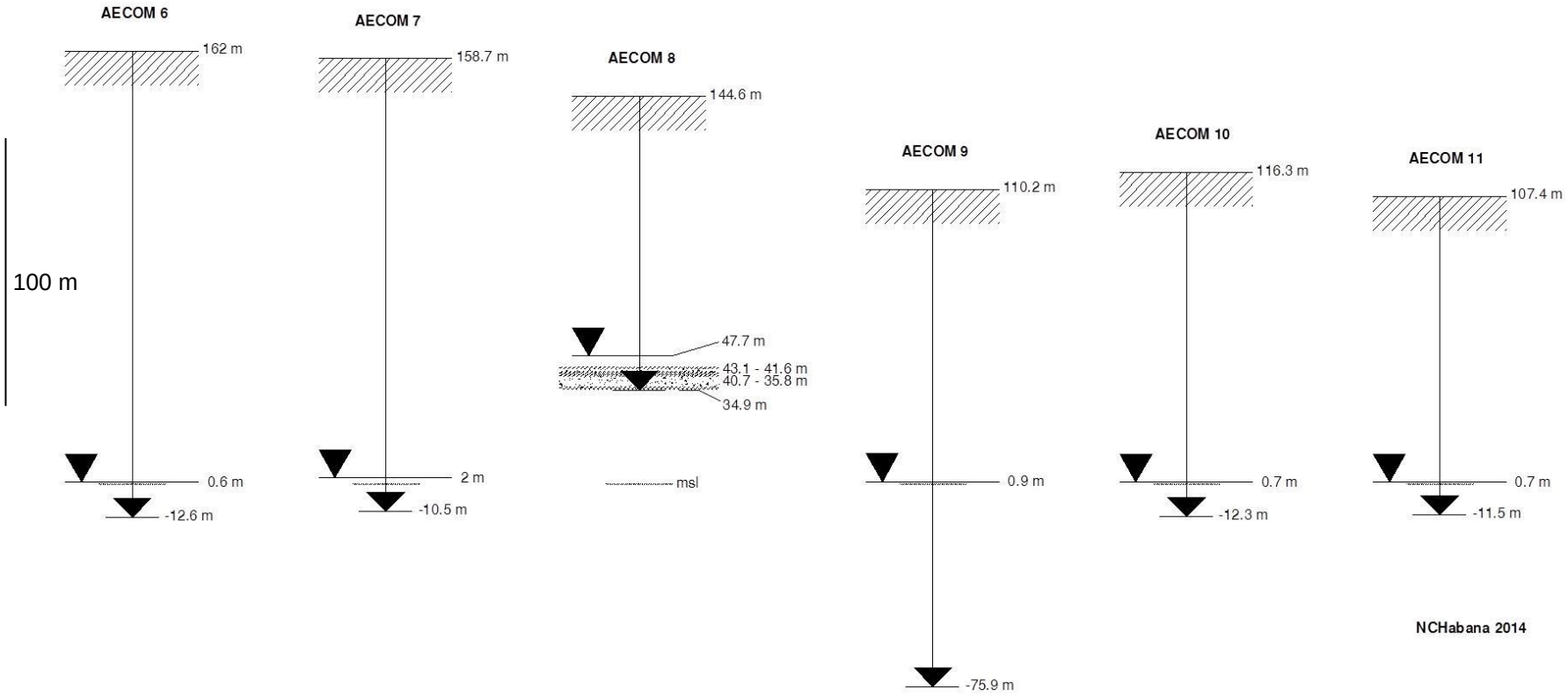

Appendix D

Map of suspect seismic data based on Vann's (2000) analysis

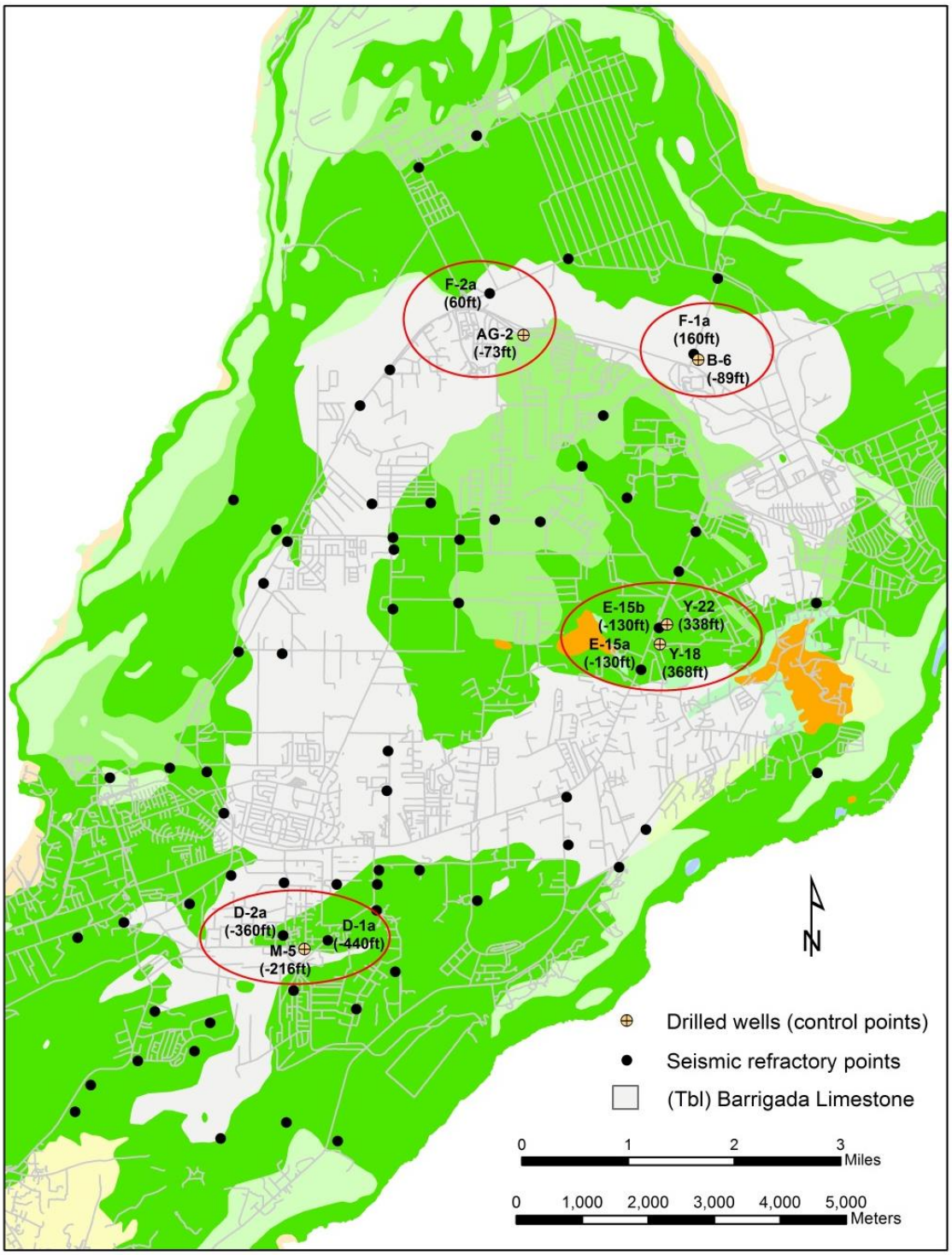

Appendix E. TDEM areas and subsequent basement revision

1) TDEM data from Hild et al. (1996)

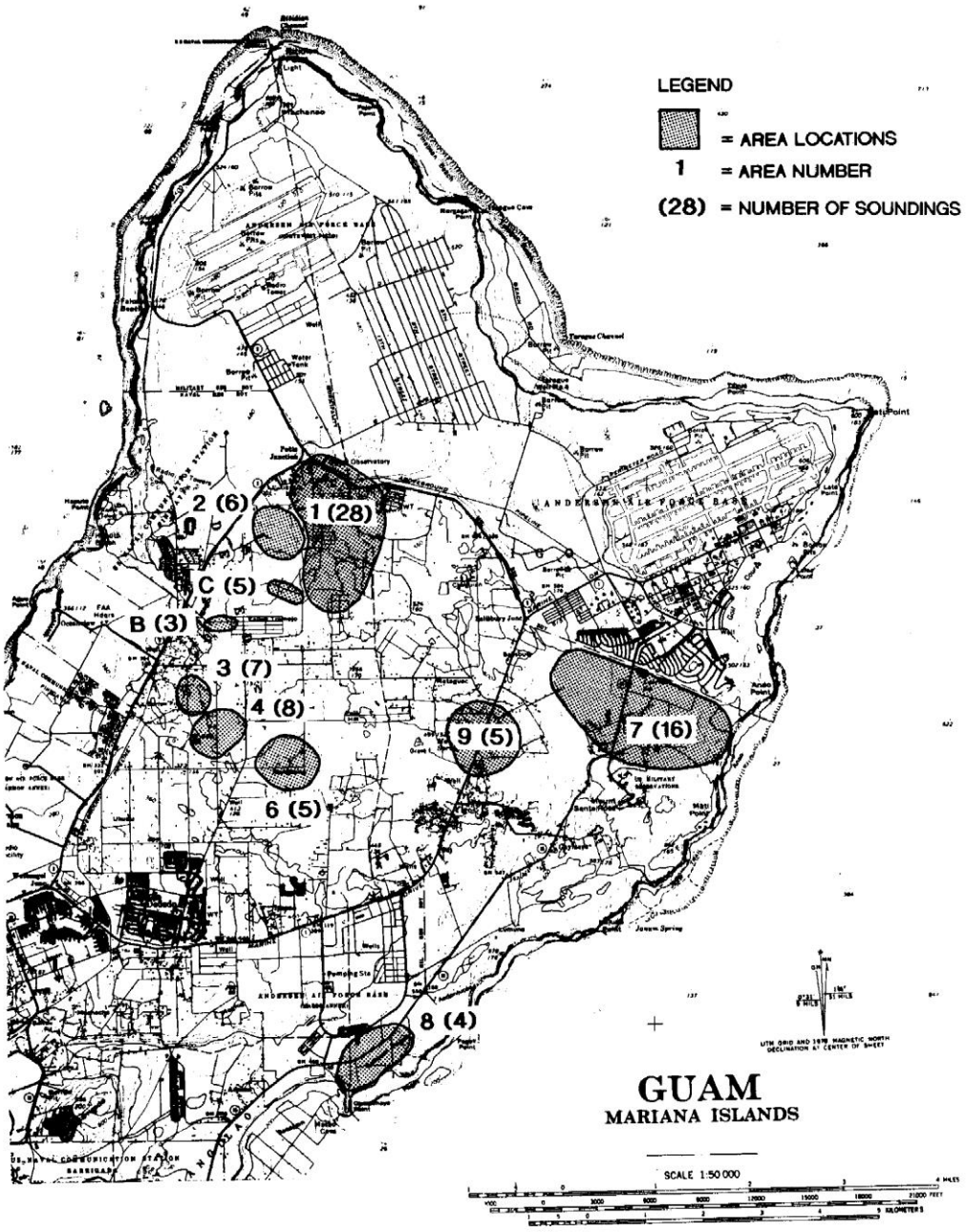

Figure 4. General location map of TDEM sounding areas.

2) 1992 basement map revision from TDEM data

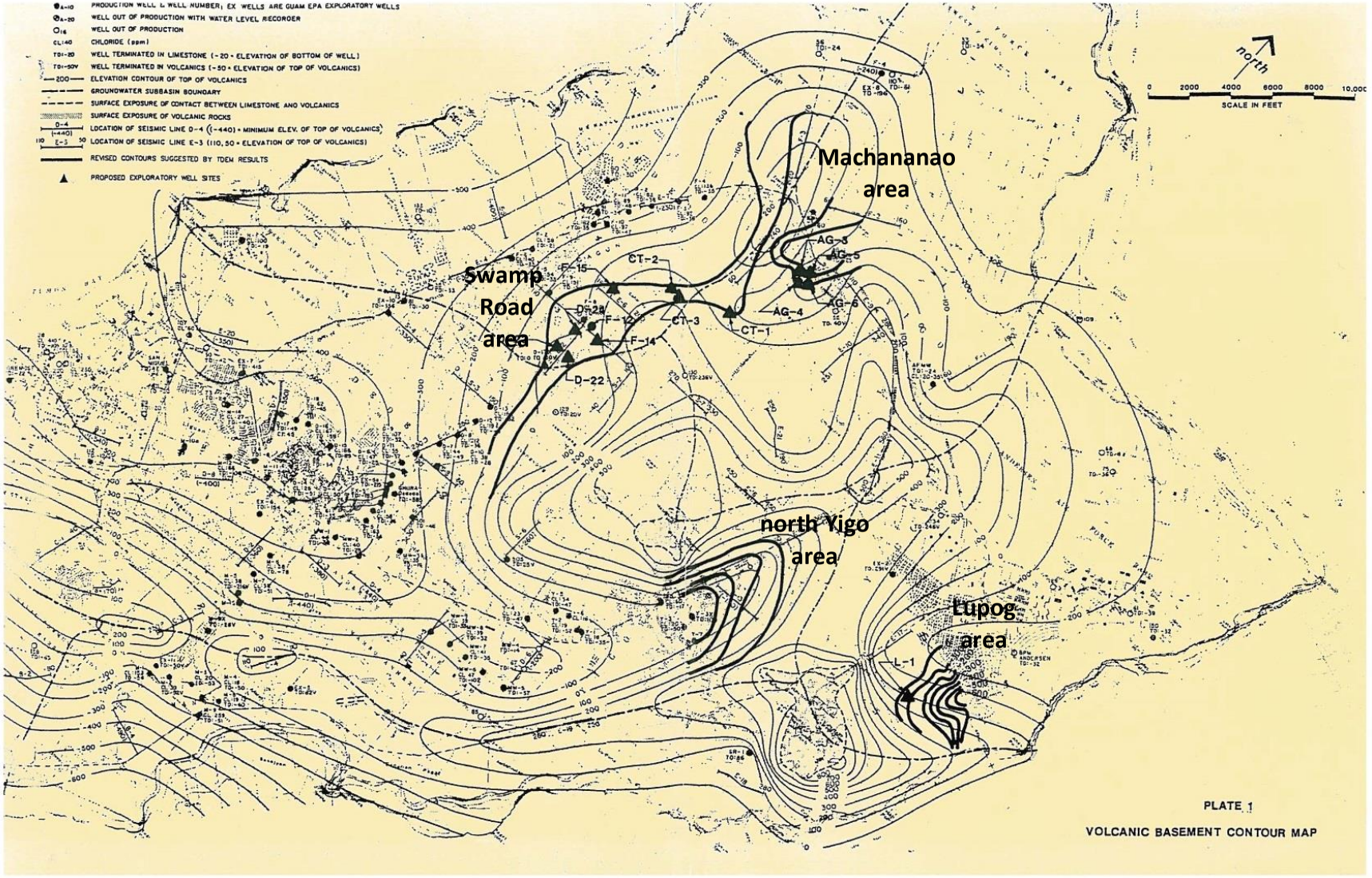

Appendix F

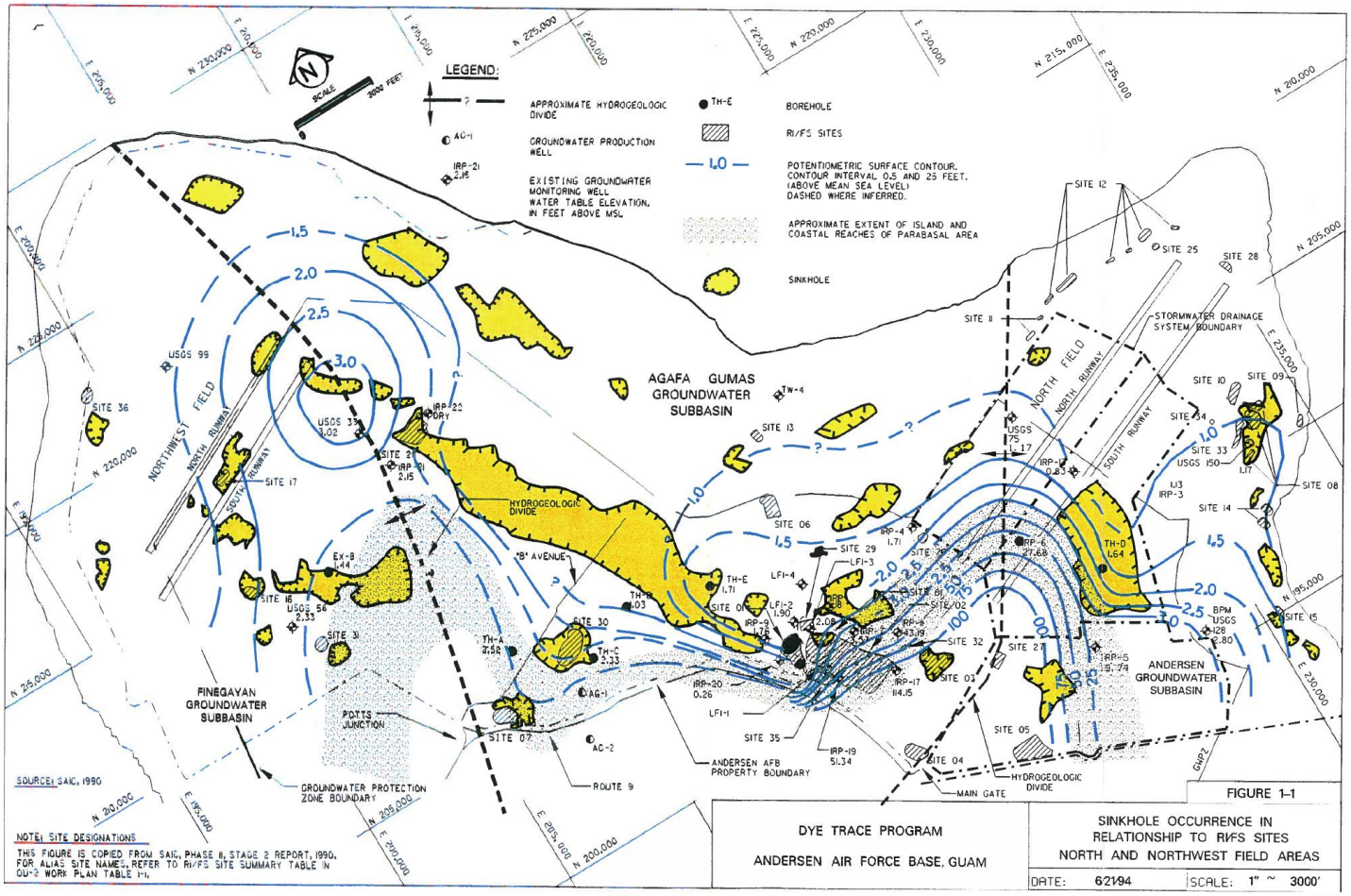

Water table beneath the North Field area, AAFB, as inferred by ICF Technology, Inc. (1995, Figure 1-1), based on borehole water level measurements. (See Section 5.1.3, paras. 2.d-e.)

AN ABSTRACT OF THE PROFESSIONAL PROJECT REPORT OF David T. Vann for the Master of Science in Environmental Science, presented April 21, 2013.

Title: Topography of the Basement Rock beneath the Northern Guam Lens Aquifer and its Implications for Groundwater Exploration and Development

Approved: _____

John W. Jenson, Chairman, Professional Project Committee

Subterranean hills and valleys in the non-productive volcanic basement rock underlying the water-bearing limestone bedrock of the Northern Guam Lens Aquifer partition it into six semi-contiguous groundwater basins. Within each basin are three zones, which pose different challenges for developing and managing water production and quality. An accurate and detailed map of basement topography is thus of central importance for successful groundwater exploration, development, and management. The pivotal 1982 *Northern Guam Lens Study* produced the first comprehensive map of basement topography, and has been in use ever since. The purpose of the project reported herein was to produce an up-to-date, state-of-the-art map to support groundwater exploration and development, and aquifer modeling, management, and protection. This revision applies the latest data screening and spatial analysis techniques to evaluate 697 records, from which 148 internal control points (80 from borehole data, 68 from geophysical surveys) were selected and applied along with 24 boundary conditions (2 Light Detection and Ranging raster-points, 17 bathymetric points, 5 specified points) to model basement topography. Elevations across the basement surface were thus estimated from 173 control points that pinned the interpolated surface to 132 positive control points. The interpolated surface was adjusted at 16 negative control points at which the deepest known depths of limestone showed it to be too high. For each control point, the new map displays the *type of data* (boundary condition, borehole, seismic, or Time Domain Electromagnetic), *type of control* (positive or negative), and *precision* (distinct or indistinct). The new map updates and more precisely defines the boundaries of the aquifer's six groundwater basins and provides for more accurate and detailed demarcation within each basin of its *basal zone* (at least 75% of the aquifer, where freshwater is underlain by saltwater), *para-basal zone* (probably less than 5% of the aquifer, where freshwater is underlain by basement rock below sea level), and *supra-basal zone* (about 20% of the aquifer, where conduits and discontinuous patches of freshwater are underlain by basement rock above sea level). The new map also incorporates new insights regarding groundwater occurrence gained from the broad-ranging 2010 Exploratory Drilling Program funded by *Naval Facilities Engineering Command Pacific*. Names from the 1982 map are retained but formal names are also assigned to previously unnamed significant features. New basin boundaries are also proposed. This report describes the elements and methodology used, including definitions of essential terms and concepts; the conceptual model of the basement geology; procedures for assembling the dataset; and the steps in preparing, statistically evaluating, and editing the interpolated basement surface. It also describes the geologic and geographic symbols used. The report concludes with recommendations regarding groundwater exploration, aquifer development, and maintenance and improvement of the basement map.

TO THE OFFICE OF GRADUATE STUDIES

The committee members approve the professional project of David T. Vann presented April 21, 2014.

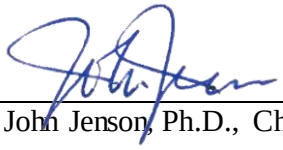

John Jenson, Ph.D., Chairman

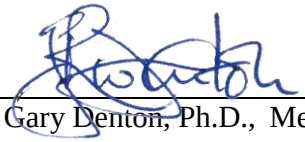

Gary Denton, Ph.D., Member

Ross Miller, Ph.D., Member

ACCEPTED:

May 2, 2014

John A. Peterson, Ph.D. Date
Assistant Vice President Of Graduate Studies,
Sponsored Programs and Research

Acknowledgments
by
David T. Vann

I would like to extend sincere appreciation to all the members of my graduate committee; Dr. John Jenson, Dr. Gary Denton and Dr. Ross Miller.

I would like to also extend appreciation to Rodney Toves and Brett Railey at Guam Water Authority and Greg Ikehara with the36th Civil Engineering Squadron at Andersen AFB for providing a wealth of historic well data. And many thanks to Doug Roff and Rob Schumann from AECOM, Steve Gingerich of the USGS in Hawaii and Nate Habana at WERI for their technical expertise, input and review on the report.

I would also like to extend my personal gratitude to my fellow graduate research colleagues Danko Taboroši, John Jocson and Maureen Quenga for their spirit and support on our many field trips.

And finally, a very special thanks to Dr. Jenson and Vivianna Bendixson. Without Dr. Jenson's leadership, guidance and determination and Vivianna's ability to organize and make sense out of a mountain of historic well data, this report would not have been possible.